Comparison of Lactate Threshold Using Plasma and Whole Blood Lactate during a Ramp-Pattern Exercise in Dyspneic Patients

Bryan S-J Ho, I-Feng Lin*, Ming-Lung Chuang, Chang-Sheng Lin, Meng-Chih Lin, Thomas, C-Y Tsao

Objective: The lactate threshold (LT) has been an important marker for physical fitness. Processing the plasma lactate assay usually requires more time and manpower to spin the deproteinated whole blood in the perchlorate solution. We decided to use whole blood (WB) lactate instead of plasma (PL) lactate to save time while we determined the LT (turning-point) of a ramp-pattern exercise test. Thus we determined the LT from WB and PL lactate levels.
Design: This study was a comparative investigation and was followed up for one year.
Setting: A referral cardiopulmonary exercise testing lab of a medical center.
Patients: Forty-eight dyspneic patients (43 COPD and five without a specific diagnosis), aged 23-76 years, were enrolled into the study.
Investigations: Each subject performed a ramp-pattern exercise test, to his limit of tolerance, using a gas exchange measurement. Blood from the brachial artery was sampled at rest, during unloaded cycling, and followed by one sample every minute during the period of increased load exercise. The WB lactate concentration was analyzed using an amperometric, enzymatic technique. The remaining blood was assayed for PL lactate concentrations.
Results: The WB lactate levels were systemically lower than the PL lactate levels. The correlation between WB lactate and PL lactate was excellent ($r = 0.97$, $P < 0.0001$). The WB lactate levels were approximately parallel to the PL lactate levels before the turning-point of each subject during the exercise test. After the LT, the slope of increase in plasma lactate was slightly steeper than that of the whole blood lactate. The LT measured with WB lactate was no different from that with PL lactate (5.4 ± 1.7 vs. 5.5 ± 1.8 min, $P > 0.05$).
In summary: The pattern of change in plasma lactate is analogous to that in whole blood in response to a ramp-pattern exercise. The LT in plasma lactate is not different from that determined from whole blood lactate, suggesting that the LT can be determined from whole blood. ***(Thorac Med 2001; 16: 80-88)***

Keywords: lactate threshold, incremental exercise; amperometric technique

Division of Pulmonary and Critical Care Medicine, Chang Gung Memorial Hospital, Taoyuan, Taiwan
*Department of Social Medicine, National Yang Ming University Taipei, Taiwan
Address reprint requests to: Dr. Bryan S-J Ho, 5 Fu-Hsin St. Kewi-Hsan, Taoyuan, Taiwan 333

Introduction

Lactic acid can be generated if the oxygen flow to tissue is inadequate for the demand. The lactate levels measured during incremental exercise are not appreciable until the onset of increased anaerobic glycolysis, after a certain level of exercise [1]. The breaking point of the increase in the lactate level is termed the lactate threshold (LT). Since the generation of lactate is due to the onset of increased anaerobic glycolysis, conceptually, an anaerobic threshold (AT) should exist and may be identical to the LT [2-3]. However, LT and AT, or lactic acidosis threshold (LAT), are appreciably different using different analytical methods, but the difference is small and the clinical significance of the difference may be neglected [3].

In recent years, there has been a growing interest in the use of blood lactate measures to define optimal training intensities, and to assess physical fitness and the effects of training [4]. The lactate threshold or AT has been an important marker for physical fitness. A normal or high AT indicates good physical fitness; a low AT indicates unfitness or circulatory impairment. In some patients with COPD, the AT is difficult to obtain by the ventilatory gas exchange method, due to an earlier ventilatory limitation or uneven breathing pattern [5]. Therefore, the technique used to analyze lactate in order to identify the LT is important for clinical use.

For the lactate assay, plasma is usually rapidly deproteinated in iced perchlorate solution and, following centrifugation, is analyzed for plasma lactate concentration. Deproteination with perchlorate and centrifugation are relatively labor- and time-consuming. This therefore could result in a further increase in the lactate produced by red cells during the spinning and processing of the specimen [6-7]. Yellow Springs Instruments (YSI) developed an equation for converting whole blood (WB) lactate to the equivalent plasma (PL) lactate value in a non-stressed condition, as follows,

$$C_{lactate}\,(PvB) = C_{lactate}\,(vB) \times 1/(1-0.22\,Hct) \quad (1)$$

Where C is concentration, PvB is venous plasma, vB is venous blood, and Hct is hematocrit.

Wandrup et al [8] found the equation inadequate and modified it as follows,

$$C_{lactate}\,(PvB) = C_{lactate}\,(vB) \times 1/(1-0.88\,Hct) \quad (2)$$

To use this equation, we must measure Hct, adding to labor and expense. Since the relationship between WB lactate and PL lactate has been reported to be extremely significant [8-9], we reasonably hypothesized that the LT measured from WB lactate should be similar to the LT measured from PL lactate. Therefore, the purpose of this study was to compare WB lactate with PL lactate for determining LT in a ramp-pattern exercise test.

Dyspnea has been the most common reason for cardiopulmonary exercise testing in our pulmonary exercise lab. Most of the patients have chronic airflow impairment. For a substantial volume of patients with COPD, the AT during a ramp-pattern exercise test is difficult to identify with gas exchange methods [5]. Since the AT has been extremely important in interpretation and exercise training in pulmonary rehabilitation, we intended to analyze the LT by lactate measurements rather than analyzing the AT with the gas exchange method.

Materials & Methods

Forty-eight patients aged 23-76 years were enrolled into this study. Forty-three subjects had stable moderate to severe chronic obstructive pulmonary disease. Five subjects were referred due to dyspnea on exertion without a specific diagnosis. The procedures and the risks of the exercise testing were clearly explained to the patients. Each subject gave informed consent. The institute ethics and research committee approved the study.

After a period of stable breathing and heart rate on the cycle ergometer ($CardiO_2^{TM}$, Medical

Graphics, MN), measurements were made during a 2-min period of resting, followed by a 2-min period of unloaded cycling, followed by a ramp-pattern exercise test to the subject's limit of tolerance. The work rate was increased at a rate of 10 to 25 watts/min, based on the subjects' fitness. During the test, the subject breathed through a mouthpiece connected to a preVent™ pneumotachograph (Medical Graphics). Expired gas was continuously sampled through a sampling line (95-105 ml/min), and analyzed with a zirconium oxygen (O_2) analyzer and an infrared absorbance carbon dioxide (CO_2) analyzer to measure the fractions of O_2 and CO_2, respectively. Minute ventilation ($\dot{V}E$), oxygen uptake ($\dot{V}O_2$), and CO_2 output ($\dot{V}CO_2$) were computed breath by breath using an on-line computer (CardiO$_2$TM, Medical Graphics).

Blood from the brachial artery was sampled with a heparinized 3-ml syringe via an indwelling catheter connected to a pressure monitor through a monitoring kit and a pressure transducer. Two blood samples were taken at rest and two samples during unloaded cycling followed by one sample every minute after the start of loaded exercise. We stick the blood at the last 15 seconds of each minute during the loaded cycling. It took approximately 15 seconds to sample each arterial blood.

With a blunt needle syringepet, a 25-μL whole blood sample was immediately pipetted and injected into the sample chamber of the lactate analyzer (YSI Model 1500 SPORT, Yellow Springs, OH) containing 350-μL buffer solution, without adding either cell lysing agents or perchloric acid [9]. The lactate concentration was analyzed using an amperometric, enzymatic technique. The processing of each sample took approximately 60 seconds, using the manual mode. The remaining blood in each syringe was stored in a test tube containing ethylenediamine tetraacetic acid (EDTA) and NaF, and was quickly iced (0-4℃) and centrifuged at 3200 rpm for five minutes [6], and then assayed for PL lactate concentrations using the same lactate analyzer (YSI Model 1500 SPORT, Yellow Springs, OH) approximately 40 minutes after blood was drawn. (Whole blood appears to be stable for at least 60 min when stored in an iced bath) [10]. Calibration of the lactate analyzer was conducted with 5-mmol/L and 15-mmol/L L-lactate standards before each testing to verify linearity [6,11]. The mean lifetime of the enzyme membranes was 4 weeks [9,12]. All assays were performed in the same laboratory under similar temperature conditions (23 ± 2℃).

Lactate levels for each subject as a function of time was used to describe the behavior of increase in lactate during the ramp-pattern exercise. We used the technique of standard regression lines of 2-segment analysis to identify the turning point where the two segments intersect. The turning point of the lactate levels, the LT for each subject, was expressed as the time after the start of the exercise test [13].

Data are shown as group mean (SD, unless otherwise indicated. Paired t tests were used to test for differences in the LT between WB and PL lactate. Two simple linear regression lines were fitted in describing the relationship of WB and PL, before and after the LT turning-point, respectively. A test of parallelism in linear regression was performed in comparing the two regression slopes of WB on PL before and after the LT. All tests were 2- sided, and significance was accepted at the $P < 0.05$ level.

Results

The total time of the exercise test was 10.5 ± 2.5 min. The mean WB lactate level was 0.4 ± 0.1 mmol/l, and the mean PL lactate was 1.1 ± 0.3 mmol/l at rest. ($P < 0.0001$). The mean WB lactate level was 3.0 (1.4 mmol/l at peak exercise and the mean PL lactate was 5.4 (2.6 mmol/l at peak exercise. ($P < 0.0001$). Figure 1 shows three representative subjects with stable lactate levels before a certain exercise intensity, and then the rapid increase in lactate after that point. The correlation between WB lactate and PL lactate

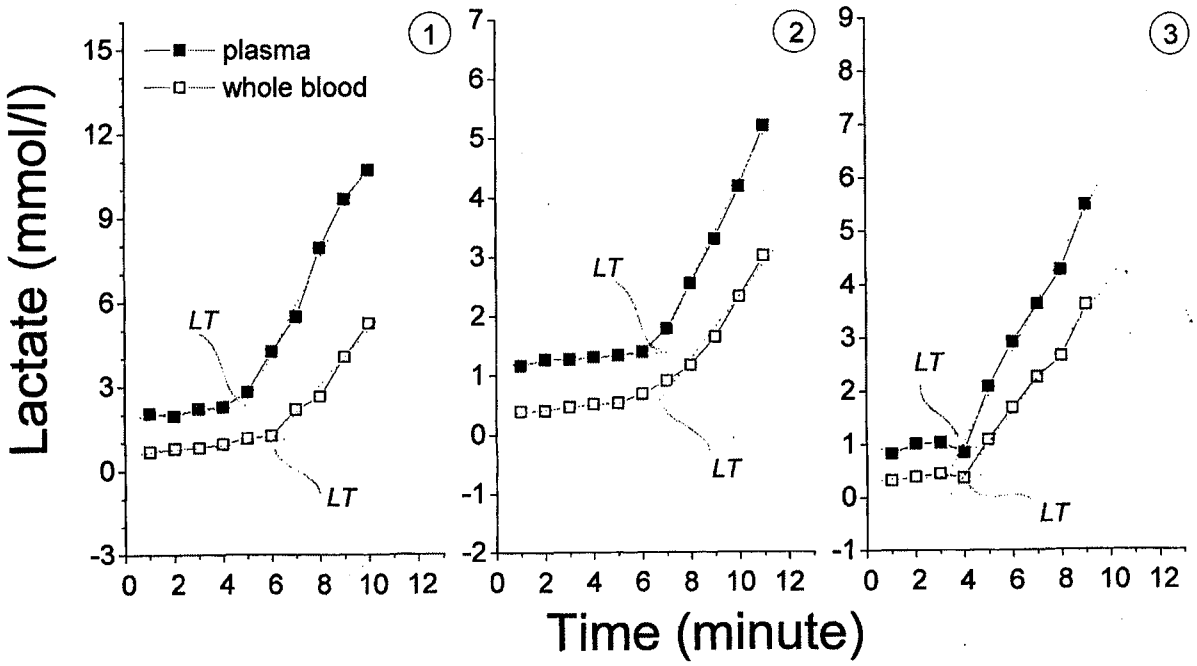

Fig. 1. Plasma (solid square) and whole blood lactate (open square) during a ramp-pattern exercise. Data in each panel are from one subject. Three representative subjects are shown. Subject number is encircled in each panel. Two-segment linear regression (dashed lines) was used to identify the turning point where the two segments intersect. LT = lactate threshold.

was excellent ($r = 0.97$, $P < 0.0001$). The PL lactate values were systemically higher than the WB lactate values. The WB lactate levels were approximately parallel to the PL lactate levels before the turning-point in each of the 48 subjects during the ramp-pattern exercise test (PL = 0.47 + 1.55 WB, $r = 0.89$, $P < 0.0001$) (Fig. 2). However, after the turning-point, the increase in PL lactate was somewhat out of proportion to and higher than the increase in WB lactate (PL = 0.2 + 1.75 WB, $r = 0.96$, $P < 0.0001$) (Fig. 2). The slope of the regression equation after the turning-point was weakly steeper than that before the turning-point ($P = 0.05$).

The mean turning point of the WB lactate was 5.4 ± 1.7 min and the mean turning point of the PL lactate was 5.5 ± 1.8 min. ($P > 0.05$). Figure 3 shows that the turning-point time of the PL lactate and that of the WB lactate were comparable for each subject.

The expense and labor for the WB lactate analysis were lower, as compared to the PL lactate analysis (Table). The latter requires additional test tubes containing EDTA, NaF, and additional labor for centrifugation (approximately 30 minutes for each subject). In contrast, we directly measured the WB lactate with the same lactate analyzer and without test tubes or centrifugation.

Discussion

Plasma lactate levels are significantly higher than WB lactate levels, because the former is measured for extracellular fluid [6,11-12,14]. The WB lactate is "diluted" by the red blood cell volume when measured for the whole blood. Plasma lactate level is also higher than blood lactate level even if the red cells are lysed [12,14]. This is due to the red cells containing ~50% of the plasma lactate level [15].

Differences in the lactate concentration between WB and PL are significant at different exercise levels, as reported previously [6]. They

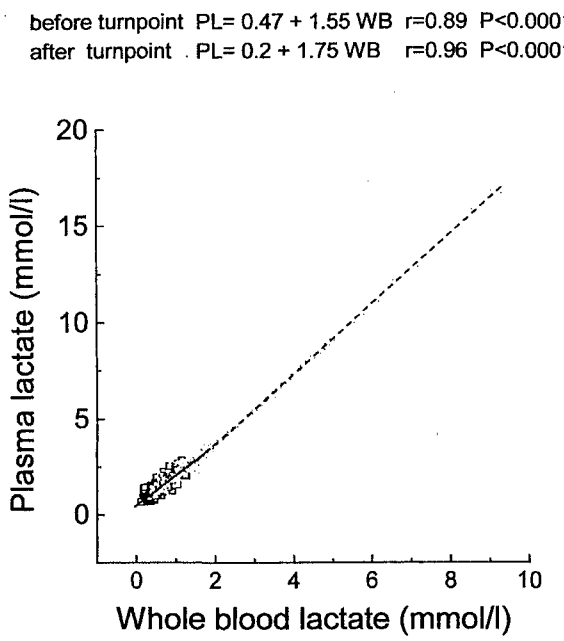

Fig 2. Relationship between plasma and whole blood lactate. All points represent the lactate levels of the 48 subjects measured during the exercise test. The thick solid line is the regression line of the plasma-whole blood lactate before the LT turning-point (open squares). The thick dashed line is the regression line of plasma and whole blood lactate after the LT turning-point (open circles). The dotted lines are the 95 C.I. lines.

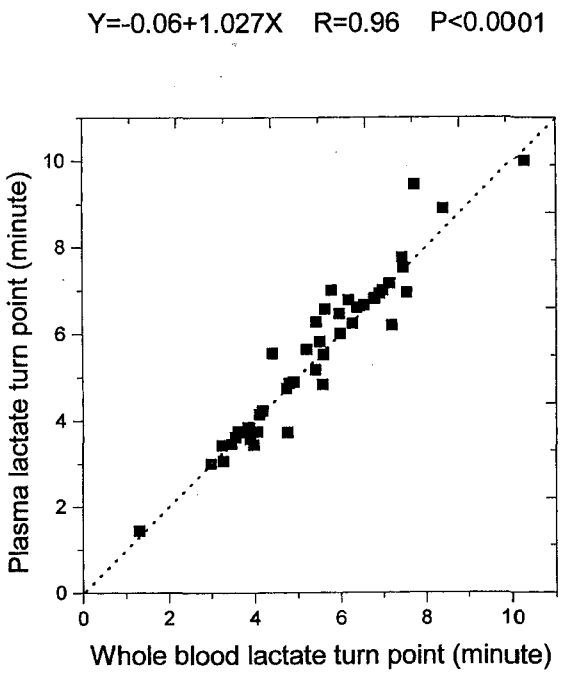

Fig 3. The relationship between the LT turning-point of the plasma lactate (n = 48) and the LT turning-point of the whole blood lactate (n = 48) in response to a ramp-pattern exercise. The unit of the turning point is time. The time is that of the lactate increase after remaining relatively constant during early exercise. Each point represents one subject.

are predictable for regression equations (R2 = 0.91-0.98). For different WB lactate levels, the prediction of the WB lactate level is slightly influenced by the PL lactate level and hematocrit. In contrast, a large variability was reported between the PL and WB levels by YSI (lactate level measured, ranging from 0.5 to 2.2 mmol/l) [10]. This could be explained by the higher variability as a percent when the lactate level is lower [6,11-12,16]. The differences in lactate levels between WB and PL were significant at different exercise levels, as shown previously [6], and based on our observation. Although the correlation of WB and PL lactates in response to a ramp-pattern exercise was highly significant in this study (y = 0.34 + 1.7 x, R2 = 0.95) and in the previous report [11], we further identified the slope of the linear regression equation after the LT to be weakly steeper than that before the LT (P = 0.05).

It was proposed that during dynamic exercise, plasma volume decreased in proportion to the increase in exercise intensity, and that the fluid shifted from the intravascular space into cells at different exercise levels on account of an accumulation of intracellular osmoles, i.e., lactate, making an osmotic gradient [17]. Thus, the Hct must be higher after the LT, and proportionally contributes to the difference between the WB and PL lactate [10]. Most of our subjects were moderate to severe COPD patients who were unable to perform at as high an intensity of exercise as that reported by Nose et al [17]. Thus, the fluid that shifted from the intravascular space into cells should have been less than in normal people. A change in Hct would be very small, and would have little effect on the LT measured using WB.

Since our study subjects were patients with COPD, their exercise capacity was lower, compared to norms, due to ventilatory limitation, and oxyhemoglobin desaturation, coexisting with

Table. Comparison of the expense and labor between WB and plasma lactate analysis

Expense			Labor		
	WB	PL		WB	PL
Syringe (NT dollars)	3600 #	3600 #	Time for blood sampling for each sample (seconds)	15	15
EDTA, NaF tube (NT dollars)	nil	1584 ^	Lactate measurement time for each sample (seconds)	60	60
Centrifuger (NT dollars)	nil	6000	Centrifugation time (minutes)	nil	1440*

WB (whole blood), PL (plasma), NT (New Taiwan)

EDTA (ethylenediamine tetraacetic acid)

each subject requires 15 syringes and each syringe costs 5 NT dollars. The cost for syringes is 15 × 48 × 5 = 3600

^ each EDTA, NaF tube costs $2.2 NT dollars. The cost for tubes is 15 × 48 × 2.2 = 1584

* 1440 min = 48 (patients) × 30 min (per patient)

pulmonary vascular impairment, or cardiovascular limitation. In normal people, the exercise limitation is due primarily to cardiovascular limitation. It may be said that the use of inter-changeable LT measured with WB lactate and LT measured with PL lactate in this study may not be able to be extrapolated to the norms. However, the inadequacy of O2 flow in response to exercise is the primary factor for anaerobic metabolism, despite its mechanisms of limitation: i.e., a circulatory or ventilatory or combined limitation. Our intention to use of WB lactate is supported by the excellent correlation between WB lactate levels and PL lactate levels, and the similar LTs measured from WB lactate and PL lactate. It should be pointed out that our derived correlation equations for PL lactate could not be applied to norms.

The measurement of the WB lactate took approximately 60 seconds for each blood sample. This was comparable to PL lactate measurement. However, the latter requires another 30 minutes for processing and centrifugation for each patient (approximately 15 samples for each patient). The expense of PL lactate analysis was also higher as compared to WB lactate analysis (Table).

The LT can be identified as an abrupt transition occurring in the rate of increase in plasma or blood lactate when the O_2 flow can not satisfy the need for cell metabolism [1,13]. Wasserman and McIlroy described this in patients with heart disease in 1964 [18]. The conceptual LT was widely used not only for the evaluation of cardiovascular dysfunction [19], but as a guide for endurance exercise training [20]. Kanarek et al reported that patients with COPD with low AT can improve their exercise capacity by exercise training; however, those who had normal AT can not [21]. Since the AT is difficult to identify with gas exchange methods in some patients with COPD, the LT as measured from the PL lactate reported by Beaver et al [1,22] or from the WB lactate reported herein emphasizes its important role in reconditioning exercise. Gas exchange, visual identification of a systemic increase in $\dot{V}E/O_2$ without an increase in $\dot{V}E/CO_2$, and a systemic increase in end-tidal PO_2 without a decrease in end-tidal PCO_2, reflected the onset of lactic acidosis. The V-slope method using a computerized regression analysis of the slopes of the $\dot{V}CO_2$ vs. $\dot{V}O_2$ plot, was reported to be superior to the visual identification method [22], and was used and termed as the gas exchange threshold (GET), which was slightly larger than the LT [3]. By an analysis of blood or plasma lactate, the LT can be identified visually using

lactate vs. time [13,23] or a log-log transformation (log $\dot{V}O_2$ vs. log lactate concentration) [23-24]. Because of the disadvantage of noise in O_2 measured breath by breath and the advantage of a fixed time interval of blood lactate sampling as the abscissa, we used lactate vs. time to identify the LT rather than a log-log transformation method in this study. We used a two-segment linear regression technique to fit the lactate data vs. time, and termed the intersect the LT turning-point measured as time. Because the behavior of WB and PL lactate are fairly parallel, the LT turning-points must be consistent, as shown here ($P > 0.05$).

Nevertheless, several experimental studies have reported that the increase in intracellular lactate production did not occur as a threshold, and therefore that a continuous function of blood lactate change might be more appropriate [25-26]. The rate of ramp-pattern exercise should be critical to the behavior of blood lactate change. In fact, most of their subjects showed a continuous function while the rate of ramp-pattern exercise was slower.

In summary, for dyspneic patients such as patients with COPD, (1) the whole-blood lactate concentration increase parallels the plasma lactate concentration increase with a slightly slower increase above the lactate threshold; and (2) the lactate thresholds measured with whole-blood and plasma samples are comparable during a ramp-pattern exercise. Thus whole-blood lactate can be used to identify the lactate threshold.

Acknowledgment

This study was supported in part by the Chang Gung Medical Research Program (CMRP #443). We thank Professor Karlman Wasserman for his critical review of the manuscript. We thank Ms. Jia-Rong Hsieh for her skillful assistance in the measurements of lactate concentrations, and Dr. Ying-Huang Tsai, Dr. Chung-Chi Huang, and Dr. Hern-Jia Chang for referring patients.

References

1. Beaver WL, Wasserman K, Whipp BJ. Improved detection of lactate threshold during exercise using a log-log transformation. J Appl Physiol 1985;59:1936-40.
2. Wasserman, K, B.J. Whipp, S. Koyal, et al. Beaver. Anaerobic threshold and respiratory gas exchange during exercise. J. Appl. Physiol 1973;35: 236-242.
3. Patessio A, Casaburi R, Carone M, et al. Donner CF, Wasserman K. Comparison of gas exchange, lactate, and lactic acidosis thresholds in patients with chronic obstructive pulmonary disease. Am Rev Respir Dis 1993;148:622-6.
4. Jacobs I. Blood lactate. Implications for training and sports performance. Sports Med 1986;3:10-25.
5. Sue DY, Wasserman K, Morrica RB, et al. Metabolic acidosis during exericse io patients with chronic obstructive pulmonary disease. Use of the V-slope method for anaerobic threshold determination. Chest 1988; 94: 931-8.
6. Bishop PA, May M, Smith JF, et al. Influence of blood handling techniques on lactic acid concentrations. Int J Sports Med 1992;13:56-9.
7. Toffaletti J, Ernst P, Hunt P, et al. Dry electrolyte-balanced heparinized syringes evaluated for determining ionized calcium and other electrolytes in whole blood. Clin Chem 1991;37:1730-3.
8. Wandrup J, Tvede K, Grinsted J, et al. "Stat" measurements of L-lactate in whole blood and cerebrospinal fluid assessed. Clin Chem 1989;35:1740-3.
9. Anonymous. YSI Model 1500 Sport lactate analyzer operations manual. Yellow Springs Instrument Co., Inc.: Yellow Springs, Ohio.
10. Toffaletti J, Hammes ME, Gray R, et al. Lactate measured in diluted and undiluted whole blood and plasma: comparison of methods and effect of hematocrit. Clin Chem 1992;38:2430-4.
11. Williams JR, Armstrong N, Kirby BJ. The influence of the site of sampling and assay medium upon the measurement and interpretation of blood lactate responses to exercise. J Sports Sci 1992;10:95-107.
12. Foxdal P, Bergqvist Y, Eckerbom S, et al. Improving lactate analysis with the YSI 2300 GL: hemolyzing blood samples makes results comparable with those for

deproteinized whole blood. Clin Chem 1992;38:2110-4.
13. Caiozzo VJ, Davis JA, Ellis JF, et al. A comparison of gas exchange indices used to detect the anaerobic threshold. J Appl Physiol 1982;53:1184-9.
14. Foxdal P, Sjodin B, Sjodin A, et al. The validity and accuracy of blood lactate measurements for prediction of maximal endurance running capacity. Dependency of analyzed blood media in combination with different designs of the exercise test. Int J Sports Med 1994;15:89-95.
15. Sahla SD MH, James LS, et al. Lactate and pyruvate gradients between red cells and plasma during acute asphyxia. J Appl Physiol 1964;19:1100-4.
16. Rodriguez FA, Banquells M, Pons V, et al. A comparative study of blood lactate analytic methods. Int J Sports Med 1992;13:462-6.
17. Nose H, Takamata A, Mack GW, Oda Y, et al. Water and electrolyte balance in the vascular space during graded exercise in humans. J Appl Physiol 1991;70:2757-62.
18. Wasserman K MM. Detecting a threshold of anaerobic metabolism in cardiac patients during exercise. Am J Cardiol 1964;14:844.
19. Matsumura N, Nishijima H, Kojima S, et al. Determination of anaerobic threshold for assessment of functional state in patients with chronic heart failure. Circulation 1983;68:360-7.
20. Casaburi R, Wasserman K. Exercise training in pulmonary rehabilitation [editorial]. N Engl J Med 1986;314:1509-11.
21. Kanarek D, Kaplan D, Kazemi H. The anaerobic threshold in severe chronic obstructive lung disease. Bull Eur Physiopathol Respir. 1979;15:163-70.
22. Beaver WL, Wasserman K, Whipp BJ. A new method for detecting anaerobic threshold by gas exchange. J Appl Physiol 1986;60:2020-7.
23. Dickstein K, Barvik S, Aarsland T, et al. A comparison of methodologies in detection of the anaerobic threshold. Circulation 1990;81:II38-46.
24. Westgard JO, Lahmeyer BL, Birnbaum ML. Use of the Du Pont "automatic clinical analyzer" in direct determination of lactic acid in plasma stabilized with sodium fluoride. Clin Chem 1972;18:1334-8.
25. Hughson RL, Weisiger KH, Swanson GD. Blood lactate concentration increases as a continuous function in progressive exercise. J Appl Physiol 1987;62:1975-81.
26. Yeh MP, Gardner RM, Adams TD, et al. "Anaerobic threshold": problems of determination and validation. J Appl Physiol 1983;55:1178-86.

比較呼吸困難病人在執行漸進式運動時使用血漿及全血乳酸鹽濃度測定乳酸閾值之差異

何松融　林逸芬* 莊銘隆　林昌生　林孟志　曹昌堯

目的：乳酸鹽閾值一直被用來做為體能狀況的重要指標。然而血漿中乳酸鹽的測定需要使用高氯酸鹽溶液將全血去蛋白化因而耗費較多的人力與成本。在本實驗中我們以漸進式運動肺功能檢查的病人為對象，分別以血漿及全血為樣本來測量乳酸鹽的濃度及測定乳酸鹽閾值，比較以兩種樣本所測量的閾值有無差異。

實驗設計：共 48 位轉介至本院運動心肺功能實驗室之病人進入本實驗，43 位慢性阻塞性肺病及 5 位無特定診斷的病人；年齡介於 23 至 76 歲。每位病人均接受漸進式運動心肺功能測驗並達到病人之運動極限。分別在休息、無負荷，及開始負荷運動起的每一分鐘接受臂動脈血取樣，並先以安培計量酵素分析法進行全血的乳酸鹽濃度分析，其餘樣本則用以分析血漿中之乳酸鹽濃度。

結果：整體上全血所測得的乳酸鹽值較血漿低而兩者的相互關連性極高 (r 值 0.97, P<0.0001)。 在運動期間血漿及全血之乳酸鹽值在閾值前大致上成平行關係；在閾值後血漿的乳酸鹽值增加幅度較全血大。分別以血漿及全血乳酸值所推定之乳酸鹽閾值在統計學上無明顯差異(5.5±1.8 min vs. 5.4 ±1.7, P > 0.05)。

結論：在漸進式運動測驗中血漿中乳酸鹽值的變化趨勢與全血中乳酸鹽值變化類似，以血漿中乳酸鹽值所推定之閾值與以全血中乳酸鹽值所推定之閾值並無不同。因此，我們推論可以測定全血之乳酸鹽值來測定乳酸鹽閾值。*(胸腔醫學 2001; 16: 80-88)*

關鍵詞：乳酸鹽閾值，漸進式運動測驗

林口長庚紀念醫院　胸腔一科　陽明大學　社會醫學科*
索取抽印本請聯絡：何松融醫師，桃園縣龜山鄉復興街五號

Diagnosis of Tuberculosis Pleurisy by Detection of Specific IgG and IgA Anti-Antigen 60 in Pleural Fluid

Min-Hsi Lin, Hong-Chung Wang, Hui-Li Liu*, Kuo-An Chu, Jau-Yoeng Lu

The diagnosis of tuberculous (TB) pleural effusion, in this study, was evaluated by means of an enzyme-linked immunosorbent assay (ELISA) of IgG and IgA antibodies to mycobacterial antigen 60 (A60). The study population consisted of 22 patients with TB pleural effusions. The control group consisted of 23 patients, comprising 16 cases of malignant pleural effusions, 4 cases of empyema/ parapneumonic effusions, and 3 cases of transudative pleural effusions. The mean titers of IgG and IgA against A60 in patients with TB pleural effusions were significantly higher than those of the mean values of the control group ($p<0.001$ in anti-A60 IgG, and $p<0.001$ in anti-A60 IgA). Using 150 ELISA units (EU) as a cutoff value, the sensitivity and specificity of the IgG measurement were 63.7% and 82.6%, respectively; and using the IgA measurement, these parameters were 54.5% and 95.6%, respectively. Serum IgG levels were simultaneously detected in 19 out of 22 patients with tuberculous pleural effusion. A positive correlation was found between the IgG titers of pleural fluids and their corresponding sera ($r=0.77$, $p<0.01$). A significant correlation was also found between pleural fluid IgG titers and IgA titers in patients with tuberculous pleural effusions ($r=0.59$, $p < 0.01$). The sensitivity and specificity of the combined test detecting pleural fluid IgG and IgA levels in patients with TB pleurisy was 81.8% and 82.6%, respectively. In conclusion, the ELISA method, using IgG and IgA against A60, is a quick test with an acceptable sensitivity and specificity for the differentiation of TB and non-TB pleural effusions. ***(Thorac Med 2001; 16: 89-94)***

Keywords: antigen 60, IgA, IgG, TB pleurisy

Introduction

Tuberculosis remains an important cause of pleural effusion in Taiwan. The ultimate diagnosis depends upon the culture and the identification of *mycobacterium tuberculosis* from the pleural effusion, or pleural biopsy. However, limitations in the usefulness of the conventional diagnostic methods do exist. Because tuberculous (TB) pleural effusion is a paucibacillar disease, mycobacteria are rarely seen on a direct smear examination of the pleural fluid. Culture identification of mycobacteria is a more definite and sensitive method. Nevertheless, six to eight weeks are required in order to

Division of Chest Medicine, Department of Internal Medicine, Veterans General Hospital-Kaohsiung, Kaohsiung, Taiwan, *College of Health Science, Kaohisung Medical University, Kaohsiung, Taiwan
Address reprint requests to: Dr. Hong-Chung Wang, Division of Chest Medicine, Veterans General Hospital-Kaohsiung, No386, Ta-Chiung 1st Road, Kaohsiung, Taiwan

complete the identification test. A histologic specimen with appropriately stained organisms or granuloma suggests the diagnosis, but this requires the performance of an invasive procedure and its positive rate is often less than 50 percent [1]. Thus, the development of a rapid serologic test for the diagnosis of active tuberculosis would be of great benefit.

The introduction of enzyme-linked immunosorbent assay (ELISA) by Nassan and his co-workers has provided an important method for tuberculosis detection [2]. Antigen 60 is a thermostable macromolecular antigen, purified from the cytoplasm of *M.Bovis* Bacillus-Calmette-Guerin [3]. It is a powerful immunogen able to induce primary and secondary responses as well as delayed hypersensitivity reactions [4]. Recent reports have demonstrated a serodiagnostic value in active pulmonary tuberculosis by using an antigen 60 (A60) ELISA test [5-10]. However, only a few examinations attempting identification of mycobacterial antibodies in the pleural effusion have been reported [11-13]. Recently, Caminero et al reported that the sensitivity and specificity was 50% and 100%, respectively, in detecting anti-A60 IgG in the pleural effusion in patients with TB pleurisy [14]. In the present work, we evaluated the usefulness of measuring anti-A60 IgG and IgA levels in the pleural fluid in the diagnosis of TB pleurisy.

Materials and Methods

We studied 45 patients who were admitted to our hospital for a diagnostic evaluation of pleural effusion. The final etiologic diagnosis was based on clinical, radiological, laboratory, and cytopathologic findings. The patients were divided into 2 major groups: the TB and non-TB pleurisy groups.

In the TB pleurisy group (n=22), the diagnosis was confirmed on the basis of a pleural biopsy, and reported as tuberculosis (n=21) or chronic granulomatous inflammation (n=1). Six out of 22 patients also showed positive pleural fluid culture results. All of the specimens were obtained before anti-tuberculosis treatment was prescribed.

In the non-TB pleurisy group (n=23), three patients presented with transudative pleural effusion secondary to heart failure (2) or uremia (1) Four patients were associated with parapneumonic effusions, and one of them could be considered as having empyema. The remaining 16 patients were cases of bronchogenic carcinoma with malignant pleural effusion. The diagnosis of malignancy was confirmed either by a cytologic study of the pleural effusion, a histology of the pleura, or both.

All of the pleural fluid specimens were tested using IgG and IgA antibodies to A60 . In addition, the anti-A60 IgG in the corresponding sera in 19 out of 22 patients with TB pleurisy were also determined. IgG and IgA antibodies to A60 were measured with the ELISA method, following Cocci et al [3]. Diagnostic kits (Anda-TBTM) were obtained from Anda Biologicals (Strasbourg, France). Briefly, in each microtiter well, 0.1ml of pleural fluid was diluted to 1:10 for IgG and 1:20 for IgA, and 0.1ml serum was diluted to 1:100 for IgG, and then incubated at 37 ^{0} C. The microtiter plates were washed, and a 0.1ml/well of conjugate was added. After incubation and a second washing cycle, an enzymatic substrate (0-phenylenediamine) was added. Finally, after 30 min of darkness, the color reaction was arrested by the addition of 4N H_2SO_4. The plates were read on a colorimetric plate reader at 450nm.

The diagnostic reliability was evaluated in terms of sensitivity and specificity. Values are expressed as mean $\pm$ SD. Cutoff values for the IgG and IgA tests were established at means $\pm$ 2SD of values measured in non-TB pleural effusions and corrected by a logistic regression analysis using 100, 150, 200, 250, 300, 400 ELISA Units (EU) to obtain an appropriate specificity and sensitivity. The Mann-Whitney U test was used for comparison between TB and non-TB groups. The relationship between pleural fluid IgG and IgA or between serum IgG and

pleural fluid IgG was calculated by a coefficiency of Spearman's correlation.

Results

The IgG test

The results of measuring pleural fluid IgG against A60 are displayed in Fig.1 Patients with TB pleurisy showed significantly ($p<0.001$) higher titers of anti-A60 IgG than did the control group. With a cutoff value of 150 EU, the test was positive in 15 of 22 (68.3%) patients with TB pleurisy. In all the subjects with transudative pleural effusions (n=3), the assay provided negative results. Positive test results were found in 2 of the 4 parapneumonic effusion patients, and in 1 of 16 patients with malignant pleural effusion. Thus, the overall sensitivity and specificity of the test were 63.7% and 82.6 %, respectively.

The IgA test

Titers of IgA against A60 were significantly higher in patients with TB pleural effusion than in those with non-TB pleural effusion ($p< 0.001$) (Fig 2). When the cutoff value was set at 150 EU, positive results were observed in 12 of 22 (54.5%) patients with TB pleurisy. For all three patients with transudative pleural effusion, the levels were lower than the cutoff value, whereas in 1 of the 4 parapneumonic/empyema patients, and in none of the 16 patients with malignant pleural effusion, the test was positive. The specificity of the IgA assay was 95.6%.

Combined use of tests

When the results of both tests were considered, the number of positive results in patients with TB pleurisy increased, yielding an overall sensitivity of 81.8%. The number of false positive increased to a lesser extent, giving an overall specificity of 82.6%.

Correlation of the tests

There was a positive correlation between pleural fluid IgG and serum IgG levels in patients with TB pleurisy ($r=0.77$, $p<0.01$). A significant correlation was also noted between pleural fluid IgG and pleural fluid IgA levels in patients with tuberculous pleurisy ($r=0.59$, $p<0.01$).

Discussion

Patients with TB pleurisy showed significantly higher titers of both IgG ($p<0.001$) and IgA ($p<0.001$) in pleural effusion against A60 compared with the non-TB control group. Both tests provided acceptable characteristics of sensitivity and specificity. The combination of both antigens showed an increase in sensitivity without a significant loss of specificity.

Anti-A60 IgG is considered a useful diagnostic tool in pulmonary tuberculosis, with a

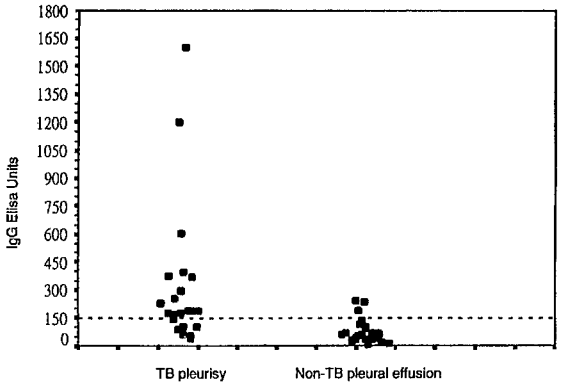

Fig. 1 . A comparison of the IgG antibody to the A60 antigen in the tuberculous pleurisy and the control groups. *Dashed line*: a cutoff value of 150 ELISA Units.

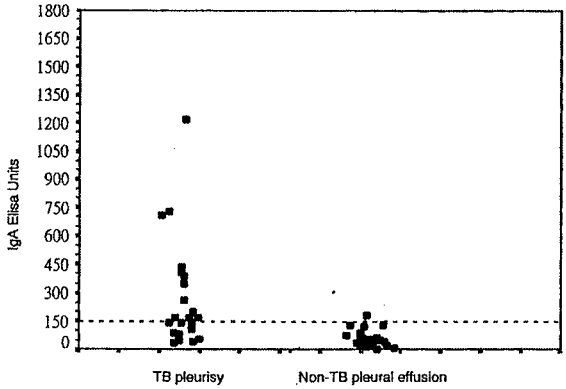

Fig 2. A comparison of the IgA antibody to the A 60 antigen in the tuberculous pleurisy and the control groups. *Dashed line*: a cutoff value of 150 ELISA Units.

sensitivity ranging from 60%-94%, as reported by different authors in different countries [5-9]. Alifano et al recently reported that the detection of serum anti-A60 IgG and IgA is characterized by good sensitivities, with 73.9% for the IgG test, 72.5% for the IgA test, and 84% for the combination of both antigens in pulmonary tuberculosis [10]. Few studies detected anti-A60 IgG or IgA in the pleural fluid of patients with TB pleurisy. A study reported by Caminero et al showed a sensitivity of 50% and a specificity of 100% among 30 patients with TB pleurisy, by detecting anti-A60 IgG in the pleural fluid [14]. Chiang et al has recently reported a sensitivity of 72.2% and a specificity of 94.4%, respectively, in the detection of pleural fluid anti-A60 IgG in 18 patients with TB pleurisy [15]. In our present work, the sensitivities in detecting the pleural fluid anti-A60 IgG and IgA were 63.7% and 54.5%, respectively, with corresponding specificities of 82.6% and 95.6%.

In our study, the detection of IgA and IgG against A60 in patients with TB pleurisy was negative in some cases. A number of studies suggested that this may be a result of immunosuppression due to the disease as well as to the presence of immune complexes that are quickly removed from the bloodstream [16,17]. Some false positive results of both tests occurred in patients with parapneumonic effusion/ empyema and in those with malignant pleural effusion. This might be due to a subclinical infection of environmental non-tuberculous mycobacteria that also express A60, or to the presence in the host of commensal non-pathologic mycobacteria. [10,18]. The disregulation of the humoral immune response that occurs frequently in several diseases might be another cause of false positive results in patients with non-TB disease [18].

The positive rates of detecting pleural fluid anti-A60 IgG and IgA were 63.7% and 54.5%, respectively. The combined use of both tests (for IgG and IgA) allowed an increase in sensitivity to 81.1% without an associated decrease in specificity. There was a positive correlation between serum anti-A60 IgG and pleural fluid anti-A60 IgG in patients with TB pleurisy ($r=0.77$, $p<0.001$). There was also a significant correlation between serum IgG titers and pleural fluid IgA titers in patients with TB pleurisy. According to the study by YU et al [7], and in our previous report [8], using 200 EU and 300 EU as cutoff values respectively (frequently used in Taiwan), the sensitivities of anti-A60 IgG for the serodiagnosis of 19 patients with TB pleurisy were 72.7% and 52.7% separately in our present work. This sensitivity is close (i.e, 63.7%) to the measurement of the pleural fluid IgG levels in patients with TB pleurisy. There are two mechanisms for the production of anti-mycobacterial antibodies in TB pleural effusions: one is passive diffusion from the serum, and the other is local antibody production from the pleura itself. Van Vooren et al favored a mechanism of local antibody production because they found higher levels of IgG and IgA anti-P32 antibodies in the pleural fluid than in the serum [11]. In contrast, Levy et al concluded that the level of antibodies in the pleural fluid is probably due to passive diffusion, not local IgG production [12]. Despite the fact that the passive diffusion mechanism may be more favored in our present study, it seems to insufficiently explain both mechanisms of antibody production in TB pleural effusion because of the small sample size and the moderate degree of correlation between the anti-A60 IgG in the pleural fluid and its corresponding serum.

In conclusion, the anti-A60 IgG and IgA tests for the diagnosis of TB pleural effusion are characterized by acceptable sensitivities and specificities. The combined use of both tests allows an increase in the diagnostic accuracy of TB pleurisy. The A60-based ELISA test may be a useful method for the rapid diagnosis of TB pleurisy.

References

1 Sahn SA. The pleura. Am Rev Resp Dis 1988;138:184.

2. Nassau E, Parasons ER, Johnson GD. The detection of antibodies to mycobacterium tuberculosis by enzyme-linked immunosorbent assay (ELISA). Tubercle 1976;57:67-70.
3. Cocito C, Vanlinden F. Preparation and properties of antigen 60 from mycobacterium bovis BCG. Clin Exp Immunol 1986;66:262-72.
4. Cocito C, Baelden MC, Benoit C. Immunological properties of antigen 60 of BCG: induction of humoral and cellular immune reactions. Scand J immunol 1987;25:579-85.
5. Charpin D, Herbault H, Gevaudan MJ. Value of ELISA using A60 in the diagnosis of active pulmonary tuberculosis. Am Rev Respir Dis 1990;142:380-4.
6. Cocitio C. Properties of the mycobacterial antigen complex A60 and its applications to the diagnosis and prognosis of tuberculosis. Chest 1991;100:1687-93.
7. Yu CJ, Yang PC, Hsieh RP, et al. Evaluation of the A-60 IgG ELISA serodiagnostic test for tuberculosis in Taiwan. J Formosan Med Assoc 1992;91:614-9.
8. Wang HC, Lu JY, Liang L, et al. Evaluation of the potential role of enzyme-linked immunosorbent assay in serodiagnosis of tuberculosis, Chin Med J (Taipei) 1993; 52:9-14.
9. Gupta S, Kumari S, Banwalikar JN, et al. Diagnostic utility of the estimation of mycobacterial antigen A60 specific immunoglobulins IgM, IgA and IgG in the sera of cases of adult human tuberculosis. Tubercle Lung Dis 1995; 76:418-24.
10. Alifano M, Sofia M, Mormile M, et al. IgA immune response against the mycobacterial antigen 60 in patients with active pulmonary tuberculosis. Respiration 1996; 63:292-7.
11. Van Vooren JP, Farber CM, De Bruyn J, et al. Actimycobacterial antibodies in pleural effusions. Chest 1990;97:88-90.
12. Levy H, Wayne LG, Anderson BE, et al. Antimycobacterial antibody levels in pleural fluid as reflection of passive diffusion from serum. Chest 1990;97:1144-7.
13. Murate T, Mizoguchi K, Amano H, et al. Antipurified-protein-deriative antibody in tuberculous pleural effusion. Chest 1990;97:670-3.
14. Caminero JA, Rodriguez F, Carrillo T, et al. Diagnosis of pleural tuberculosis by detection of specific IgG anti-antigen 60 in serum and pleural fluid. Respiration 1993;60:58-62.
15. Chiang CS, Yeh SZ, Chang TL, et al. Detection of specific antibody to mycobacterial antigen 60 in tuberculous pleural effusion. Chin Med J (Taipei) 1994;53:204-7.
16. Johnson NM, McNicol MW, Burton-Kee EJ, et al. Circulating immune complexes in tuberculosis. Thorax 1981;36:610-7.
17. Katz P, Goldstein RA, Fauci AS, et al. Immunoregulation in infection causes by M.tuberculosis: the presence of suppressor monocytes and the alteration of subpopulation of T lymphocytes. J Infect Dis 1979;140:12-21.
18. Cocci C. Properties of the mycobacterial antigen complex A60 and its applications to the diagnosis and prognosis of tuberculosis. Chest 1991;100:1687-93.

藉由偵測肋膜積液中抗 A60 IgG 及 IgA 特異抗體來診斷結核性肋膜炎

林旻希　王鴻昌　劉慧俐* 朱國安　盧朝勇

利用 ELISA 偵測 IgG 及 IgA 對分枝桿菌 A60 抗原的抗體來診斷結核性肋膜積液。研究的群體包括 22 個結核性肋膜積液的病人。非結核性肋膜積液組有 23 個病人，包括 16 個惡性肋膜積液的病人，4 個膿胸/肺炎旁積液，及 3 個滲出性肋膜積液的病人。結核性肋膜積液組對分枝桿菌 A60 抗原的 IgG 及 IgA 抗體的血清濃度平均值比非結核性肋膜積液組的血清濃度平均值有意義的升高(在抗 A60 IgG 抗體 P<0.001,在抗 A60 IgA 抗體 p<0.001）。若以 150 IU 為切點，IgG 的敏感度及特異度分別是 63.7%及 82.6%。若測量 IgA,則其敏感度及特異度分別是 54.5%及 95.6%。22 個結核性肋膜積液的病人中有 19 個同時測量了血清 IgG 的濃度，這些病人的肋膜積液與血清的 IgG 濃度成正相關（r=0.77,p<0.01）。同時，在這些結核性肋膜積液的病人中，肋膜積液裡的 IgG 及 IgA 抗體亦有相關（r=0.59,P<0.01）。藉由同時偵測結核性肋膜積液裡的 IgG 及/或 IgA 抗體，敏感度及特異度分別是 81.8%及 82.6%。總之，藉由 ELISA 偵測抗 A60 抗原的 IgG 及 IgA 抗體是一個迅速且敏感度及特異度均可以接受的鑑別結核及非結核性肋膜積液的方法。*(胸腔醫學 2001; 16: 89-94)*

關鍵詞：A60 抗原，IgG，IgA，結核性肋膜炎

高雄榮民總醫院　胸腔內科　高雄醫學大學　健康科學院*
索取抽印本請聯絡：王鴻昌醫師，高雄市左營區大中一路 386 號

Pulmonary Metastasis of Hepatocellular Carcinoma

Wen-Yuh Liou*, Jen-Yu Hung, Jew-Wu Chen**, Jiunn-Jiun Hou, Te-Hung Hsu, Tung-Heng Wang, Inn-Wen Chong, Jhi-Jhu Hwang, Ming-Shyan Huang

Hepatocellular carcinoma (HCC) is one of the leading causes of malignancy in Taiwan and in the world. Pulmonary metastasis is the most common extrahepatic metastasis, according to antemortem and postmortem studies. We reviewed 964 HCC patients who were admitted to Kaohsiung Medical University Hospital from Jan 1998 to Dec 1999. Among them, there were 51 (5.3%) HCC cases with pulmonary metastasis. The main presentations of HCC with pulmonary metastasis on the chest x-ray were multiple nodules (43 cases) and pleural effusion (16 cases). Five patients with a solitary nodule, and one with lymphangitic carcinomatosis of the lung, were also found. The common characteristic of these metastases was that most cases arose from the lower right lung field.

Additionally, we studied the survival time of the HCC patients with pulmonary metastasis. The median survival time of these 51 cases was 10 months. Once pulmonary metastasis was found, the mean survival time was 3.3 months. ***(Thorac Med 2001; 16: 95-101)***

Keywords: hepatocellular carcinoma (HCC), chest X-ray, pulmonary metastasis, survival time

Introduction

Hepatocellular carcinoma (HCC) is one of the most common cancers in the world. It is also one of the most deadly, with a 5-year survival rate of less than 5%, if untreated [1]. In Taiwan, HCC is one of the leading causes of malignancy [2]. Since 1965, it has had the highest mortality ranking of male malignancies. The mean survival time is less than 6 months after diagnosis, if left untreated. The introduction of alpha-fetoprotein (AFP), real-time ultrasound, and CT has improved the ability to screen for HCC. However, patients with small HCC are often free from symptoms. Patients usually present to the hospital with a large HCC or late-stage HCC, thus the prognosis is very poor. At the present time, surgical resection and liver transplantation are the only treatment options that offer the potential for long-term survival or cure of HCC.

Due to the high incidence rate of HCC in Taiwan, we were interested in studying the extrahepatic metastasis of HCC patients. Previous studies have showed that the most common extrahepatic metastatic site of HCC is the lung [3-13]. In postmortem series, the incidence ranged from 23 to 70 percent. Therefore, HCC may be the most common primary malignancy with pulmonary metastasis in Taiwan. In this study,

Department of Internal Medicine, Saint Joseph Memorial Hospital*, Division of Chest Medicine, Department of Internal Medicine, School of Medical Sociology**, Kaohsiung Medical University, Taiwan.
Address reprint requests to: Dr. Ming-Shyan Huang, Division of Chest Medicine, Department of Internal Medicine, Kaohsiung Medical University, 100, Shih-Chuan 1st Road, Kaohsiung, 80708, Taiwan

the plain chest x-ray examination was used as a tool to detect possible pulmonary metastasis in HCC cases. The chest x-ray patterns in those patients and their survival time were reviewed.

Materials and Methods

We reviewed the clinical records of hepatocellular carcinoma (HCC) patients diagnosed at and admitted to Kaohsiung Medical University Hospital between January 1998 and December 1999. A total of 964 HCC cases were registered during this period. Out of the 964 cases, there were 51 cases (5.3%) of HCC with pulmonary metastasis. Those 51 cases were analyzed using several criteria at the time of diagnosis: age, sex, HCC location and tumor size as shown on abdominal echography, serum AFP level, co-existing liver disease, and survival time (time between diagnosis and death).

The chest x-ray presentation patterns of lung metastasis in these 51 cases were further classified into four main groups: solitary nodule, multiple nodules, lymphangitic carcinomatosis, and pleural effusion. These 51 patients had at least one chest x-ray examination during admission. As a control, another 51 cases were selected from the remaining 913 HCC cases in a random fashion. These control group patients were analyzed in the same manner.

All data analyses were made using the SPSS for Windows Statistical Software package (SPSS, Chicago, IL). The results are expressed as mean ± standard deviation (SD). The Kaplan-Meier method was used to estimate the probability of overall survival as a function of time, and differences in the survival of subgroups of patients were compared with Mantel's log-rank test. Overall survival duration was measured to the date of death from any cause. Statistically significant differences were reported when the p value was less than 0.05.

Table 1 Patient characteristics

Characteristics	Patient groups	
	Cases	Controls
Total No.	51	51
Age, years		
Median	55	60
Range	24-89	36-86
Sex		
Male	41	39
Female	10	12
HCC location		
Right lobe	30	28
Left lobe	5	10
Both lobes	16	13
HCC tumor size		
<5cm	18	29
5-10cm	12	14
>10cm	21	8
Serum AFP		
<20 ng/ml	10	16
20-40 ng/ml	11	24
>400 ng/ml	30	11
Underlying liver disease		
Hepatitis B	39	18
Hepatitis C	7	26
Liver Cirrhosis	27	47
Survival time, months		
Median	10.0	15.5
Range	0-66	2-72

Results

The characteristics of our study cases (HCC with lung metastasis) and controls (HCC without lung metastasis) are stated in Table 1. Both groups showed a male-patient predominance. Most HCC, when first diagnosed, were located on the right lobe of the liver. Patients in the case group had a shorter median survival time when compared to that of the control group (case/control: 10.0/15.5 months). However, there was no significant difference ($p>0.05$) (Fig. 1).

Among the 51 HCC patients with pulmonary metastasis, other sites of metastases were also seen: there were seven cases with bone metastases, three cases with brain metastases, one case with spleen metastasis, and two cases with

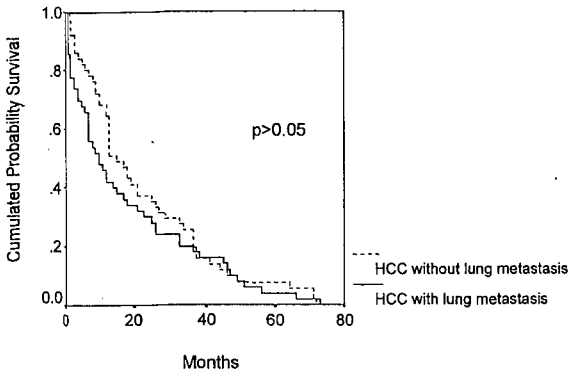

Fig 1. Comparison of survival time in HCC with and without pulmonary metastasis.

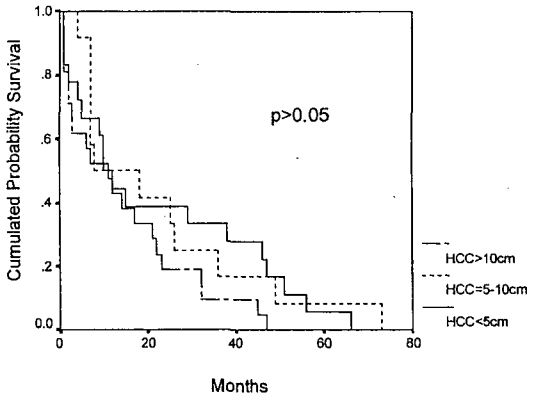

Fig 2. Comparison of survival time in HCC with pulmonary metastasis, with a different HCC tumor sizes.

right adrenal gland metastases.

Concerning the survival time of our study cases, there were no statistically significant differences based on HCC tumor size (Fig. 2) or serum AFP level (Fig. 3). The median survival time of the study group was 10 months. The mean survival interval between initial diagnosis and the appearance of pulmonary metastasis was 14.8 months. Once lung metastasis was present, the mean survival time was 3.3 months.

The main chest x-ray presentations of lung metastasis in HCC were a solitary nodule (Fig. 4A), multiple nodules (Fig. 4B), pleural effusion (Fig. 4C), and lymphangitic carcinomatosis (Fig. 4D). We identified five cases with a solitary nodule (two cases located in the right upper lobe, one in the right lower lobe, one in the left upper lobe, and one in the left lower lobe; the tumor size varied from 0.5-2.8 cm); 43 cases of multiple nodules (one case in the left lung field, 42 cases in bilateral lung fields; tumor size 0.3-3 cm), and one lymphangitic carcinomatosis of the lung. There were 16 cases of pleural effusion: 12 cases were unilateral (11 cases on the right side, one on the left side) and four cases presented with bilateral pleural effusion (Table 3). We found that there was no correlation between the lung metastatic pattern and the HCC tumor size.

Table 2 Survival Time (Months)

	Survival times (months)	
HCC size		p>0.05
<5cm	22.39 ± 22.20	
5-10cm	22.25 ± 21.29	
>10cm	13.48 ± 14.68	
Serum AFP		p>0.05
<20 ng/ml	15.90 ± 16.54	
20-400 ng/ml	27.18 ± 21.87	
>400 ng/ml	16.40 ± 18.86	

Survival times: Mean ± standard deviation

Discussion

We have reviewed and compared serial references (Table 4). In this study, there were only 51 cases, out of 964 HCC cases (5.3%), with pulmonary metastasis. The frequency of lung lesions seen in our study was correlated with the findings of a previous autopsy meta-analysis, in which the lung was found to be the most common site of extrahepatic metastasis disease (range, 23%-70%) and antemortem x-ray findings (6.9-28 %) [3-13].

The most frequent site of the first detectable metastasis of HCC is also the lung [12]. The pulmonary nodules of most patients were less than or equal to 1.0 cm in diameter, but the largest pulmonary nodule measured up to 3.0 cm. The lower lobes of the lungs were more commonly involved than the upper lobes. Hematogenous dissemination to the pulmonary capillary network is the presumed mechanism of

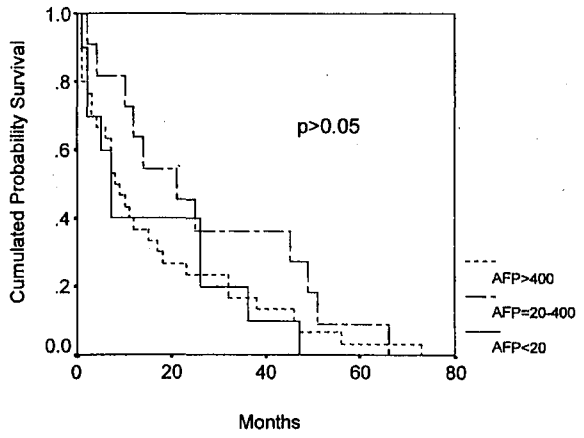

Fig 3. Comparison of survival times in HCC with pulmonary metastasis, with different serum AFP.

spread. As with hematogenous metastasis from other extrathoracic malignancies, the lower lung zones were involved more frequently than the upper lung zones [14].

The development of surgical techniques, TACE and PEI, have increased the survival time of HCC patients with intrahepatic recurrence. But in our study, if the patient had pulmonary metastasis, the prognosis would be poor. The mean survival time was 3.3 months after diagnosis of lung metastasis in our series. Six patients died in less than one month after diagnosis of lung metastasis. One report even showed that the pulmonary metastasis of HCC patients associated with transcatheter arterial chemoembolization (TACE) had a strong adverse impact on patient survival [15].

Among the 51 cases of HCC with lung metastasis, one patient still survived at this writing. He was diagnosed with lung metastasis in April 1998. After diagnosis, he received a complete course of radiotherapy, and the lung nodules disappeared. He also received TACE 4 times and PEI once. He is still making OPD follow-up visits.

HCC metastasis to the lungs is spread by hematogenous, lymphatic, and direct invasion [4,9,16]. Due to the abundant blood supply, a close relationship between the lungs and liver, and the fulminating course of the hepatoma have been noted. The main chest x-ray manifestations are multiple nodulation [5,7,17] and pleural effusion. Multiple round foci are a typical radiological sign of hematogenous metastasis. This finding is explained by the radiating growth pattern surrounding the mostly centrally, later sometimes eccentrically, localized embolized blood vessels [18].

Table 3. The chest X –ray presentations in HCC with pulmonary metastasis.

Chest X-ray presentations	Case no.
Solitary nodule	5
Multiple nodules	43
Unilateral	1
Bilateral	42
Lymphangitic carcinomatosis	1
Pleural effusion	16
Right side	11
Left side	1
Bilateral	4

There was only one lymphangitic carcinomatosis of the lung in our study. Since not every patient received a thin section CT examination or pathology proof, the rate of lymphangitic carcinomatosis may be underestimated. Lymphangitic dissemination of the tumor within the lung, due to HCC, is less common. When it does occur, it is usually seen with carcinomas of the breast, lungs, stomach, pancreas, prostate, uterus, thyroid, etc. [17,19]. Lymphangitic carcinomatosis almost always results from hematogenous metastasis to small capillaries, with a secondary invasion of the peripheral lymphatic channels [20].

There were limitations to our study. First, it was a retrospective study. Within the two-year period, the rate of HCC with lung metastasis was lower. If we traced a longer period (five or more years), we would find a higher incidence rate. Second, we recognize that not all of the extrahepatic lesions were proven metastatic HCC by biopsy. Third, lung metastasis has not been well-studied because of poor follow-up after

Table 4. The incidences of HCC with pulmonary metastasis

Reference	Patients no.	Incidence percent (%)	
		Antemortem x-ray study	Autopsy
Sung et al.[3]	313	13	53
Lai & Lin [4]	87	--	63
Okuda .[5]	134	28	43
Patton & Horn[6]	60	--	70
Gustafson [7]	62	--	23
MacDonald [8]	108	--	37
Lin [9]	313	8	--
Tsai et al.[10]	470	11	--
Chen [11]	231	6.9	--
Katyal et al. [12]	403	20.9	--
Lam et al. [13]	380	12.6	--
Liou et al.	964	5.3	--

diagnosis and treatment. However, in a patient with known HCC and with no other primary tumor, the development of a new lesion in the lungs strongly suggests metastatic HCC. This criteria is used by oncologists and surgeons when planning therapy.

In conclusion, a series of chest x-ray examinations are useful in the detection of pulmonary metastasis in HCC patients, and are also a good modality for the prognosis of HCC cases during treatment.

Reference

1. Ulmer SC. Hepatocelluar carcinoma. Postgraduate Medicine 2000; 107 : 117-24.
2. 陳定信,賴明陽,陳健弘.肝細胞癌--台灣三十年的經驗. 行政院衛生署八十年度委託研究計畫研究報告 2001/1/7 擷取自網：http://formosan.mc.ntu.edu.tw/data/肝癌.html
3. Sung JL, Wang TH, Yu JY. Clinical study on primary carcinoma of the liver in Taiwan. Am J Dig Dis 1967; 12: 1036-49.
4. Lai YH, Lin WSJ. A pathological study of primary carcinoma of the liver (thesis). Taiwan, Institute of Pathology, School of Medicine, National Taiwan University, 1976.
5. Okuda K. Clinical aspects of hepatocellular carcinoma: analysis of 134 cases. In: Okuda K, Peter RL,eds. Hepatocellular carcinoma. New York: John Wiley and Sons 1976: 428-30.
6. Patton RB, Horn RC. Primary liver carcinoma: autopsy study of 60 cases. Cancer 1964; 17: 757-68.
7. Gustafson EG. An analysis of 62 cases of primary carcinoma of the liver based on 24,400 necropsies at Bellevue hospital. Ann Intern Med 1937; 11: 889-900.
8. MacDonald RA. Primary carcinoma of the liver: clinicopathologic study of 108 cases. Arch Intern Med 1957; 99: 266-79.
9. Lin TY. Tumor of the liver. In: Bockus HL (ed). Gastroenterology, 3rd ed. Philadelphia: WB Saunders Co, vol 3, 1976: 522-32.
10. Tsai GL, Liu JD, Siauw CP, et al. Thoracic roentgenologic manifestations in primary carcinoma of the liver. Chest 1984; 86: 430-34.
11. 陳信成.門靜脈侵犯對肝細胞癌轉移之影響.高雄醫學大學醫學研究所博士論文.1993:75-86.
12. Katyal S, Oliver III JH, Peterson MS, et al. Extrahepatic metastases of hepatocellular carcinoma. Radiology 2000; 216: 698-703.
13. Lam CM, Lo CM, Yuen WK, et al. Prolonged survival in selected patients following surgical resection for pulmonary metastasis from hepatocellular carcinoma. British Journal of Surgery 1998; 85:1198-200.
14. Davis SD. CT evaluation for pulmonary metastasis in patients with extrathoracic malignancy. Radiology 1991;

180: 1-12.

15. Liou TC, Shih SC, Kao CR, et al. Pulmonary metastasis of hepatocellular carcinoma associated with transarterial chemoembolization. Journal of Hepatology 1995;23:563-8.
16. Liu JD. Peritoneoscopic diagnosis of hepatocellular carcinoma. Gastroenterol Endoscope 1982; 24:3-13.
17. Eppstein S. Primary carcinoma of the liver. Am J Med Sci 1964;247:137-44.
18. Muller K-M, Respondek M. Pulmonary metastases : pathological anatomy. Lung 1990; 168 (Suppl): 1137-44.
19. Yang SP, Lin CC. Lymphangitic carcinomatosis of the lungs: the clinical significance of its roentgenological classification. Chest 1972;62:179-87.
20. Janower ML, Blennerhassett JB. Lymphangitic spread of metastatic cancer to the lung. A radiologic-pathologic classification. Radiology 1971;101:267-73.

肝細胞癌之肺部轉移

劉文玉* 洪仁宇 陳九五** 侯俊君 許德宏 王東衡 鍾飲文 黃吉志 黃明賢

肝細胞癌（肝癌）是台灣和世界常見癌症死因之一，肝癌病人的轉移不管生前或死後的研究都是以肺部最多。我們研究了 964 個肝癌病人，他們是從 1998 年 1 月到 1999 年 12 月住在高雄醫學大學附設中和紀念醫院的病人。從胸部 X 光的檢查追蹤總共有 51 位肺部移轉的病人被診斷出來。這些肺部轉移的病人在肺部 X 光片上的主要表現是多發性結節（43 名病人）和肋膜積水（16 名病人），另外有 5 名病人是單一結節和一名肺部癌性淋巴管炎的病人。大部分的病例是從右下肺野開始發生。

此外，我們研究肺癌病人肺部轉移的生存時間。51 位病人的中間存活時間是 10 個月，一旦肺部轉移被發現後期平均存活時間是 3.3 個月。*(胸腔醫學 2001; 16: 95-101)*

關鍵詞：肝細胞癌，胸部X光，肺部轉移，存活時間

高雄縣聖若瑟醫院內科* 高雄醫學大學 內科部胸腔內科 醫學社會學系**
索取抽印本請聯絡：黃明賢醫師，高雄市三民區十全一路 100 號 高雄醫學大學內科部胸腔內科

Physical Findings and Cephalometric Variables as Risk Factors for Obstructive Sleep Apnea Syndrome— A Preliminary Report

Yu-Lun Lo, Kang-Yun Lee, Hsih-Shin Hsiao, Chao-Kai Yang, Yu-Chih Liu, Han-Pin Kuo

Obstructive sleep apnea syndrome (OSAS) results from the repeated collapse of the upper airway during sleep, accompanied by arousal from sleep. Increased pharyngeal collapsibility and abnormal anatomic structures have been postulated to contribute to the pathophysiology of OSAS. To determine the risk factors of the oropharyngeal structure and the morphological characteristics specific to patients with OSAS, 20 adults with an AHI higher than 10, and 15 adults with an AHI less than 10, were recruited for oropharyngeal physical examination and cephalometry evaluation. The OSAS patients had a higher mean AHI (41.0 ± 20.2 vs 4.1 ± 3, P<0.01) than the control group. The neck circumference (NC) (40.8 ± 3.7 cm vs 37.1 ± 5.1 cm, P<0.05) and the percentage of males (75 % vs 40 %, P<0.05) were significantly higher compared to the control subjects. Soft palate length (SPL) (42.9 ± 9.0 mm vs 37.6 ± 3.9 mm, p<0.05) and superior posterior airway space (SPAS) (5.9 ± 2.6 mm vs 7.9 ± 2.8 mm, p<0.05) were found to be significantly different between the OSAS and control groups. The physical findings of lateral pharyngeal wall narrowing, tonsillar enlargement, uvula enlargement, overjet, and retrognathia were not significantly associated with OSAS patients. In addition, NC was found to be highly correlated with AHI (r= 0.52, p=0.002). As to cephalometric variables, AHI was strongly associated with SPL (r=0.55, p=0.001), and negatively associated with SPAS (r= -0.33, p=0.04). Our results suggest that males with an expanded neck circumference, elongated soft palate length, and a short superior posterior airway space, were at an increased risk for OSAS. ***(Thorac Med 2001; 16: 102-111)***

Keywords: obstructive sleep apnea syndrome, cephalometry

Introduction

Obstructive sleep apnea syndrome (OSAS) is a condition in which repetitive episodes of apnea and hypopnea occur during sleep. OSAS affects 2-4% of middle-aged people, and poses a major health problem to the public [1]. The clinical presentations and severity are variable. The minor complaints are sleep disturbance, excessive daytime somnolence, narcolepsy, sexual dysfunction, and mental retardation [4]. Its major

Department of Thoracic Medicine II, Chang Gung Memorial Hospital, Taipei, Taiwan
Address reprint requests to: Dr. Yu-Lun Lo, Thoracic Medicine II, Chang Gung Memorial Hospital, 199 Tun Hwa N Rd. Taipei, Taiwan

sequels include systemic or pulmonary hypertension, life-threatening arrhythmia, myocardial infarction, stroke, and chronic respiratory failure. OSAS has a significant impact on quality of life, and also carries a high cardiovascular and cerebrovascular morbidity and mortality [2-3]. Nevertheless, only a small proportion of OSAS subjects is properly diagnosed. This is attributed to a lack of awareness of OSAS among the public and physicians [5].

Previous studies have focused on anatomic parameters to predict apnea density. Multisegmental narrowness or closure of the upper airway has been observed in the unstable pharynx [6-8]. The soft tissue of the pharynx, including the lateral pharyngeal wall, uvula, tonsils, and soft plate, was thought to be important in mediating airway size [9]. Furthermore, the airway size has also been determined by the craniofacial bony structure of the mandible [10]. Cephalometry studies have shown several parameters relative the OSAS, including relative collapsibility in the position of the hyoid bone, the long mandibular-plane-to-hyoid-bone distance, the width of the posterior airway space, and the diameter and length of the soft palate and the tongue [11-12, 16]. The available cephalometry results were all from Caucasians, and might not reflect the pathophysiology of OSAS in Chinese. The purpose of our study is to identify the upper airway soft tissue and bony structural characteristics in Chinese with OSAS. We approached this study with physical examinations and cephalometric radiography to linearize the risk factors for OSAS.

Methods

Study design and patients

Seventy adult patients were recruited from the outpatient clinic from July 1999 to February 2001, for an evaluation of their sleep disorder. They were all either Taiwanese or Hakka. They were divided into OSAS and non-OSAS groups, based on their polysomnography results. All of them were asked to come back for clinical evaluation and cephalometry measurement. Twenty patients in the OSAS group completed all the evaluations. They were aged from 35 to 76, and had a mean apnea-hypopnea index (AHI) of 41. Fifteen patients in the control group completed all the evaluations; they were aged from 31 to 67, with a mean AHI of 4.1 (Table 1).

Clinical evaluation

Each patient's sex, age, weight, and height were recorded. Body mass index (BMI) was calculated based on the patient's height and weight in standard units of kilograms per meter-squared (Table 1). Neck circumference (NC) was measured at the level of the thyroid cartilage. Upper airway soft tissue and bony structures were evaluated in the upright position. During these measurements, the patient's head was placed in the Frankfurt plane (defined by a line extending from the tragus of the ear to the inferior edge of the ipsilateral orbit) parallel to the floor. A single physician performed all measurements [13]. All patients were asked to open their mouth as widely as possible during the examination, while the

Table 1 Subject Demographics

Measurement	OSAS(AHI>10)(n=20)		CONTROL(AHI<10)(n=15)		P Value
	Mean	SD	Mean	SD	
AHI,events per hour	41	20.2	4.1	3	<0.01
Age,yr	55.9	13.4	49.9	11.8	0.179
BMI,kg/m^2	31.7	4.7	28.9	4.6	0.102
Neck size,cm	40.8	3.7	37.1	5.1	0.02
Percent male%	75		40		0.035

Definition of abbreviations. AHI=apnea-hypopnea index; BMI=body mass index; OSAS=Obstructive sleep apnea syndrome.

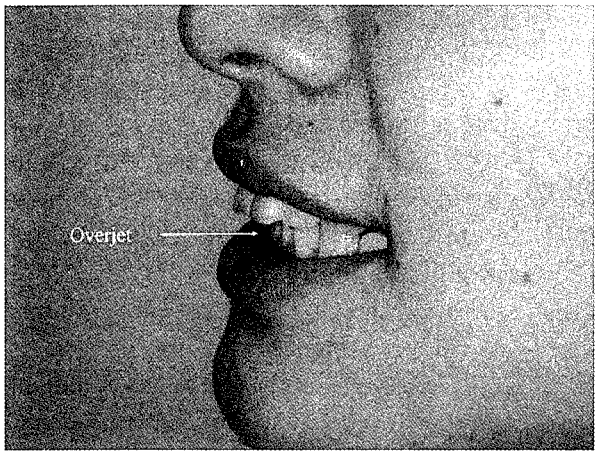

Figure 1a. A lateral view of the jaw demonstrates a over 3mm overjet. Overjet is seen when the maxilla expand forward compared with the mandible.

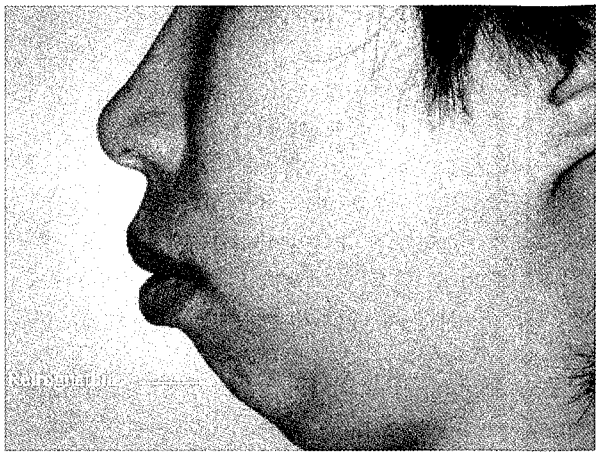

Figure 1b. A lateral view of the entire face demonstrates retrognathia. Retrognathia exists when that the position of the gnathion is posteriorly displaced compared with the nasion.

tongue remained in the mouth in a relaxed position. The posterior pharynx was directly visualized with the aid of a penlight and tongue blade. Phonation was initiated only to assess the full size of the uvula, soft palate, and lateral peritonsillar tissue, when not fully visible without phonation. Tonsillar enlargement was defined as the presence of a lateral impingement greater than 50% of the posterior pharyngeal airspace (clinical grade 2+ or greater). The uvula was considered enlarged if it was more than 1.5cm in length or greater than 1.0cm in width. Lateral peritonsillar narrowing was defined as impingement, greater than 25%, of the pharyngeal space by the peritonsillar tissues, excluding the tonsils, which were evaluated independently as described above. Overjet was defined as the distance greater than 3mm, between the upper and lower incisors during occlusion (Figure 1a). Retrognathia was defined as a retroposition of the gnathion (the most inferior point in the contour of the chin) greater than 0.5cm relative to the plane of the nasion (the deepest point of the superior aspect of the nasal bone) and the subspinal (the deepest point on the pre-maxillary outer contour) (Figure 1b).

Cephalometry

Cephalometric radiographs were obtained according to the methods described previously [14-15]. The distance from the focus to the median plane of the head was 150 cm, while the distance from the median plane of the head to the film was kept at 14 cm, in all cases. The patients were in a sitting natural head posture at the end-expiration phase, and did not swallow. No corrections were made for linear enlargement. One experienced operator measured the cephalography twice, at an interval of several days. Discrepancies less than one degree or one millimeter were kept for this study. The cephalometric parameters included soft tissue, airway size, and hyoid bone position variables. The soft tissue variables were measured as follows: the length of the soft palate (Spl) from the posterior nasal spine of the maxilla to the lower edge of the uvula; the soft palate width (Spw); the tongue length (Tl) measured from the lowest part of the epiglottis to the tip of the tongue; and the tongue width (Tw). Upper airway size was defined as the superior (SPAS) and inferior (IPAS) posterior airway space measured, respectively, as the shortest distance from the posterior pharyngeal wall to the posterior soft palate (SPAS) and to the dorsum of the tongue (IPAS). Hyoid position variables included the distance of the hyoid bone to the posterior pharyngeal wall (H-Ph); the distance of the hyoid bone to the mandibular plane

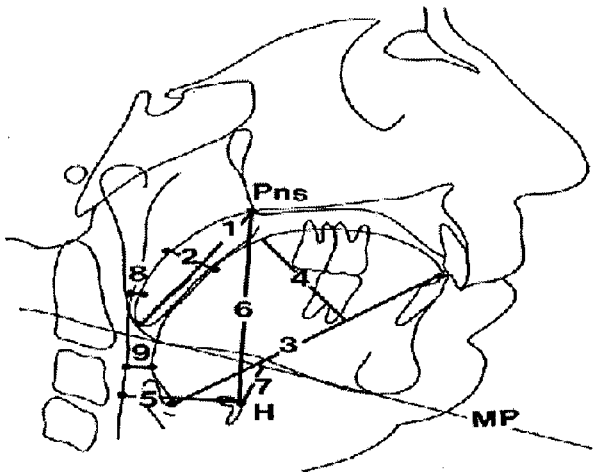

Figure 2a. Cephalometric landmarks, soft tissue, airway size variables, and the hyoid position in the study. Landmarks: H, hyoid bone; MP, mandibular plane; Pns, posterior nasal spine. Variables: 1] Spl, the length of thesoft palate; 2] Spw, the width of the soft palate; 3] Tl, the length of the tongue; 4] Tw, the width of the tongue; 5] H-Ph, the distance from the hyoid bone to the posterior wall of the pharynx; 6] H-Pns, the distance from the hyoid bone to the Pns; 7] H-MP, the distance from the hyoid bone to the mandibular plane; 8] SPAS, the upper posterior pharyngeal space; 9] IPAS, the upper posterior pharyngeal space.

(H-MP); and the distance of the hyoid bone to the posterior nasal spine (H-Pns) (Figure 2).

Polysomnographic study

A one-night polysomnography (Embla, Flaga hf, Iceland) for one night was performed with all patients. During the polygraphic recording, the monitored variables included central, occipital, and frontal electroencephalograms, electro-oculograms, chin electromyogram, electrocardiogram, and chest and abdominal wall motion tests. Airflow was measured by thermistor, and oxygen saturation by pulse oximeter. Snoring was measured with a microphone attached to the lateral surface of the thyroid cartilage. Sleep was scored using the criteria of Rechtschaffen and Kales [16] for 30-s epochs, and respiratory events were scored using standard criteria. Diagnostic definitions were: (1) apnea, a cessation of airflow for at least 10s; and (2) hypopnea, a greater than 50% reduction in airflow for at least 10 s, associated with a more than 4% fall in oxygen saturation. Only those patients, who had more than 10 episodes of apnea/hypopnea per hour, with at least 80% of the episodes of an obstructive or mixed type, were considered for enrollment in the OSAS group.

Statistical Analysis

A chi-squared test was used to evaluate the influence of the lateral peritonsillar structure, uvula, tonsils, overjet, or retrognathia, as risk factors for OSAS. The relative magnitude of association between individual variables and the likelihood to have AHI>10 were compared by odds ratios (ORs). The precision of the estimated ORs was assessed by 95% confidence intervals (CIs). The association between OSAS and a specific physical finding was considered significant when the lower bound of the 95% CI excluded 1. All the numeric data, such as anthropometric and cephalometric parameters, were presented as means and standard deviation. The Student's T test was used for comparison between the OSAS group and the control group. A separate variance T or pooled T was used depending on the results of the Levene test for equality of variances. A statistical significant difference was considered when the P value was smaller than 0.05. Pearson's correlation coefficient was used to evaluate the relationship between those variables with a significant difference and the AHI score. SPSS software, version 10, was used for all statistical analysis.

Results

The anthropometric variables of the OSAS and control groups are presented in Table 1. The OSAS patients had a higher mean AHI (41.0 ± 20.2, N=20 vs 4.1 ± 3, N=15, P<0.01) than the control group. The neck circumference (NC) (40.8 ± 3.7 cm vs 37.1 ± 5.1 cm, P<0.05) and percentage of males (75 % vs 40 %, P<0.05) in the OSAS group were significantly higher compared with the control subjects (Table 1), whereas these two groups had comparable mean age and BMI.

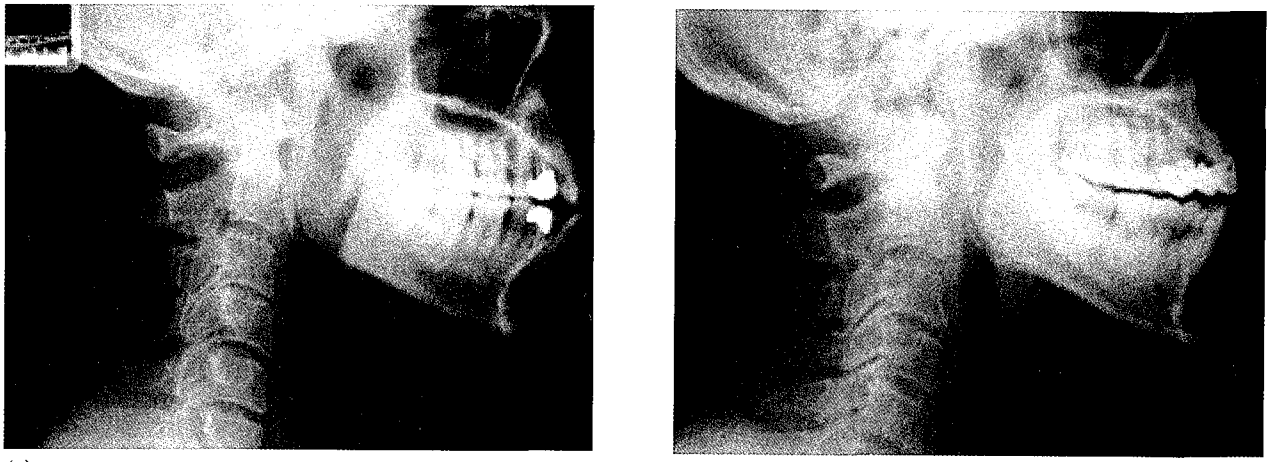

(a) (b)

Figure 2b. Cephalometric radiographies from a normal subject (a) and a patient with OSAS (b). The soft palate length is elongated and the posterior airway space is narrowed in this OSAS patient.

The results of the oropharyngeal physical findings and the craniofacial bony structure are presented in the Table 2. We found that the size of the lateral peritonsillar narrowing, the uvula size, tonsil size, overjet, and retrognathia, were not significantly different between the two groups.

The cephalometric cranial and soft tissue parameters are presented in Table 3. A significant difference between the two groups was observed in the soft palate length (SPL) (42.9 ± 9.0 mm vs 37.6 ± 3.9 mm, $p<0.05$), and the shortest distance from the soft palate to the posterior wall of the pharynx (SPAS) (5.9 ± 2.6 mm vs 7.9 ± 2.8 mm, $p<0.05$). There was no significant difference between these two groups in terms of soft palate width, tongue width or length, hyoid bone position, or inferior posterior airway space.

Figure 3 presents the correlation coefficients between NC, SPL and SPAS, and AHI, respectively. NC was found to be highly correlated with AHI ($r=0.52$, $p=0.002$). As to cephalometric variables, AHI was strongly associated with SPL ($r=0.55$, $p=0.001$), and moderately associated with SPAS ($r=-0.33$, $p=0.04$).

Discussion

We found that neck circumference, rather than oropharyngeal physical findings, showed a significant difference between the OSAS and control groups. The cephalometric evaluation showed that the length of the soft palate and the shortest distance from the soft palate to the posterior wall of the pharynx (SPAS) were significantly different in these two groups. The relationship between the soft palate length and the shortest distance from the soft palate to the posterior pharyngeal wall, and the severity of OSAS, were found to be moderately to highly correlated. This implied that those who had a longer soft palate and a shorter superior posterior airway space might have more severe OSAS.

OSAS is characterized by recurrent closure of the pharyngeal airway during sleep. It is widely accepted that the patency of the upper airway during sleep is determined by the balance between the negative luminal pressure during inspiration and the upper airway dilating muscle activity. Two hypotheses have been used to explain the tendency toward collapsibility in OSAS patients. One is the neural mechanism, in which the peak phasic and tonic airway dilating muscle activities are mediated by continuous chemical or physical stimulation during wakefulness, e.g., a change of upper airway pressure. The loss of wakeful stimulation and the generation of greater luminal

Table 2 Chi-Squared , Or, And 95% Ci Between Morphometric Variables And Osas

Structure	OSAS(AHI>10) (n=20)	CONTROL(AHI<10) (n=15)	OR	95% CI		P Value
				Lower	Upper	
Lateral narrowing						
Present	16	9	2.67	0.59	12.02	0.266
Absent	4	6				
Tonsils enlarged						
Present	7	4	1.48	0.34	6.43	0.721
Absent	13	11				
Uvula enlarged						
Present	4	0				0.119
Absent	16	15				
Retrognathia						
Present	7	3	2.15	0.45	10.29	0.458
Absent	13	12				
Overjet						
Present	8	4	1.83	0.34	7.84	0.489
Absent	12	11				

Definition of abbreviations. CI=Confidence interval; OR=odds ratio; OSAS=Obstructive sleep apnea syndrome

Table 3 Clinical And Cephalometric Data Of Osas And Control Patients

Measurement	OSAS(AHI>10)(n=20)		CONTROL(AHI<10)(n=15)		P Value
	Mean	SD	Mean	SD	
AHI,events per hour	41	20.2	4.1	3	<0.01
Age,yr	55.9	13.4	49.9	11.8	N
Spl,mm	42.9	9	37.6	3.9	0.048
Spw,mm	10.2	2.7	9.9	2.4	N
Tl,mm	81	9.4	77.9	5.4	N
Tw,mm	36.7	4.8	36.1	5.2	N
H-MP,mm	14.7	4.3	11.2	6.7	N
H-Pns,mm	69.8	7.9	65.8	8.8	N
H-Ph,mm	32.6	5.5	32.6	3.4	N
SPAS,mm	5.9	2.6	7.9	2.8	0.039
IPAS,mm	11.8	2.4	10.4	2.4	N

Definition of abbreviations. AHI=apnea-hyponea index; H-MP=distance of the hyoid bone to the mandibular plane; H-Pns=distance of hyoid bone to the posterior nasal spine; IPAS=inferior posterior airway space; H-Ph=shortest distance of the hyoid bone to the posterior pharyngeal wall; N=no significant; OSAS=Obstructive sleep apnea syndrome; SPAS=superior posterior airway space; SPl=lengh of the soft palate; Spw=soft palate width; Tl=tongue length; Tw=tongue width.

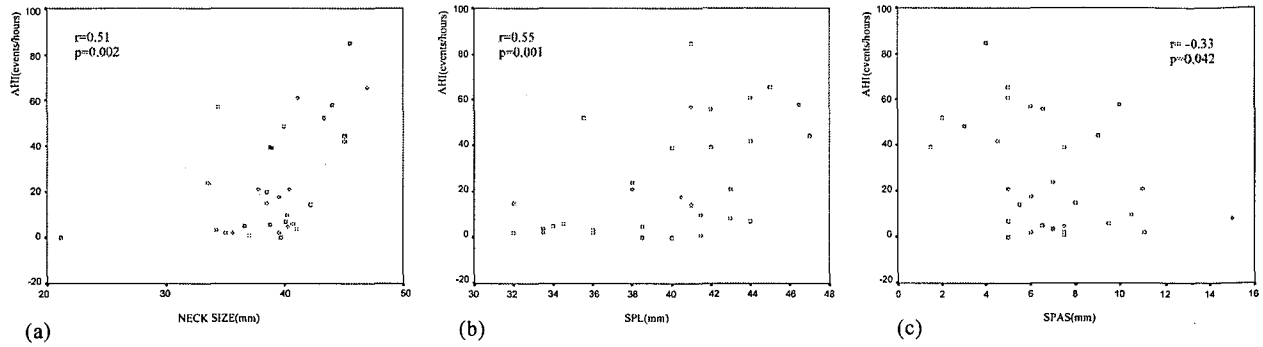

Figure 3. Correlation between AHI and BMI (a), Spl (b), and SPAS (c) in all patients. Pearson's correlation coefficient was used to evaluate the relationship between those variables and the AHI score. AHI=apnea-hypopnea index; BMI=Body mass index; Spl=Length of the soft palate; SPAS=Shortest distance from the posterior pharyngeal wall to the posterior soft palate

pressure without activating the dilator muscle will increase the airway collapsibility. The second is the anatomic theory indicating that maintenance of oropharyngeal patency is determined by the area of the oropharyngeal cross-section. Anatomic factors, such as neck soft tissue mass, parapharyngeal fat, and craniofacial bony structure, are likely to be important determinants in OSAS. Upper airway patency might not be able to be maintained during sleep if the pharyngeal luminal cross-section becomes too narrow for the dilator muscle to counteract in inspiration. The more narrow the pharyngeal airway, the more the increase of compliance, which has been found in OSAS patients [17]. The relationship between the pharyngeal cross-sectional area and the transmural pressure is curvilinear,implying that a stiff pharynx will become more collapsible as it narrows. In addition, certain anatomic anomalies, such as in those with an enlarged uvula [18] or in micrognathic infants [19], may increase the collapsibility of upper airway due to their high closing pressure. Taken together, it is reasonable to assume that particular features of the craniofacial bony and soft tissue structure might increase pharyngeal collapsibility, and that these differences will be significant between OSAS and control groups.

The significantly elongated soft palate and the short distance of the soft palate to the posterior pharyngeal wall in OSAS patients have been postulated as the consequence of long-term vibration trauma and high negative pressure [20]. The widening of the soft palate is due to repeated stretching, and its thickening is caused by prolonged edema [20]. A previous study showed that the elongated soft palate contributed to upper airway collapsibility [12], which is consistent with our observation. Uvuopalatopharyngoplasty is widely used as a first-step procedure for the surgical correction of obstructive sleep apnea, but the benefit is small [21]. This suggests that the change in soft palate length and the superior posterior airway space patency in OSAS might be a result of breathing against increased upper airway resistance rather than a cause of the increased resistance. In this study, the shorter the superior posterior airway space the more severe the OSAS, but this parameter seems not to be important in the Caucasian study [12]. A lower hyoid bone position is associated with OSAS in the Caucasian study [12], but this factor was not critical in our observation. As such, there might be some anatomic difference between Western and Eastern people in the cephalometric evaluation of the pathophysiology of OSAS..

We found that the OSAS group had a significantly high percentage of males and also an increased neck size compared with the non-OSAS controls. These results are similar to previous observations [22]. Men are predisposed to OSAS presumably because androgens distribute body fat

deposition centrally, particularly in the neck area. The influences of obesity and gender in developing OSAS vary by age, being stronger among middle-aged people. This is probably associated with the actions of sex hormones before and after puberty. Apart from this, sex hormones may modulate upper airway and respiratory muscle activities, to some extent. Neck circumference was thought to be a more useful predictor than general obesity [23]. Our data is consistent with this result and the correlation between neck circumference and AHI was highly significant. Expanded neck circumference not only increases fat deposition but also increases muscle mass in the neck [9], which will advance extraluminal pressure and promote obstruction of the upper airway. The BMI of the two groups was not significantly different; this result varied from the Caucasian studies, indicating that the mechanisms governing OSAS might differ between Western and Eastern people.

Some limitations in this study need to be addressed. First, we evaluated these patients and took cephalometry during wakefulness in the sitting position, which might not reflect the pathophysiology during sleep. Not only were the patients not in a supine position, but the sleeping stimulation of the pharyngeal muscle was removed. Second, the physical examination and cephalometry provide two-dimensional parameters of the skeletal and soft tissue structures, but not volumetric data. However, the aim of this study was to use a physical examination and skull plain film to identify those who were at risk for OSAS on an outpatient basis. The evaluation of soft tissue and skeletal structures during sleep are not as convenient to do as a routine assessment of patients in the clinic. Third, the percentage of males was significantly higher in the OSAS group in this study. We were not able to exclude the influence of gender on anthropometry and cephalometry in this study. A further study will be planned to investigate the influence of gender on cephalometry and neck size.

In summary, the soft tissue structural characteristic of the pharynx and neck size were important determinants of OSAS in this study. Soft palate length and the superior posterior airway space were shown to be involved in the pathogenesis of this syndrome. Patients with obstructive sleep disorder and an elongated soft palate and smaller superior posterior airway space are at risk for the development of OSAS. Cephalometric radiography and neck size measurement provide an easy way to identify patients at risk for OSAS and plan for their further management.

References

1. Young T, Palta M, Badr S, et al. The occurrence of sleep-disordered breathing among middle-aged adults. N Engl J Med 1993;328:1230-5.
2. He J, Kryger MH, Roth T, et al. Mortality and apnea index in obstructive sleep apnea: experience in 385 male patients. Chest 1988;94:9-14.
3. Partinen M, Jamieson A, Guilleminault C. Long-term outcome for obstructive sleep apnea syndrome patients: mortality. Chest 1988;94:1200-4.
4. Yamashiro Y, Kryger MH. Why should sleep apnea be diagnosed and treated? Clin Pulm Med 1994;1:250-9.
5. Rosen RC, Rosekind M, Dement WC, et al. Physician education in sleep and sleep disorders: a national survey of U.S. medical schools. Sleep 1993;16:249-54.
6. Hudgel DW. Mechanisms of obstructive sleep apnea. Chest 1992;101:541-9.
7. Bonsignore MR, Marrone O, Bonsignore G et al. The cardiovascular effects of obstructive sleep apnoeas: analysis of pathogenic mechanisms. Eur Respir J 1994;7:786-805.
8. Shepard JW Jr, Thawley SE. Localization of upper airway collapse during sleep in patients with obstructive sleep apnea. Am Rev Respir Dis 1990;141:1350-5.
9. Schwab R, Gupta K, Pack A. et al. Upper airway and soft tissue anatomy in normal subjects and patients with sleep-disordered breathing: significance of the lateral pharyngeal walls. Am J Respir Crit Care Med 1995;152: 1673-89.
10. Rivlin J, Hoffstein V, Bryan A. et al. Upper airway morphology in patients with idiopathic obstructive sleep apnea. Am Rev Respir Dis 1984;134: 355-60.

11. Partinen M, Guilleminault C, Jamieson A. et al. Obstructive sleep apnea and cephalometric roentgenograms: the role of anatomic upper airway abnormalities in the definition of abnormal breathing during sleep. Chest 1988;93: 1199-205.
12. Sforza E, Bacon W, Krieger J. et al. Upper airway collapsibility and cephalometric variables in patient with obstructive sleep apnea. Am J Respir Crit Care Med 2000;161:347-52.
13. Schellenberg JB, Greg M, Schwab RJ. Physical findings and the risk for obstructive sleep apnea. Am J Respir Crit Care Med 2000;162:740-8.
14. Bacon WH, Turlot JC, Stierle JL, et al. Cephalometric evaluation of pharyngeal obstructive factors in patients with sleep apnea syndrome. Angle Orthod 1989;60: 115-21 .
15. Bacon WH, Krieger J, Stierle JL, et al. Craniofacial characteristics in patients with obstructive sleep apneas syndrome. Cleft Palate J 1988;25: 374-378.
16. Rechtschaffen A, and Kales A. 1968. A Manual of Standardized Terminology: Techniques and Scoring System for Sleep Stages of Human Subjects. Brain Information Service/Brain Research Institute, UCLA, Los Angeles. NIH Publication No. 204.
17. Brown IG, Bradley TD, Hoffstein V, et al. Pharyngeal compliance in snoring subjects with and without obstructive sleep apnea. Am Rev Respir Dis 1985;132: 211-15.
18. Morrison DL, Launois SH, Remmers JE, et al. Pharyngeal narrowing and closing pressure in patients with obstructive sleep apnea. Am Rev Respir Dis 1993;148: 606-11.
19. Roberts JL, Reed WR, Thach BT, et al. Assessment of pharyngeal airway stability in normal and micrognathic infants. J Appl Physiol 1985;58: 290-9.
20. Woodson BT, Garancis JC, Toohill RJ. Histopathologic changes in snoring and obstructive sleep apnea syndrome. Laryngoscope 1991;101:1318-22.
21. Senior BA, Rosenthal L, Day R, et al. Efficacy of uvulopalatopharyngoplasty in unselected patients with mild obstructive sleep apnea. Otolaryngol Head Neck Surg 2000;123(3):179-82.
22. Davies RJO, Stradling JR. The epidemiology of sleep apnea. Thorax 1996;51(Suppl. 2):S65-S70.
23. Davies RJ, Ali NJ, Stradling JR. Neck circumference and other clinical features in the diagnosis of the obstructive sleep apnoea syndrome. Thorax 1992;41(2):101-5.

阻塞性睡眠窒息症候群(OSAS)在理學檢查及頭顱X光危險因子的表現－初步報告

羅友倫　李岡遠　蕭世欣　楊朝凱　劉育志　郭漢彬

阻塞性睡眠窒息症候群(OSAS)導因於睡眠時上呼吸道重複阻塞所致，是一個嚴重的大眾健康問題，主要影響 2~4%的中年族群。阻塞性睡眠窒息症候群(OSAS)的嚴重度及臨床表現差異極大，可透過心肺呼吸衰竭表現，亦可以精神意識不正常表現。咽部呼吸道的塌陷增加及結構上的異常被認為與阻塞性睡眠窒息症候群(OSAS)的病理機轉有關，為了正確了解阻塞性睡眠窒息症候群(OSAS)病人理學檢查及結構型態上的特殊差異，本研究比較二十個阻塞性睡眠窒息症候群(OSAS)病人及十五個對照組病人有關理學檢查及頭顱 X 光的差異。研究結果顯示二組病人間性別、頸圍、軟顎長度及後上呼吸道空間有明顯差異；理學檢查部分，有關側咽壁狹窄與否、扁桃腺大小、懸垂雍大小、咬合不正(Overjet)、縮下巴與否(Retrognathia)，則二組病人間無明顯差異，研究結果認為男性、頸圍較長、軟顎較長及後上呼吸道空間狹窄的病人，易得到阻塞性睡眠窒息症候群(OSAS)。 ***(胸腔醫學 2001; 16: 102-111)***

關鍵詞：阻塞性睡眠窒息症候群，頭顱測量

林口長庚紀念醫院　胸腔二科
索取抽印本請聯絡：羅友倫醫師，桃園縣龜山鄉復興街五號

Unilateral Gynecomastia and Lung Cancer— A Case Report

Jen-Feng Liu, Shi-Chuan Chang

Gynecomastia is a common condition found in different age groups. It can be caused by puberty, hormonal imbalance, liver disease, renal disease, medication, genetic factors, and even malignancy. Unilateral gynecomastia in elderly males might alert us to the possibility of underlying carcinoma. We report a case of unilateral left gynecomastia in a 73-year-old man who was later found to have lung cancer in the upper right lobe. After excluding other possible causes, we speculated that gynecomastia is highly related to primary lung cancer. Gynecomastia may be the only early sign of some life-threatening disease, especially breast cancer, lung cancer, and gonadotropin-releasing malignancies. Though gynecomastia is not uncommon in normal elderly males, we can not overlook it if it appears unilaterally. To avoid overshooting, taking a careful history of medications and other systemic disease is important, as is a precise physical examination. ***(Thorac Med 2001; 16: 112-118)***

Keywords: gynecomastia, lung cancer, calcium-channel blocker

Introduction

Gynecomastia has been a diagnostic dilemma for middle-aged males since it has been linked to a long list of conditions. Some are daunting, but most are not. One study reported that 36% of 306 asymptomatic, healthy individuals, aged 17-58 years, had gynecomastia, and its incidence increased with age: 57% of the 28 men between 45 and 59 years had gynecomastia [1]. The gynecomastia in the above study was bilateral in all but seven cases. By and large, bilateral gynecomastia is not uncommon as a normal physical finding, especially in elderly males. Unilateral breast enlargement, however, is quite another. Although the unilateral phenomenon may be only a transient stage to bilateral gynecomastia, certain studies imply that multiple factors may contribute to this phenomenon, including drugs [2-3], malignancies [4-5], trauma [6-7], and idiopathy. Gynecomastia is reported to be associated with a variety of carcinomas, and its relationship to lung cancer has received special attention [4-5]. Herein, we present a patient with both adenocarcinoma of the lung and unilateral gynecomastia.

Case report

A 73 year-old married veteran was admitted for hemoptysis which had recently exacerbated. He had suffered pulmonary tuberculosis infection about 40 years ago, and had received complete anti-tuberculosis treatment. Bronchiectasis was diagnosed based on the clinical features and results of chest imaging studies in the early 1990s; thereafter, hemoptysis was noted intermittently. He also had paroxysmal atrial fibrillation with

Chest Department, Taipei Veterans General Hospital, Taipei, Taiwan
Address reprint requests to: Dr. Shi-Chuan Chang, 201, Sec 2, Shih-Pai Road, Taipei, Taiwan 112.

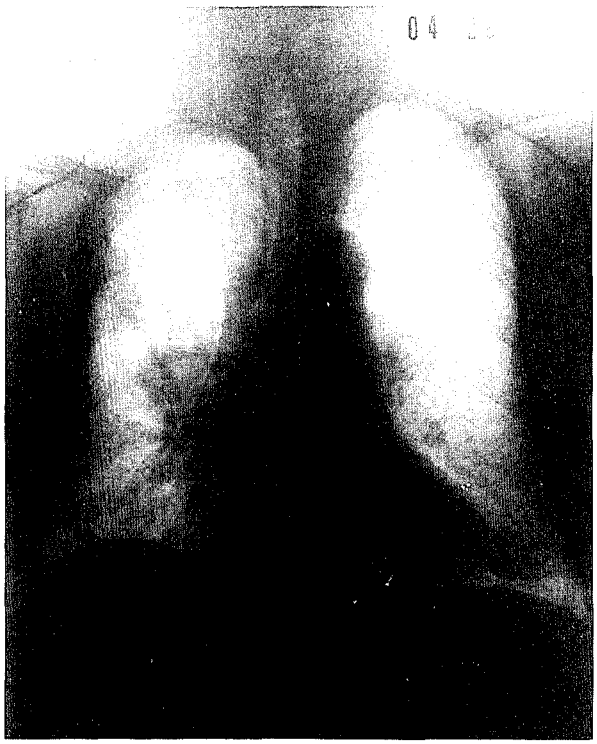

Fig 1. Chest radiograph obtained in 2000 shows a lung tumor in the upper right lung, and a left breast shadow

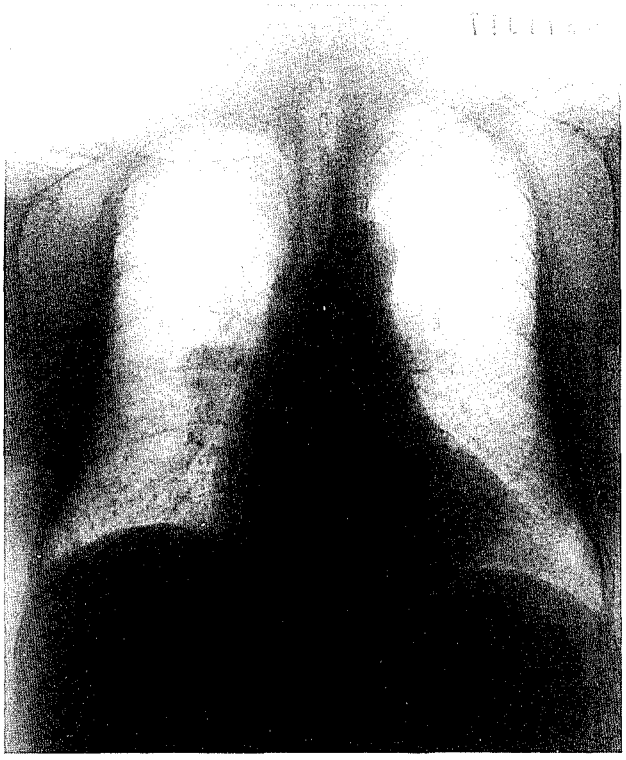

Fig 2. Chest radiograph obtained in 1997 does not show a left breast shadow

medication control. He was issued a mucolytic agent and a calcium channel blocker (slow-releasing diltiazem) at our outpatient clinic. Unfortunately, the hemoptysis had increased in amount and frequency within the recent 6 months, as had his right chest pain. The chest radiograph disclosed newly-developed opacity in the upper right lung field, and the patient was admitted with a suspected lung neoplasm.

On physical examination, he was a well-developed, well-nourished male, and not ill-looking. Bilateral lower lung field crackles were noted on auscultation. Incidentally, we noticed a left breast enlargement in the subareolar area without tenderness, about 4x5cm in size, and without fixation to the skin or discharge from the nipple. The patient was not aware of its existence. The thyroid gland seemed normal on palpation, as were the testes and penis on inspection. The chest radiograph showed a prominent left breast shadow (figure 1), which had not been found on the chest X- ray films taken before 1997 (figure 2). Computerized tomography of the chest also revealed an irregular 4cm-sized soft tissue mass in the upper right lung (figure 3). In addition, prominent subcutaneous soft tissue, which was compatible with gynecomastia, was noted in the left anterior chest wall. Both of the above findings were absent in the chest CT done in 1997 (figure 3). Adenocarcinoma of the lung was proven by a sono-guided biopsy of the mass in the upper right lobe. Because the cancer had metastasized to the right 3rd rib, as evidenced by bone scan, he began receiving chemotherapy.

We checked the hormone levels in relation to breast development. Estradiol was 33.81 pg/ml (reference level: < 80 pg/ml); testosterone was 2.04 ng/ml (reference level: 2.36-9.96 ng/ml); LH was 10.03 mIU/ml (reference level: 0.6-12 mIU/ml); HCG was 0.78mIU/ml (reference level: <10 mIU/ml); and FSH was 12.74 mIU/ml (reference level: 1-8 mIU/ml). His medication history showed that he had received diltiazem irregularly, since early 1990 at our cardiovascular

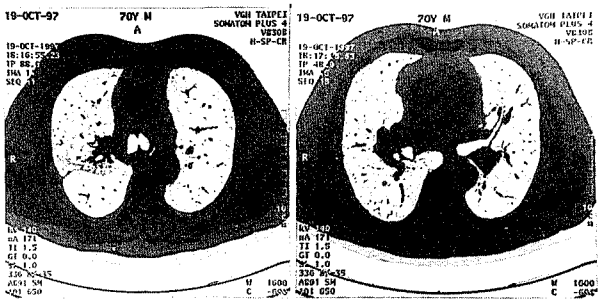

Fig. 3-1

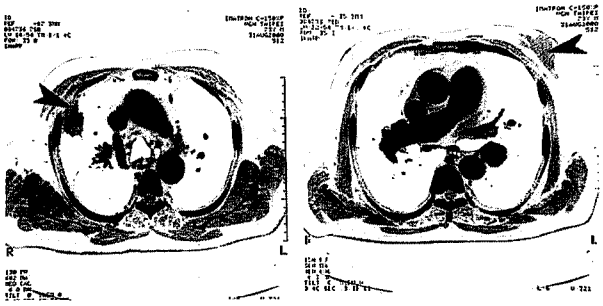

Fig. 3-2

Fig 3. Computed tomography obtained in 1997 (Figs.3-1) and 2000 (Figs. 3-2) of the same levels. Prominent left breast glandular tissue and an upper right lung tumor, which were absent in the 1997 images, are noted in the CT images taken in 2000.

clinic, for paroxysmal atrial fibrillation. He began taking the drug regularly at monthly intervals since early 1997, a week after he had undergone chest CT. The patient had no evidence of thyroid diseases.

The patient underwent chemotherapy for advanced lung cancer. Unfortunately, he succumbed to severe septic shock after 3 cycles of chemotherapy, about 1 month after diagnosis.

Discussion

Gynecomastia, a benign enlargement of the male breast due to a proliferation of the glandular component, is a common clinical condition. Three distinct age-related peaks are readily discerned: the neonatal period, the pubertal period, and the adult period [8-9]. The highest prevalence in the adult period was found to be between 50 and 80 years of age. Braunstein [8] reviewed 6 articles on the prevalence of gynecomastia. With different diagnostic methods, the prevalence varied from 32% to 65%. Considering the high prevalence rate, it is not surprising that it may coexist with an array of disorders without clear causal relation. So, finding out which one is really clinically important requires some sophistication. Table 1 summarizes the conditions that have a well-documented association with clinically important gynecomastia.

Some gynecomastias appear to be due to a change in the estrogen-to-androgen ratio, such that there is an absolute or relative increase in the estrogen. Some believe that the physiological gynecomastia, which emerges with age, results from varying degrees of testicular failure. Our patient had no sign of testicular atrophy, and no evidence for primary or secondary hypogonadism. The blood FSH level was slightly elevated, but the LH value was not. The testosterone was slightly depressed, but the estradiol was normal. HCG was also within the normal limit. Hyperthyroidism increases sex hormone-binding globulin, and leads to a greater increase in free estrogen than free testosterone. The peripheral conversion of androstenedione to estrogen is also increased in hyperthyroidism. However, this was unlikely in our patient because of his lack of clinical features suggesting of hyperthyroidism. There was no evidence of renal failure, liver cirrhosis, or alcoholism.

Bannayan and Hajdu indicated that pubertal and hormone-induced gynecomastia tended to be diffuse and bilateral, while nonhormonal enlargements were usually unilateral and discrete [11]. Sbar [4] demonstrated the unilaterality of gynecomastia in diseases of the chest, especially carcinoma of the lung and renal cells. Even when the gynecomastia is bilateral, it usually appears first and seems larger on the ipsilateral side. These findings imply that local factors, such as neurovascular reflexes, may be important.

Some reports have attributed gynecomastia to chest trauma or thoracotomy. Field et al [6] described a patient who developed right gynecomastia after removing a cancer from the upper right lobe. After excluding other possible

Table 1. Conditions associated with gynecomastia

Physiologic
Neonatal
Pubertal
Involutional
Pathologic
Neoplasms
Testicular (germ cell, leydig cell, or sertoli cell)
Adrenal (adenoma or carcinoma)
Ectopic production of human chorionic gonadotropin
Other carcinomas (especially lung, colon)
Hypogonadism
Enzymatic defects of testosterone production
Liver disease
Renal disease and dialysis
Starvation, especially during the recovery phase
Hyperthyroidism
Drugs (table 2)
Idiopathic gynecomastia

causes, they attributed it to thoracotomy. Camiel et al [7] described 3 other patients who developed gynecomastia on the ipsilateral side of a thoracotomy about 3-6 weeks after operation. They reported it is quite possible that involvement of the thoracic nerves secondary to a surgical incision is an important factor. Obviously, our patient had not undergone a previous thoracotomy.

Many different drugs were reported to be related to gynecomastia (Table 2) [8-9]. Ketoconazole and spironolactone have been shown to decrease testosterone synthesis and to interfere with testosterone binding to target cell receptors. Cimetidine has a weak antiandrogenic activity. It also blocks the binding of androgen to androgen receptors, which normally suppresses the growth of breast tissue. Digoxin could be responsible because of its structural homology with estrogen. Incidental exposure to estrogen, e.g., through percutaneous absorption from anti-balding creams, or from a partner's estrogen-containing vaginal creams, may also occur. These above are accepted to have a strong relationship with gynecomastia.

What attracts our attention is the relationship between calcium-channel blockers and gynecomastia, though its relationship was established on the basis of challenge–rechallenge studies on individuals or small groups of patients. Tanner et al [3] reported 30 patients with gynecomastia during the treatment with calcium-channel blockers, out of 48 million prescriptions. Of these 30 patients, 11 were treated with nifedipine, 18 with verapamil, and 1 with diltiazem. The pathogenesis is still unknown and no hormonal abnormality was noted. Some of the cases had unilateral gynecomastia. Otto et al [2] presented another case, whose left gynecomastia developed 9 months after diltiazem (360mg/d) usage. It resolved a few weeks after dose-reduction (180mg/d). Our patient had received irregular medication with diltiazem since 1990, to control against atrial fibrillation-related tachycardia. The prescription became regular with slow-releasing diltiazem 90mg per day, beginning in 1997. We can not exclude the possibility that his left gynecomastia might be related to the diltiazem. But the probability, however, is less than that of lung cancer, based on the time sequence and the dose of diltiazem. The only way to prove this would be to observe changes in the breast after discontinuing the drug.

Gynecomastia has been described in patients with all types of lung carcinoma. The first convincing evidence came in 1941, when the gynecomastia of 3 patients with lung cancer disappeared after radiotherapy. Thereafter, numerous clinical reports supported the relationship. Most of the 80 patients with gynecomastia and lung disease reported by Sbar [4] had primary lung cancer. Thirty-four patients had unilateral gynecomastia which was found on the ipsilateral side of the disease. Some anaplastic large-cell lung cancer may secrete gonadotropin [5], but most lung cancer patients do not have hormonal abnormalities. Some believe gynecomastia is one of the paraneoplastic signs of lung cancer. Our patient's gynecomastia was on

Table 2. Drugs implicated as causing gynecomastia

Category	Drug
Hormones	Androgens and anabolic steroids
	Estrogens and estrogen agonists
Antibiotics	Isoniazid
	Ketoconazole
	Metronidazole
Antiulcer drugs	Cimetidine
	Omerprazole
	Ranitidine
Cardiovascular drugs	Amiodarone
	Captopril
	Digitoxin
	Enalapril
	Nifedipine
	Verapamil
	Diltiazem
Psychoactive agents	Diazepam
	Haloperidol
	Tricyclic antidepressants
Drugs of abuse	Alcohol
	Heroin
	Amphetamines
	Marijuana
Other	Phenytoin
	Penicillamine

the left side, though, opposite to the lung cancer. Based on the time sequence and the exclusion of other causes, the gynecomastia might have been related to the lung cancer and may be the only early sign of underlying malignancy.

Since gynecomastia is common in men, the mere presence of non-tender, palpable breast tissue on a routine examination should not lead to an extensive laboratory evaluation. In most instances, the taking of a careful history pertaining to the use of drugs and alcohol, with specific questions about symptoms related to hepatic dysfunction, testicular insufficiency (decreased libido or impotence), pulmonary symptoms suggestive of lung cancer, and hyperthyroidism is sufficient to uncover most of the conditions associated with gynecomastia. If no abnormalities are found on physical examination or after the assessment of hepatic, renal, and thyroid function by blood biochemistries, further specific evaluation is unlikely to be useful. The patient should be reexamined in six months [8].

In conclusion, we presented a patient who had right side lung cancer and left-side gynecomastia. Though we could not prove the direct relationship between the two, lung cancer is most likely the cause of this unilateral gynecomastia by exclusion of other possible causes. Gynecomastia is a common finding in normal elderly males, but we shouldn't neglect it when it emerged unilaterally. It might be the only early sign of some life-threatening diseases. To avoid overshooting, taking a careful history of medications and other systemic disease is important, as is a precise physical examination.

Reference

1. Nuttall FQ. Gynecomastia as a physical finding in normal men. J Clin Endocrinol Metab 1979; 48: 338-40.
2. Otto C, Richter WO. Unilateral gynecomastia induced by treatment with diltiazem. Arch Intern Med 1994; 154: 351.
3. Tanner LA, Bosco LA. Gynecomastia associated with calcium channel blocker therapy. Arch Intern Med 1988; 148: 379-80.
4. Sbar S. Unilateral gynecomastia. N Eng J Med 1972; 286: 1367-8.
5. Fusco FD, Rosen SW. Gonadotropin-rpoducing anaplastic large-cell carcinoma of the lung. N Eng J Med 1966; 275: 507-15.
6. Field JB, Solis RT, Dear WE. Unilaeral gynecomastia associated with thoracotomy following resection of carcinoma of lung: case report. Am J Med Sci 1989; 298: 402-6.
7. Camiel MR, Benninghoff DL, Alexander LL. Gynecomastia after incision on the thoracic cage. Ann Thorac Surg 1968; 5: 42-6.
8. Braunstein GD. Gynecomastia. N Eng J Med 1993; 328: 490-5.
9. Leung AK. Gynecomastia. Am Fam Physician 1989;

39:215-22.
10. Carlson HE. Gynecomastia. N Eng J Med 1980; 303: 795-9.
11. Bannayan GA, Hajdu SI. Gynecomastia. Clinicopathologic study of 351 cases. Am J Clin Pathol 1972; 57: 431-7.

單側男性女乳化和肺癌－病例報告

劉人鳳　張西川

男性女乳症在不同年齡的男性都相當常見，可能原因包括新生兒期和青春期的正常生理現象，或是非生理性的荷爾蒙失調，肝腎疾病，藥物副作用，或甚至是癌症的初期表現。在中老年男性出現單側乳房變大，其原因常是病理性的，因此須特別注意。在此提出一例 73 歲男性病人，其左側男性女乳化伴隨右肺肺癌，在排除目前已知的其它因素，並佐以影像學上時間性證明，我們認為肺癌是造成此病患單側男性女乳化最可能的原因。單側男性女乳化對於一些危及生命的疾病也許是唯一的早期病徵，小心的病史，藥物史詢問及高度的臨床警覺性是最重要的。 ***(胸腔醫學 2001; 16: 112-118)***

關鍵詞：男性女乳症，肺癌，鈣離子阻斷劑

台北榮民總醫院　胸腔部
索取抽印本請聯絡：張西川醫師，台北市石牌路二段 201 號

Primary Pulmonary Rhabdomyosarcoma— A Case Report

Chien-Chih Ou*, Tung-Ying Chao, Young-Fa Lai, Sui-Liong Wong, Shun-Chen Huang**

Rhabdomyosarcoma is not an uncommon malignant tumor of the soft tissue, but primary pulmonary rhabdomyosarcoma in adults is rare. We present the case of a 79-year-old man, including clinical symptoms, image pictures, surgical intervention, and detailed pathological studies. Early surgical excision of the tumor appears to be the most effective means of therapy. However, most patients reported in the literature did not survive more than 2 years after diagnosis. ***(Thorac Med 2001; 16: 119-123)***

Keywords: Primary pulmonary rhabdomyosarcoma

Introduction

Rhabdomyosarcomas are not uncommon malignant neoplasms of the soft tissue. The head, neck, extremities, genito-urinary tract, and trunk are the most common primary sites [1]. Although metastatic lesions of the lung are sometimes found, primary pulmonary rhabdomyosarcomas in adults are extremely rare.

The occurrence of rhabdomyosarcomas in the lung parenchyma has been previously described in children and adults [2,3] in the form of case reports without detailed documentation. In this article, we present a case of primary pulmonary rhabdomyosarcoma in an adult, with its clinical, chest radiograph, pathologic, and immunohistochemical features.

Case Report

A 79-year-old man with a 40-year smoking history was admitted to Kaohsiung Chang Gung Memorial Hospital due to a prolonged dry cough and progressive dyspnea for one year. The patient had a history of bilateral forearm skin cancers, and had received operational excision about 2 years ago. The pathology showed squamous cell carcinoma.

In this admission, the physical examination showed a blood pressure of 140/87 mmHg, body temperature of 36.4 °c, pulse rate of 98 beats per minute, and a respiratory rate of 18 breaths per minute. Mild expiratory wheezing of the bilateral lungs, and a decreased breathing sound in the upper left lung fields, were audible. The rest of the physical examination was normal. The laboratory data showed a white blood cell (WBC) count of 9100 / uL, with a normal differential count, hemoglobin of 12.8 g/ dL, and a platelet count of 215000/ uL. Routine serum biochemistry and coagulation profiles were in the normal range. The pulmonary function test showed moderate obstructive ventilatory impairment with no

Department of Internal Medicine*, St. Martin de Porres Hospital, Chia-Yi, Department of Chest Medicine, Department of Pathology**, Chang Gung Memorial Hospital, Kaohsiung
Address reprint requests to: Dr. Tung-Ying Chao, Department of Chest Medicine, Chang Gung Memorial Hospital, Kaohsiung,123, Ta-Pei Road, Niao-Sung Hsiang, Kaohsiung, Taiwan

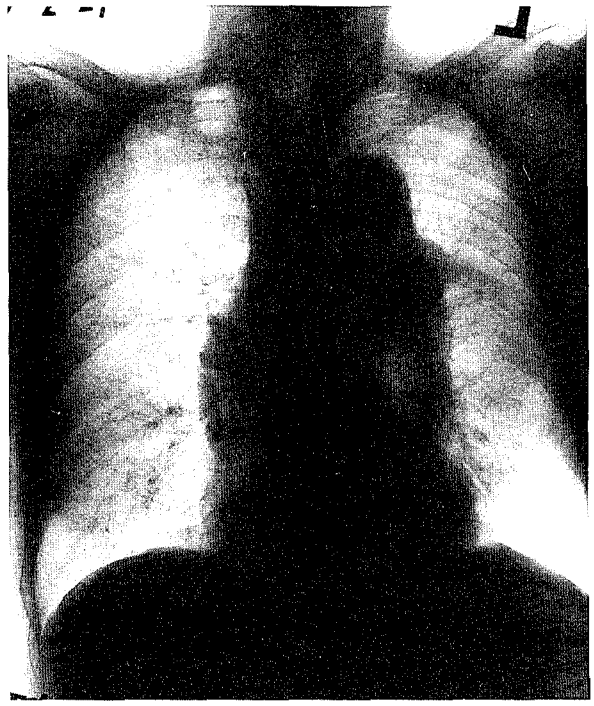

(A)

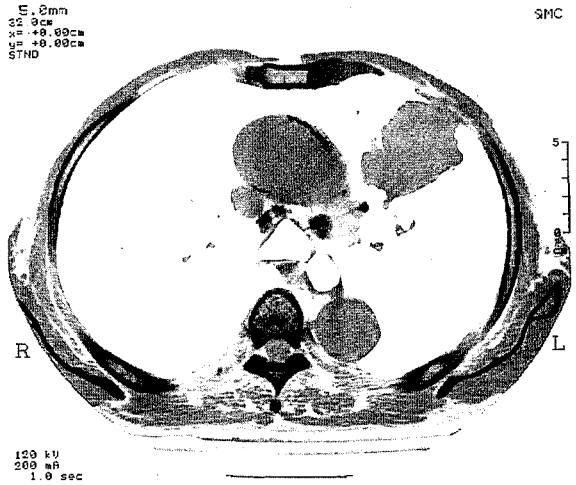

(B)

Fig. 1. (A) Chest X-ray shows an upper left lung mass.
(B) Chest CT shows an upper left lung lobulated mass about 6×5×4 cm.

response to a bronchodilator (forced expiratory volume in one second [FEV1] of 1.16L, forced vital capacity [FVC] of 1.92 L, and FEV1/ FVC of 60,45%).

The chest radiograph revealed an upper left lung mass (fig. 1.A), in an area which had been normal 6 months ago. Computed tomography (CT) of the chest showed a lobulated mass (6×5×4 cm) in the upper left lung (fig.1.B). Bronchoscopy showed an endobronchial tumor at the anterior segment of the upper left lobe, with nearly 80% of the lumen obstructed (fig.2). A biopsy was performed at the same time, and the pathology showed embryonic rhabdomyosarcoma. A bone scan indicated active bone lesions in the right knee joint, probably due to osteoarthritis, rather than malignancy.

An upper left lobe lobectomy and mediastinal lymph nodes dissection were then performed. The specimen measured 13×6×2.2 cm, with a 6-cm well-defined, friable and whitish tumor in the middle section. Light microscopic examination revealed sheets of spindle-shaped, hyperchromatic cells in myxoid or fibrovascular backgrounds (fig.3.A). No evidence of perihilar node involvement or tumor spread beyond the capsule was found. The tumor did not appear to be connected to any surrounding structure. Immunohistochemical studies revealed positive staining for myoglobin, vimentin, and desmin (fig.3.B), and negative staining for S-100 in the tumor cells, which was consistent with rhabdomyoblastic differentiation [4]. After a thorough examination of the patient, no other primary lesion was found. Therefore, the final diagnosis of a primary pulmonary rhabdomyosarcoma was rendered.

The patient was in stable condition after the lobectomy, but suddenly experienced apnea one month later. The EKG showed ventricular fibrillation (Vf), and cardiopulmonary resuscitation (CPR) was performed. Unfortunately, the patient died at home after being discharged in critical condition.

Discussion

Bronchogenic carcinoma was considered

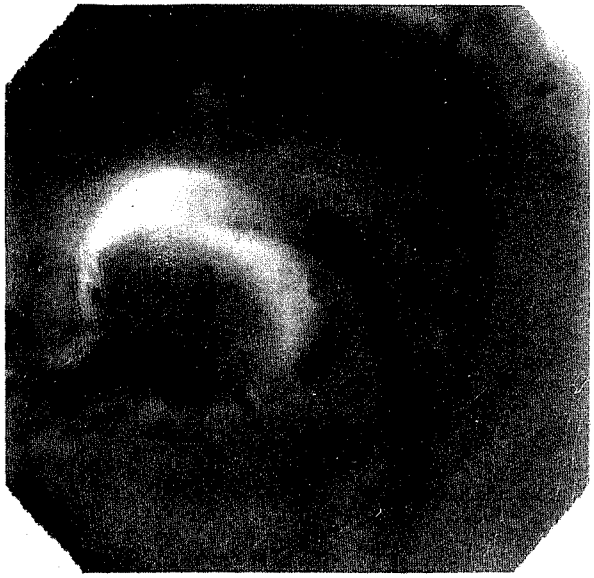

Fig. 2. Bronchoscopy revealed an endobronchial tumor in the anterior segment of the upper left bronchus, with nearly 80% of the lumen obstructed.

first, based on the patient's age, smoking history, and the location of the tumor. But we found that the tumor cell growth rate seemed to be faster than that of lung carcinoma. The tumor became a 6-cm mass within six months. Therefore, other malignancies, such as sarcoma or lymphoma, were also considered.

Primary pulmonary rhabdomyosarcomas are rare pulmonary neoplasms, and the majority occur in the fifth and sixth decades of life [5]. The etiological factors predisposing adults to the development of pulmonary rhabdomyosarcoma are unknown. In children, pulmonary rhabdomyosarcoma can originate within congenital adenomatoid cystic malformations [1]. Rhabdomyosarcomas are classified as embryonic, alveolar, and pleomorphic types. The alveolar subtype was associated with the poorest prognosis [6]. The recurrence and mortality rates are significantly higher for those with the alveolar subtype.

Clinically, primary pulmonary rhabdomyosarcoma is similar to any other pulmonary tumor. The symptoms are related, for the most part, to the location of the tumor within the lung [7]. The tumors usually are large, spherical masses that are located within or between the lobes of the lung. The radiological manifestations are varied, but a rapidly growing soft tissue mass with compression of the adjacent structure is the most common feature. Magnetic resonance imaging (MRI) may be more helpful in diagnosing the presumed site of the primary rhabdomyosarcoma presenting as metastatic disease than computed tomography (CT) [8]. The diagnosis of primary pulmonary rhabdomyosarcoma requires thoracotomy and biopsy for evaluation. Identification frequently relies on histologic findings and immunohistochemical studies. In the excised specimens, packed spindle cells with a hyperchromatic nucleus, ample

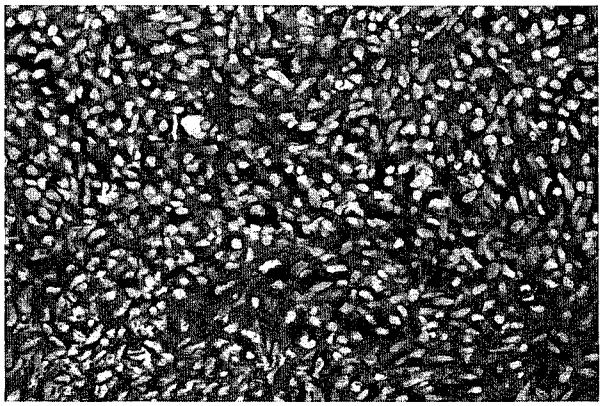

(A)

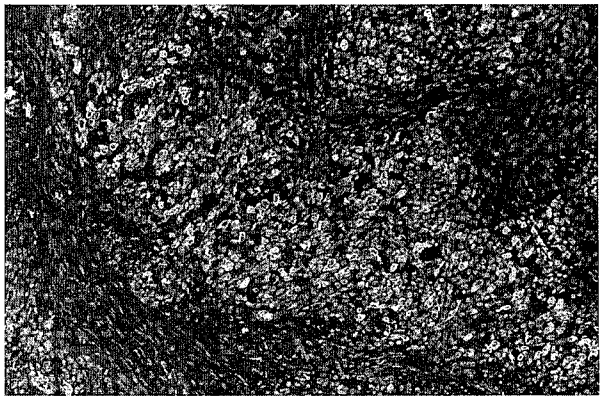

(B)

Fig. 3. (A) The tumor cells were spindle-shaped and hyperchromatic with eosinophilic cytoplasm in a fibromyxoid background. (H & E ×100).

(B) Many tumor cells were strongly positive for Desmin. × 40.

eosinophilic cytoplasm, and the probable presence of striation are virtually diagnostic. However, with a biopsy specimen, a crushing artifact may hinder the diagnosis. Final judgement will rely on the immunohistochemical studies. The tumor cells are usually positive for antibodies against desmin, myoglobin, and vimentin [6], and negative for S-100 and keratin. Adequate sampling of the lesion is necessary to reach a definite diagnosis.

Pulmonary rhabdomyosarcoma has been suggested to arise from the myoblastic differentiation of the primitive mesenchymal cells present in the bronchial walls and pulmonary interstitial tissue. Due to the rare occurrence of primary pulmonary rhabdomyosarcomas, it is important to exclude other primary pulmonary sarcomas or the possibility of a metastases from the bone or soft tissue. Some primary pulmonary neoplasms, such as pulmonary blastoma and carcinosarcoma, may exhibit rhabdomyoblastic differentiation [9]. Therefore, adequate sampling is necessary for diagnosis.

Primary pulmonary rhabdomyosarcomas are considered to be aggressive pulmonary tumors that lead to a fatal outcome in a very short time [7]. Most patients have not survived more than 2 years after diagnosis. One study showed that the mean duration of the tumor from onset to death was about 29.5 months, ranging from 3 to 152 months [10]. Pulmonary rhabdomyosarcoma has shown a tendency to metastasize to unusual organs such as the heart, liver, and small intestine, as has been noted in previously reported cases [7].

The treatment of rhabdomyosarcoma is usually multimodal. The first choice will be surgical excision [11]. Radiotherapy and chemotherapy are effective adjuvant remedies. Chemotherapy with vincristine, actinomycin-D, and cyclophosphamide plays a major therapeutic role following surgical resection [12].

Reference

1. J.J. Murphy, G.K. Blair, G.C. Fraser, et al.: Rhabdomyosarcoma arising within congenital pulmonary cysts: report of three cases. Journal of Pediatric Surgery 1992;27(10): 1364-67.
2. Fordon LZ. Boss H: Primary rhabdomyosarcoma of lung. Cancer 1955;8:588.
3. Forbes GB: Rhabdomyosarcoma of bronchus. J Pathol 70: 427. 1955 Bradford T. Allan, Deborah L. Day, Louis P. Dehner: Primary Pulmonary rhabdomyosarcoma of the lung in children. Cancer 1987; 59: 1005-11.
4. Willian J. Thomas, Harold M. Koenig, F. R. Ellwanger, et al.: Primary pulmonary rhabdomyosarcoma in childhood. Am J Dis Child 1981;135: 469-70.
5. Takuo Noda, Takuji Todani, Yasuhiro Watanabe, et al.: Alveolar rhabdomyosarcoma of the lung in a child. Journal of Pediatric Surgery 1995;30(11): 1607-8.
6. Ronakd M. Przygodzki, Cesar A. Moran, Saul Suster, et al.: Primary rhabdomyosarcomas: A clinicopathologic and immunohistochemical study of three cases. Modern Pathology 1995;8(6): 658-61.
7. Neil M. Rofsky, Nancy B. Genieser, Michael M. Ambrosino, et al.: Diagnosis of occult primary rhabdomyosarcoma by magnetic resonance imaging. New York State J of Medicine 1993;93(2): 142-3.
8. Heckman CJ, Truong LD, Cagle PT, et al.: Pulmonary blastoma with rhabdomyosarcomatous differentiation. Am J Surg Pathol 1988;12:35.
9. Graham Fallon, Medad Schiller, James W. Kilman: Primary rhabdomyosarcoma of the bronchus. The Annals of Thoracic Surgery 1971;12(6): 650-4.
10. Dinesh Chandra Doval, V. Kannan, Rani Acharya, et al: Bronchial embryonal rhabdomyosarcoma - A case report. Acta Oncologica 1994;33(7): 831-3.
11. Shameem Shariff, John A. Thomas, Nithyananda Shetty, et al.: Primary pulmonary rhabdomyosarcoma in a child, with a review of literature. Journal of Surgical Oncology 1988;38: 261-4.

原發性肺橫紋肌肉瘤－病例報告

歐建志* 趙東瀛 賴永發 王瑞隆 黃純真**

橫紋肌肉瘤在軟組織中是並非少見的惡性腫瘤，但是成人原發性肺橫紋肌肉瘤卻是一種罕見的病症。我們在此報告一位患咳嗽、漸進性呼吸困難的 79 歲男性病患。理學檢查顯示兩肺輕度呼氣期喘鳴及左上肺呼吸音減弱。胸部 X 光及電腦斷層顯現出左上肺葉狀腫瘤。經由切片、肺葉切除，再以免疫組織化學染色作顯微檢查，確定為肺橫紋肌肉瘤。早期腫瘤切除是最有效的治療方法，然而、文獻上大部分病例在診斷後的存活率不超過兩年。 ***(胸腔醫學 2001; 16: 119-123)***

關鍵詞：原發性肺橫紋肌肉瘤

嘉義天主教聖馬爾定醫院 內科* 高雄長庚紀念醫院 胸腔內科 病理科**
索取抽印本請聯絡：趙東瀛醫師，高雄縣鳥松鄉大埤路 123 號

Castleman's Disease Presenting with Massive Pleural Effusion—A Case Report

Mao-Chang Su, Young-Fa Lai, Ming-Jang Shieh*

Castleman's disease is an unusual disorder characterized by the abnormal proliferation of B lymphocytes and plasma cells in the lymphoid organs. It is subdivided into three histologic variants: hyaline-vascular, plasma cell, and mixed. Most patients are asymptomatic and found incidentally. Pleural effusion is an uncommon manifestation of Castleman's disease. We report a 23-year-old female with localized Castleman's disease associated with massive pleural effusion. This patient is surviving well and has experienced no recurrence since undergoing a surgical resection of the giant lymph node mass. ***(Thorac Med 2001; 16: 124-128)***

Keywords: Castleman's disease, giant lymph node hyperplasia, pleural effusion

Introduction

Castleman's disease, also known as angiofollicular or giant lymph node hyperplasia, or lymph node hamartoma, was first described by Castleman et al in 1956 [1]. It is subdivided into three histologic variants: hyaline-vascular, plasma cell, and mixed. This disorder is rare, and most cases are asymptomatic and usually confined to a single lymph node group. Pleural effusion is an uncommon manifestation of Castleman's disease [2]. Here, we report a case of localized Castleman's disease presenting with massive pleural effusion.

Case Report

A 23-year-old female, a resident of southern Taiwan, came to our hospital with a complaint of progressive exertional dyspnea for the past 2 weeks. She had also experienced occasional chest pain and dry cough. There was no fever, hemoptysis, or weight loss. The patient was a non-smoker and had no history of contact with tuberculosis or exposure to asbestos or other industrial agents. On examination she was apyrexial and looked well, with a respiratory rate of 28 breaths per minute. There were decreased breathing sounds and dullness to percussion in the left chest. No other abnormality was noticed.

The chest X-ray (fig. 1) confirmed a massive left-sided pleural effusion with a slight mediastinal shift to the right. Blood tests, includeing biochemistry and cell counts, were within normal range. A diagnostic thoracetesis was performed, yielding a yellowish-colored pleural fluid with a protein concentration of 4.1 gm/dL. The cytological examination showed

Division of Chest Medicine, Department of Internal Medicine; Division of Thoracic and Cardiovascular Surgery, Department of Surgery*, Chang Gung Memorial Hospital, Kohsiung
Address reprint requests to: Dr. Mao-Chang Su, Divison of Chest Medicine, Department of Internal Medicine, Chang Gung Memorial Hospital, Kaohsiung, No.123, Ta-Pei Road, Niao-Sung Hsiang, Kaohsiung Hsien, Taiwan

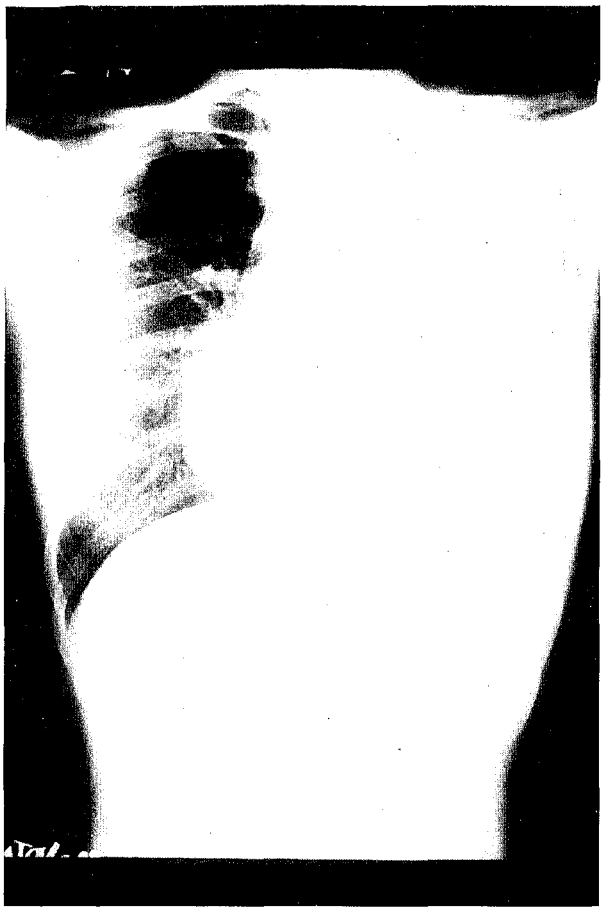

Fig. 1 The chest X-ray confirmed a massive left-sided pleural effusion with a slight mediastinal shift to the right.

numerous lymphocytes and monocytes. No organisms were found by Gram or Ziehl-Neelsen staining, or on cultures. A pleural biopsy was done simultaneously, showing chronic inflammatory changes and no caseous granulomas or malignant cells.

A computerized tomography of the thorax revealed a left side massive pleural effusion with a resultant collapse of the left lung. A 7-cm-in-diameter and well-enhanced mass with some inhomogeneity was disclosed in the left posteriomedial pleural cavity (fig. 2). No definite space-occupying lesion in the liver and adrenal glands was noted.

The patient received an exploratory thoracotomy, and an en bloc resection of the left posterior mediastinal tumor was performed. No obvious tumor spreading was observed during the

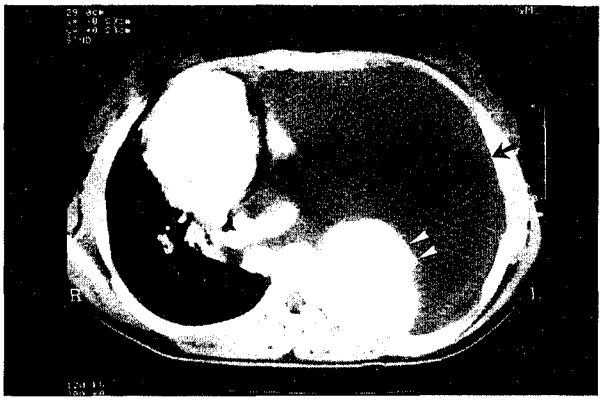

Fig. 2 Computerized tomography of the thorax revealed a left side massive pleural effusion (arrow), with a resultant collapse of the left lung. A well-enhanced mass with some inhomogeneity was revealed in the left posteriomedial pleural cavity (arrowheads). No obvious hypervascularity was noted.

operation. The tissue removed during thoracotomy consisted of a well-capsulated solid mass measuring 7.0 × 5.5 × 3.0cm, and weighing 77.98gm. Microscopically, this mass was composed of many lymphoid follicles separated by wide zones of proliferative hyperplastic capillaries. The mantle zone and follicular center cells were organized into concentric "onionskin" patterns. Many mature small lymphocytes and plasma cells were also noted (fig. 3).

The post-operative course was quite smooth, and the patient was discharged home soon thereafter. After 10 months of follow-up, she remained well without systemic complaints. No signs of recurrence were observed.

Discussion

Castleman's disease is an unusual disorder characterized by an abnormal proliferation of B lymphocytes and plasma cells in the lymphoid organs. Three histologic variants (hyaline-vascular, plasma cell, and mixed) have been classified. The hyaline-vascular variant features abnormal follicles with a striking interfollicular vascularity, expanded mantle zones composed of small lymphocytes, and one or more small blood vessels. These vessels may have thickened walls that form hyalinized germinal centers. The

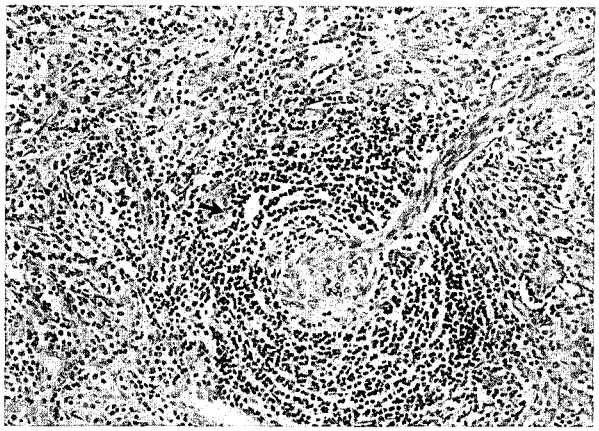

Fig.3 Microscopically, this mass was composed of many lymphoid follicles and the germinal center was surrounded by an expanded mantle zone. The mantle zone and follicular center cells were organized into concentric "onionskin" arrangements (arrow). Vascularity was increased within the interfollicular area, mantle zone, and germinal center. Hematoxylin-Eosin, × 100.

plasma cell variant displays lymph nodes with an intact mantle zone surrounded by sheets of mature plasma cells and no vascular proliferation [3].

Clinically, patients with Castleman's disease may present with an asymptomatic abnormality on the chest radiograph, localized symptoms caused by compression, or systemic symptoms (the "B" symptoms) such as fever, cold sweating, or weight loss. The latter symptoms, known as multicentric disease, is most often associated with the plasma cell variant. Patients with multicentric disease tend to be older (median age, 56 years). The multicentric variant is aggressively malignant-like, with the associated features of an elevated sedimentation rate, hepatosplenomegaly, hypergammaglobulinemia, granulocytosis, and plasmacytosis of the bone marrow [3]. Despite aggressive treatment, the median survival time for multicentric disease is 26 months, compared with a nearly 100% 5-year survival with the localized hyaline-vascular variant [4].

The presence of pleural effusion is uncommon in patients with Castleman's disease. Less than ten cases of Castleman's disease presenting with pleural effusion have been reported in the literature [5]. Two of these cases presented with chylous pleural effusion: one a plasma cell variant [6] and the other a mixed variant [5]. Chylous pleural effusions result from the disruption of the thoracic duct with a subsequent leakage of lymphatic fluid or chyle into the pleural cavity. The pleural fluid triglyceride level exceeds 110 mg/dL. The nonchylous pleural effusions reported in the literature are mostly present in multicentric disease. Pleural effusion due to localized Castleman's disease, as in this case, is especially rare. The impairment of pleural fluid resorption due to the mass effect of this tumor might be the cause of the pleural effusion, because operative findings showed no obvious tumor spreading.

Complete surgical excision is the primary modality of therapy, with radiation therapy reserved for rare unresectable cases. Awotedu et al [7] reported a young African man with a left lower lobe giant lymph node hyperplasia associated with recurrent pleural effusion, who was treated with a pneumonectomy, and survived for at least 3 years without relapse. Even though total tumor removal is not possible, subtotal excision of the tumor may be associated with good results without the recurrence of pleural effusion [2]. Medical therapy, including the use of prednisolone, chlorambucil, cyclophosphamide, and anti-interleukin-6 antibody [8,9] have been tried with multicentric disease with varying results. No complication or recurrence was noted after this patient's tumor resection, and neither medical nor radiation therapy was needed. The lack of systemic symptoms, the previous laboratory and image studies, and no evidence of recurrence indicated that the patient's Castleman's disease was a localized disease. There was a low probability of this case being a multicentric disease because the histologic picture revealed a typical hyaline-vascular variant rather than a plasma cell variant.

In conclusion, we report a unique case of Castleman's disease presenting with a massive pleural effusion - a very rare presentation of this disease. To our knowledge, this is the first case

report of Castleman's disease presenting with massive pleural effusion in Asia. This patient is surviving well and has experienced no recurrence since undergoing a surgical resection of the giant lymph node mass.

References

1. Castleman B, Iverson L, Menendez VP. Localized mediastinal lymph-node hyperplasia resembling thymoma. Cancer 1956; 9:822-30.
2. Renolds SP, Gibbs AR, Weeks R, et al. Massive pleural effusion: an unusual presentation of Castaleman's disease. Eur Respir J 1992; 5:1150-3.
3. Shahidi H, Mayers JL, Kvale PA. Castleman's disease. Mayo Clin Proc 1995; 70:969-77.
4. Weisenburger DD, Nathwani BN, Winberg CD, et al. Multicentric angiofollicular lymph node hyperplasia: a clinicopathologic study of 16 cases. Hum Pathol 1985; 16:162-72.
5. Hoor TT, Hewan-Lowe K, Miller JI, Moss M. A transitional variant of Castleman's disease presenting as a chylous pleural effusion. Chest 1999; 115:285-8.
6. Blankenship ME, Rowlett J, Timby LCJW, et al. Giant lymph node hyperplasia (Castleman's disease) presenting with chylous pleural effusion. Chest 1997; 112:1132-3.
7. Awotedu AA, Otulana BA, Ukoli CO. Giant lymph node hyperplasia of the lung (Castleman's disease) associated with recurrent pleural effusion. Thorax 1990; 45:775-6.
8. Smith RM, Dubinett SM, Grudko K, et al. Clinical conference on management dilemmas: A young woman with a 10-cm chest mass. Chest 1998; 114:295-306.
9. Nishimoto N, Sasai M, Shima Y, et al. Improvement in Castleman's disease by humanized anti-interleukin-6 receptor antibody therapy. Blood 2000; 95: 56-61.

Castleman's Disease 以大量肋膜積水表現－病例報告

蘇茂昌　賴永發　謝敏暲*

Castleman's disease 為一種罕見淋巴組織內 B 淋巴球或漿性球不正常增生之疾病。它可區分為三種組織學分類：透明血管型，漿性球型，以及混合型。大多數病患都是意外發現且無症狀，而肋膜積液是 Castleman's disease 之少見徵候。我們報告一位 23 歲女性之局限性 Castleman's disease 患者，以左側大量肋膜積液為其表現症狀。患者接受手術將其左後縱膈淋巴腫塊切除，術後病人情況良好且無復發現象。 ***(胸腔醫學 2001; 16: 124-128)***

關鍵詞：Castleman's disease 巨淋巴結增生，肋膜積液

高雄長庚紀念醫院　胸腔內科　胸腔暨心臟血管外科*
索取抽印本請聯絡：蘇茂昌醫師，高雄縣鳥松鄉大埤路 123 號

Sjögren's Syndrome and Systemic Amyloidosis Associated with Pulmonary Bullae Formation— A Case Report

Chieh-Jen Wang, Pei-Jan Chen*, Ming-Jen Peng*, Tien-Ling Chen**, Chin-Yin Sheu***, Hung-Chang Liu****, T-Y Wang*****

We report a 58-year-old female patient with Sjögren's syndrome (SS) and amyloidosis who presented with chronic cough. Her initial chest roentgenograph showed multiple bilateral nodules, linear infiltrates and cysts. Her condition remained stable for three years, but then deteriorated progressively a few months after beginning levamisole treatment. Multiple pulmonary bullae were recognized concurrently. A open lung biopsy disclosed nodular amyloidosis and a low-grade malignant lymphoma. SS associated with amyloidosis and pulmonary bullae formation has rarely been reported. We also believe it is the first report of the effects of levamisole in such a condition. A determination of the possible detrimental effects of levamisole may require further study. ***(Thorac Med 2001; 16: 129-135)***

Keywords: Sjögren's syndrome, amyloidosis, bullae, levamisole

Introduction

Amyloidosis is a disease characterized by tissue deposits of fibrillar protein with a β-pleated sheet conformation [1], which specifically binds Congo red stain, yielding apple-green birefringence under polarized light. Amyloid fibrils can be deposited locally or may involve virtually every organ system, including the lungs. Pulmonary involvement in systemic amyloidosis is common, with well-described manifestations. [2-6]. On the other hand, pulmonary involvement in Sjögren's syndrome (SS), a chronic inflammatory autoimmune disorder characterized by keratoconjunctivitis sicca and xerostomia, does not have such clearly defined characteristics. [7]. When SS and amyloidosis occur simultaneously, the thoracic radiographic manifestations may be confusing. We herein present a patient with these two conditions, further complicated by drug side effects.

Department of Emergency Medicine, *Division of Pulmonary Medicine, Department of Internal Medicine, **Division of Rheumatology, Department of Internal Medicine, ***Department of Radiology, ****Division of Thoracic Surgery, Department of Surgery, *****Department of Pathology, Mackay Memorial Hospital, Taipei, Taiwan

Address reprint requests to: Dr. Chieh-Jen Wang, Department of Emergency Medicine, Mackay Memorial Hospital, 92 Chung-Shan North Road, Sec.2. Taipe, Taiwan

Case history

A 58-year-old woman presented with the complaint of chronic cough in August 1994. She did not smoke and reported no major health problems except for occasional dry eyes. The initial chest film revealed bilateral interstitial infiltrates and emphysematous changes, interpreted as consistent with bronchiectasis. The pulmonary function tests suggested hyperinflation and air trapping (see Table 1) without response to bronchodilators. At the same time, she also consulted a surgeon for an enlarging left thigh and abdominal wall mass that had been present for 3 years with "slow growth". A biopsy report from the left thigh revealed amyloid tumor. She was followed in the OPD for her pulmonary symptoms, which showed no deterioration.

In March, 1997, she was admitted to the hospital again for weight loss, enlarging abdominal wall masses (both in size and number), and persistent dry eyes. The biopsy (from the abdominal wall) again showed an amyloid tumor. The abdominal CT revealed a diffuse peritoneal infiltration but no intra-abdominal masses. All tumor markers were negative except for an elevated CA-125 (47ng/dl, normal range: <35ng/dl), and gynecologic studies failed to find any abnormality. A positive Schirmer's test, anti-Ra auto-antibody, and the findings on sialoscintigraphy confirmed a diagnosis of SS. A HRCT of her chest was performed to look for any pulmonary involvement of systemic amyloidosis and/or lymphoma. The findings were consistent with those of the previous plain films, but further demonstrated multiple cysts of varying size and enlarged hilar lymph nodes. A Ga67 scan revealed increased uptake over the right hilum, left inguinal region, and abdomen. Surgical exploration for tissue confirmation was suggested, but she refused. Other immunologic studies included a negative rheumatoid factor, positive ANA (640x, speckled), normal C3, C4, CH50, and negative anti-dsDNA. The serum IEP showed a polyclonal gammopathy with a monoclonal peak (Ig M, λ), compatible with an elevated serum Ig M titer (901 ng/dl, normal range: 95-188). Other studies, including a complete blood cell count and peripheral smear, renal and cardiac echo, and urinary Bence Jones protein excretion, were all negative. She was then discharged.

A few months later, she returned complaining of dyspnea, exercise intolerance, and chronic fatigue. Repeat pulmonary function tests (see Table I) disclosed a restrictive pattern, in contrast to the previous obstructive pattern, and moderate impairment in diffusing capacity (47%). The chest film (fig.1) and HRCT (fig.2) exhibited bilateral hilar adenopathy, multiple ill-defined areas of alveolar consolidation, interstitial fibrosis and bullae formation. The patient admitted she had taken levamisole 50mg q8h for 3 days every 2 weeks for a few months, under another physician's instructions. She also reported her abdominal and thigh masses were enlarging and increasing in number. An open lung biopsy was performed in September 1998. The presence of amyloid deposits was confirmed by a positive Congo red stain that resisted permanganatic treatment, and by typical electron microscopic findings. However, discrete foci of neoplastic small lymphocytes without the formation of a germinal center, positive Dutcher bodies, and plasmacytoid cells with positive λ chain staining suggested the possibility of a low-grade malignant lymphoma. Her cardiac and renal

Table I

PFT	Dec, 1995	Jul, 1998
FVC	1.82 l (72%)	1.68 l (70%)
FEV_1	1.58 l (87%)	1.28 l (65%)
FEV_1/FVC	86%	76%
$FEF_{25\%-75\%}$	2.04 l (91%)	1.04 l (49%)
VC	2.25 l (89%)	1.68 l (70%)
TLC	4.82 l (120%)	3.78 l (89%)
RV	2.57 l (168%)	2.10 l (116%)
RV/TLC	53%	56%
FRC	2.97 l (118%)	2.47 l (82%)
DLCO	13.8 (99%)	9.0 (47%)

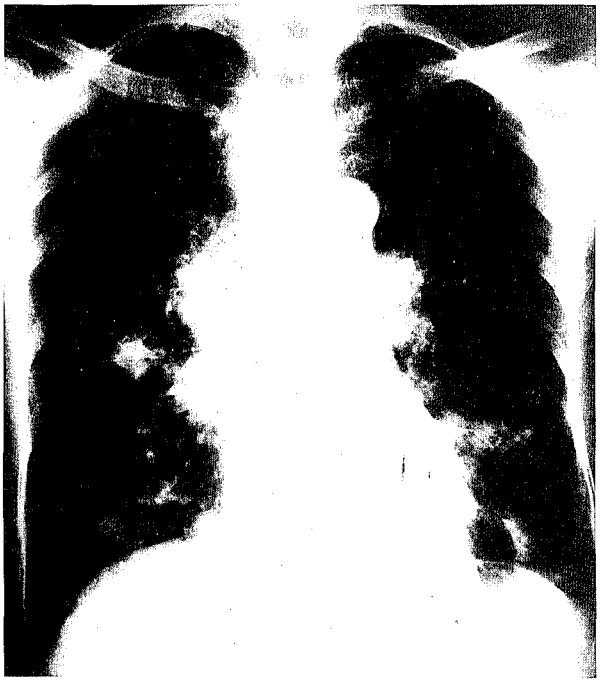

Fig.1. The chest X-ray obtained before operation. Notice the pulmonary parenchyma was severely destructed.

function were still normal, as was a bone marrow examination. The serum □*2-microglobulin level* was normal, however, her serum Ig M titer had increased to 2910 ng/dl (230% increase).

She was persuaded to stop levamisole, but her condition didn't improve. Chemotherapy (melphalan plus prednisolone) was then given, but her condition continued to deteriorate over the following months. She has been admitted to the hospital repeatedly because of dyspnea, and her daily activities have been severely limited.

Discussion

Systemic amyloidosis and SS are both diseases of insidious onset. Accompanying pulmonary manifestations may also be vague, making diagnosis difficult. Patients can be asymptomatic or present with non-specific symptoms and signs [6,8-9,10]. Grosbois et al [21] suggested that, since SS itself is frequently accompanied by a B cell lymphoproliferative disorder, amyloidosis may not be an extraordinary complication of SS. Recently, Ideura et al [11]

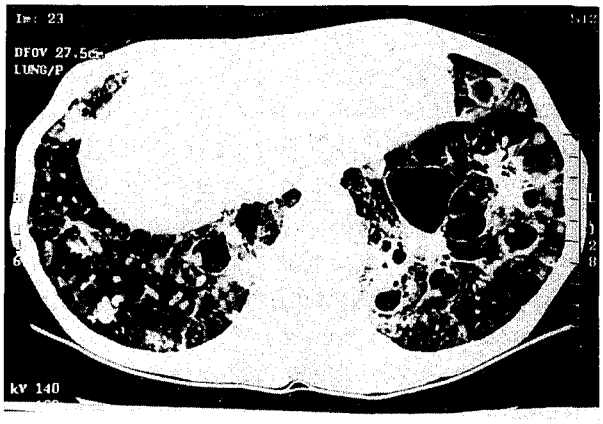

Fig.2. The HRCT obtained before operation. Notice the progression of cysts and bullae.

reviewed the 19 available English-language case reports describing the association of SS with amyloidosis or amyloidoma. They suggested that a patient with primary SS might have a tendency to accumulate amyloid precursor protein in various organs and soft tissues; alternatively, SS can occur secondarily as a manifestation of systemic amyloidosis. Several aspects of our patient's case, as below, led us to postulate that her amyloidoma and amyloidosis may have been a complication of SS: (1) amyloidoma as an initial presentation is less common than systemic amyloidosis [12]; (2) she had no heart or kidney involvement with plasma cell dyscrasia [10,23], which is more common in primary systemic amyloidosis; and (3) extensive thoracic lymph node involvement [13] and pathologic findings of malignant lymphoma are more consistent with SS.

Some cases of SS associated with amyloidosis have reportedly been complicated by pulmonary bulla formation [14-18]. Although about one fourth of SS patients have pulmonary involvement [19], there are no clearly pathognomonic pulmonary findings [8]. The radiographic spectrum in pulmonary amyloidosis has been well described [3,5,20], but the relationship between amyloidosis and cyst or bulla formation has not been emphasized. Several cases have been described, however. Kobayashi et al [16] speculated that extensive inflammatory cell infiltration (which can be intensive in SS)

around small airways might result in amyloid deposition, thereby inducing a ball-valve mechanism and bulla formation. This speculation has been supported by Ohdama et al [20], though other mechanisms have also been hypothesized. In this patient, we observed a correlation between the radiographic deterioration and the increased severity of inflammation (rising serum IgM titer) and peribronchial lymphocytic infiltration (slide not shown). This finding may support the ball-valve hypothesis. Of the 6 reported patients with pulmonary cysts or bullae (including the present case), 4 have been Asians. This suggests a possible ethnic predisposition.

The range of B cell lymphoproliferative disorders related to SS is wide, from benign lymphocytic interstitial pneumonitis to malignant lymphoma [8]. In one study, the risk of malignant lymphoma in patients with SS was 44 times higher than that of the general population [22]. For this reason, when patients with SS present with extensive thoracic lymphadenopathy, it is prudent to consider the diagnosis of malignant lymphoma. However, intrathoracic adenopathy is also the single most common abnormality identified in patients with systemic amyloidosis (up to 75%) [5]. In the same report, the authors declared that systemic amyloidosis should be considered when a combination of adenopathy, multiple small pulmonary nodules, and interlobular septal thickening or diffuse irregular lines are present on the chest CT. Although the radiographic finding in our patient shared several features with this description and remained unchanged for years, the surgical biopsy yielded evidence of malignant lymphoma. We therefore recommend a policy of early exploration in patients with SS and adenopathy, regardless of whether they are symptomatic or not.

There is no known effective therapy for amyloidosis [23]. Chemotherapy with melphalan and prednisolone have frequently been used in an attempt to reduce the production of amyloid fibril precursor protein [24], but it has seldom halted disease progression [25]. SS is also an incurable disease and treatment is aimed at symptomatic relief [26]. There have been no reports of successful treatment when both diseases are present [27].

Levamisole, an agent frequently used with fluorouracil in the treatment of colon cancer, is an immunomodulator. It stimulates formation of antibody to various antigens, enhances T-cell responses, potentiates monocyte and macrophage functions, and increases neutrophil mobility, adherence, and chemotaxis [28]. Because of its "immunomodulating" property, levamisole was once used in the treatment of patients with rheumatoid arthritis and SS [29], but it was abandoned because of complications (mainly pruritic skin rash) in 90% of those patients treated with it. We were unable to find any information in a MEDLINE literature search to support the use of levamisole for amyloidosis. Whether our patient's clinical deterioration was related to the natural course of her disease or to the effect of levamisole remains uncertain. The rapid deterioration (within a few weeks) after drug initiation is compatible with a previous report of adverse effects [29]. The profound elevation of serum IgM is also suggestive, but her condition did not improve or stabilize after discontinuing the drug. It is also very difficult to determine which component of her disease contributed to her deterioration, or whether they both had a role. However, her hypergammopathy, which is more common in amyloidosis [10] than in SS, especially SS with malignant lymphoma [30], intensified after levamisole treatment. For this reason, it is reasonable to regard amyloidosis with particular suspicion, although this type of occurrence has not been previously reported.

SS associated with amyloidosis and pulmonary bullae formation is very rare [14-18]. Treatment is empirical and the outcome is difficult to predict. However, using a previously untried therapy without any experimental support may be very dangerous. We think the use of levamisole in this patient was a tragedy. Although levamisole is thought to restore a depressed

immune function rather than to stimulate it to above-normal levels [28], our report suggests this is not always the case. The possible detrimental effect of levamisole on inflammatory disorders requires further study.

Reference

1. Glenner GG. Amyloid deposits and amyloidosis, the beta-fibrilloses. N Engl J Med 1980; 302: 1183-1232, 1333-42.
2. Wilson SR, Sander DE, Delarue NC. Intrathoracic manifestations of amyloid disease. Radiology 1976; 120: 283-9.
3. Himmelfarb E, Wells S, Rabinowitz JG. The radiologic spectrum of cardiopulmonary amyloidosis. Chest 1977; 72: 327-32.
4. Celli BR, Rubinow A, Cohen AS, et al. Patterns of pulmonary involvement in systemic amyloidosis. Chest 1978; 74: 543-7.
5. Pickfor HA, Swensen SJ, Utz JP. Thoracic cross-sectional imaging of amyloidosis. AJR 1997; 168: 351-5.
6. Utz JR, Swensen SJ, Gertz MA. Pulmonary amyloidosis, the Mayo clinic experience from 1980 to 1993. Ann Intern Med 1996; 124: 407-13.
7. Fox RI. Sjögren's syndrome. Curr Opin Rheumatol 1995; 7: 409-16.
8. Strimlan CV, Rosenow EC, Divertie MB, et al. Pulmonary manifestation of Sjogren's syndrome. Chest 1976; 70: 354-61.
9. Quismorio Jr. EP. Pulmonary involvement in primary Sjögren's syndrome. Curr Opin Pulm Med 1996; 2: 424-8.
10. Kyle RA, Gertz MA. Primary systemic amyloidosis: clinical and laboratory features in 474 cases. Semin Hematol 1995; 32: 45-59.
11. Indeura H, Tsukada Y, Maezawa A, et al. Sjogren syndrome and multiple amyloidoma. J Rheumatol 2000; 27: 1325-6.
12. Krishnan J, Chu W-S, Elrod JP, et al. Tumoral presentation amyloidosis (amyloidomas) in soft tissue, a report of 14 cases. Am J Clin Pathol 1993; 100: 135-44.
13. Gross BH. Radiographic manifestation of lymph node involvement in amyloidosis. Radiology 1981; 138: 11-4.
14. Bonner HJ, Ennis RS, Geelhoed GW, et al. Lymphoid infiltration and amyloidosis of lung in Sjögren's syndrome. Arch Pathol 1973; 55: 42-4.
15. Tsunoda N, Saito K, Kobayashi H, et al. A case report of multiple nodular pulmonary amyloidosis associated with Sjögren's syndrome and multiple bullae. Nihon Kyobu Shikkan Gakkai Zasshi 1987; 25: 1364-9. [Japanese; English abstract]
16. Kobayashi H, Natsuoka R, Kitamura S, et al. Sjögren's syndrome with multiple bullae and pulmonary nodular amyloidosis. Chest 1988; 94: 438-40.
17. Schlegel J, Kienast K, Storkel S, et al. Primary pulmonary nodular amyloidosis and multiple emphysematous bullae in Sjögren's syndrome. Pneumolgie 1992; 46: 634-7. [In German; English abstract]
18. Fujimoto T, Hiyai T, Yamanaka A, et al. Multiple nodular pulmonary amyloidosis with multiple bullae. Nihon Kokyuki Gakkai Zasshi 2000; 38: 59-62. [In Japanese English abstract]
19. Garniner P. Primary Sjogren's syndrome. Bailliere's Clin Rheumatol 1993; 7: 59-77.
20. Ohdama S, Akagawa S, Matsubara O, et al. Primary diffuse alveolar septal amyloidosis with multiple cysts and calcification. Eur Respir J 1996; 9: 1569-71.
21. Grosbois B, Jego P, Leblay R, et al. Sjögren's syndrome and malignant lymphoproliferative syndrome. Rev Med Interne 1998; 19: 319-24.
22. Kassan SS, Thomas TL, Moutsopoulos HM, et al. Increased risk of lymphoma in sicca syndrome. Ann Intern Med 1978; 89: 888-92.
23. Friman C, Pettersson T. Amyloidosis. Curr Opin Rheumatol 1996; 8: 62-71.
24. Tan SY, Pepys MB, Hawkins PN. Treatment of amyloidosis. Am J Kidney Dis 1995; 26: 267-85.
25. Merlini G. Treatment of primary amyloidosis. Semin Hematol 1995; 32: 60-79.
26. Fox RI, Tomwall J, Michelson P. Current issues in the diagnosis and treatment of Sjögren's syndrome. Curr Opin Rheumatol 1999; 11: 364-71.
27. Wong BC, Wong KL, Ip MS, et al. Sjögren's syndrome with amyloid A presenting as multiple pulmonary nodules. J rheumatol 1994; 21: 165-7.
28. Anonymous. Levamisole HCl. Drug facts and comparisons. St. Louis; Wolters Kluwer, 1999: 3521-3.
29. Balint G, EL-Ghobarey A, Capell H, et al. Sjogren's syndrome: a contraindication to levamisole treatment? Br

Med J 1977; 26: 1386-7.
30. Anderson LG, Talal N. The spectrum of benign to malignant lymphoproliferation in Sjogren's syndrome. Clin Exp Immunol 1972; 10: 199-221.

索格倫氏症候群及類澱粉樣沉積病併有肺部大泡形成－病例報告

王玠仁 陳培然* 彭明仁* 陳天令** 許清寅*** 劉洪彰**** 王道遠*****

我們報告一 58 歲女性病患，合併有索格倫氏症候群及類澱粉樣沉積病，而以慢性咳嗽呈現。其初始胸部 X 光影像呈雙側肺野多發性結節，囊腫及線狀浸潤陰影。此病人維持穩定狀況達三年之久而後在經 levamisole 治療後數月間急速惡化。追蹤之肺部影像檢查顯示嚴重的肺實質破壞及大泡形成。肺部生檢結果顯示廣泛之類澱粉樣陳積及早期輕度惡性淋巴瘤之徵兆。索格倫氏症候群及類澱粉樣沉積病合併肺部大泡形成在以往很少被報告出來，我們相信這是首例此類病人接受 levamisole 治療的報告。Levamisole 對此類病人可能有害，不宜使用。*(胸腔醫學 2001; 16: 129-135)*

關鍵詞：索格倫氏症候群，類澱粉樣沉積病，大泡，levamisole

台北馬偕紀念醫院 急診部 胸腔內科* 風濕免疫科** 放射科*** 胸腔外科**** 病理科*****
索取抽印本請聯絡：王玠仁醫師，台北市中山區中山北路二段 92 號

Endobronchial Hamartoma—A Case Report

Chen-Yi Huang, Ching-Chi Lin, Hung-Chang Liu*, Chin-Yin Sheu**, Chi-Yuan Tzen***

Endobronchial hamartoma is a rare benign tumor arising in the bronchial wall. We present a 64-year-old male patient who suffered from cough with bloody sputum and dyspnea. Chest X-ray revealed atelectasis of the upper left lobe. The gross bronchoscopic finding was that the orifice of the upper left lobe was obstructed totally by a lobulated nodule with a smooth surface, and the bronchoscopic biopsy showed chronic inflammatory mucosa. Due to the finding of fat tissue and calcification in the nodule on CT, an endobronchial hamartoma was diagnosed preoperatively. Later, the patient underwent a sleeve-lobectomy resection, without incident.

The symptons of endobronchial hamartoma are related to bronchial obstruction. The findings on the chest X-ray and bronchoscopy are nonspecific. Because CT can effectively detect the characteristic findings of fat tissue and calcification in the endobronchial hamartoma, an accurate diagnosis becomes possible preoperatively. ***(Thorac Med 2001; 16: 136-142)***

Keywords: endobronchial hamartoma

Introduction

Hamartoma is the most common benign lung tumor. Its incidence in the general population, as found in autopsies, is 0.25% [1], accounting for approximately 8% [2] of all lung tumors. Hamartoma is more prevalent in adults and only rarely occurs in infants[3]. Patients are usually 50 – 60 years old, and the male to female ratio is 1.5:1-3:1 [4,5]. Hamartomas can be classified as parenchymal or endobronchial. The latter is rather uncommon, accounting for 1.4-10% of all hamartoma cases [4,6]. The incidence of endobronchial hamartoma is approximately 1:1000, if compared with lung cancer [7]. Although rare, endobronchial hamartoma is the most common benign endobronchial tumor, accounting for 24.3% of all cases [8]. Its clinical symptoms are primarily associated with endobronchial obstruction [9]. Radiographic changes are mainly the result of this obstruction [5], while the bronchoscopic biopsy usually reveals chronic inflammation or squamatous metaplasia [10, 11]. These findings are non-specific, making the preoperative diagnosis of endobronchial hamartoma difficult. Currently, the use of the CT scan, on which fatty tissues and calcification consistent with hamartoma can be seen, helps in the preoperative diagnosis of the

Chest Divison, Departments of Internal Medicine, *Thoracic Surgery, **Radiology, ***Pathology, Mackay Memorial Hospital, Taipei, Taiwan
Address reprint requests to: Dr. Chen-Yi Huang, Division of Chest Medicine, Department of Internal Medicine, Mackay Memorial Hospital, 92, Sec.2, Chung-Shan N. Road, Taipei, Taiwan

tumor [12]. The case presented here is the first case of endobronchial hamartoma in our hospital. It displayed typical CT imaging and was accurately diagnosed before the operation. Because of its rarity, we report this case and reviewed the literature.

Case Report

The patient was male, 64-years-old, and a retired cook with a 15-year smoking history (about one pack per day). He had suffered fractured ribs in an auto accident when he was young, and once received a ventricular-peritoneal shunt due to increased intracranial hypertension. The patient's chief complaint was a cough that started about one month before hospitalization. The sputum was greyish-white with occasional traces of blood. He also complained about a poor appetite and experienced dyspnea from time to time on exertion. He lost body weight of 4 kilograms in one month. Physical examination was unremarkable except for a decreased breathing sound in the upper left lung field. The blood routine was as follows: red blood cells: $4.17x10^6$/ul; hemoglobin: 10.9g/dL; white blood cells: 15720/ul; and platelets: $187x10^3$/ul. The general biochemical test values were within normal range. Urinolysis was normal, as was the pulmonary functions test, which showed no obstructive or restrictive defects and FEV_1: 3.11L. The front chest X-ray showed an ill-defined, semi-transparent shadow in the upper left lung field (Figure 1); a left lateral chest X-ray revealed a nearly vertical left major fissure (Figure 2). These findings pointed to an upper left lobe collapse. Endobronchial obstruction was suspected at that time. Thus a bronchoscopy examination was arranged and we found that the upper left lobe orifice was blocked by a lobulated nodule with a smooth surface (Figure 3). The pathological report of its biopsy indicated bronchial mucosa infiltrated by chronic inflammatory cells. A CT scan of the

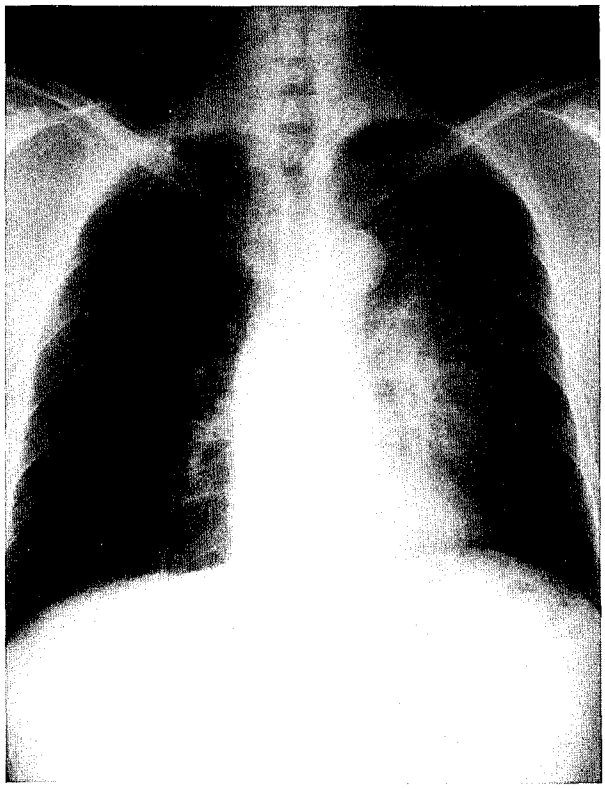

Figure 1. Chest PA on presentation shows an ill-defined, semi-transparent shadow in the upper left lung field.

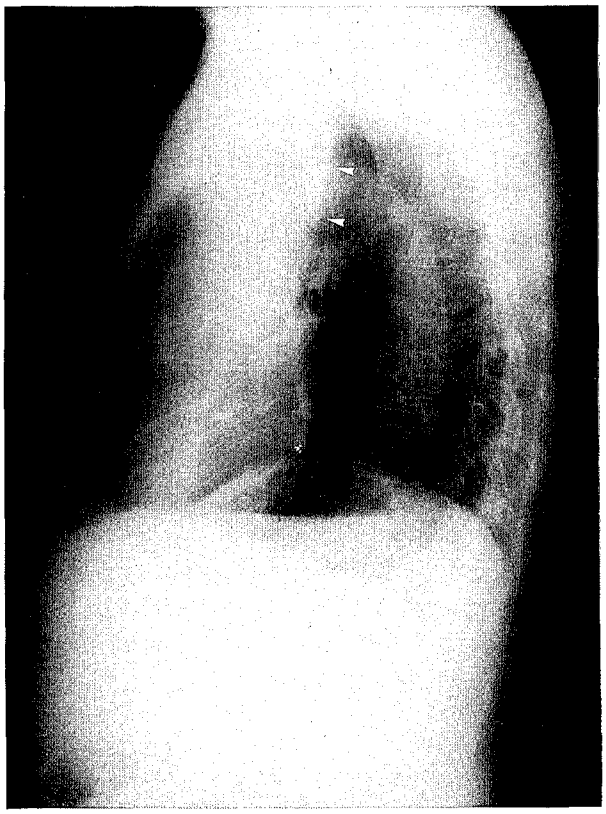

Figure 2. Left lateral chest X-ray shows the nearly vertical left major fissure (arrow).

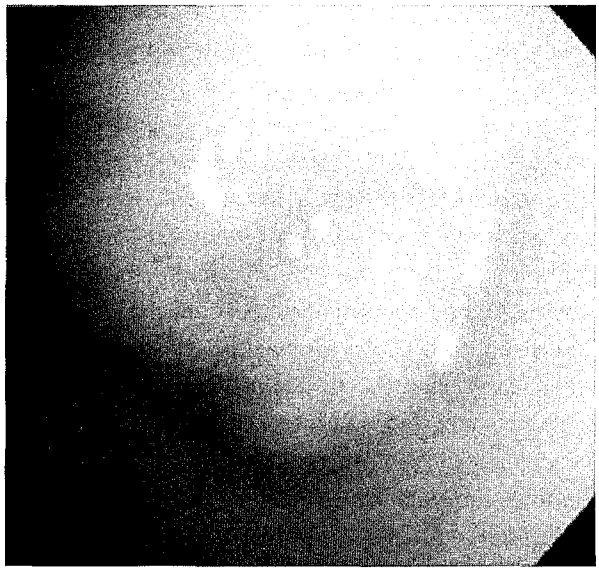

Figure 3. The upper left lobe orifice was blocked by a lobulated nodule with a smooth surface.

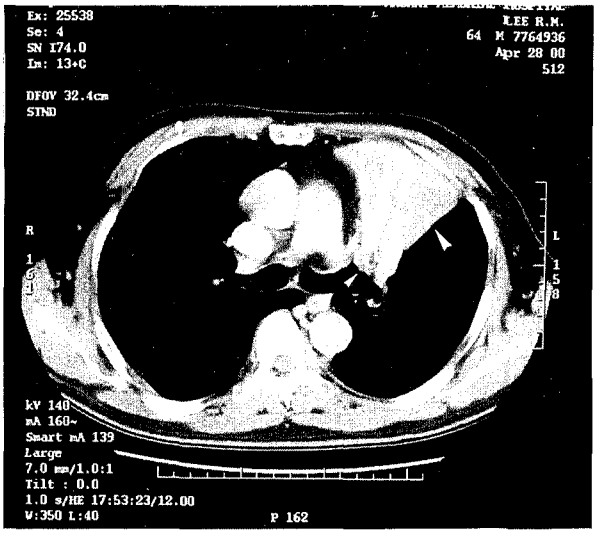

Figure 4. CT scan of the lung revealed a solitary 1.5cm nodule (thin arrow) in the upper left lobe orifice. The nodule contained fatty tissue (-30HU) and calcification, with the collapsed upper left lobe distal to it (thick arrow).

lung revealed a solitary 1.5cm nodule at the upper left lobe orifice which contained fatty tissue (-30HU) and calcification. There was a collapsed upper left lobe distal to it (Figure 4). The preoperative diagnosis was endobronchial hamartoma combined with a collapsed upper left lobe. The patient subsequently underwent surgical resection. During the operation, the upper left lobe was found to be suppurative. To prevent post-surgical infection, the surgical approach of choice was a sleeve lobectomy. The patient recovered well after the operation and was discharged in one week. The surgical specimen was a grey, firm, lobulated nodule, 2cm in diameter grossly. The pathological biopsy showed that there was some fibromyxoid tissue, fat, and cartilage within the nodule which was covered with normal respiratory epithelium (Figure 5). Some of the cartilage was ossified. The obstructed end of the lung showed organizing pneumonia and fibrosis. The pathological diagnosis was hamartoma with obstructive pneumonia.

Discussion

Albrecht defined hamartoma in 1904 as a tumor-like malformation derived from an abnormal mixture of the tissues that constitute the organ. These tissues could be of different proportions and have variable degrees of differentiation and arrangement [13]. McDonald et al. had a similar point of view [1]. Because the hamartoma can grow gradually [4, 14], and it has been found to have an identical chromosomal aberration to that of other benign tumors [15, 16], the general consensus at the present time is that it is a benign tumor [4, 17, 18].

Endobronchial hamartoma is composed of the connective tissues of the mesenchyma. The most dominant mesenchymal component is cartilage, followed by fat, fiber, and skeletal tissue [5]. The hamartoma can be lobulated or polypoid in appearance [14], is covered with normal respiratory epithelium, and contains some respiratory epithelial tissue enveloped during its growth [17, 19]. Although the tumor is benign, there have been occasional reports of malignant degeneration [20, 21, 22]. Karasik et al. reported that the risk of lung cancer in patients with hamartoma was 6.3 times greater than that of the general population [23]. But, in the 215 hamartoma cases reported by Gjevre, no evidence of either a malignant transformation or an unexplained association with other lung

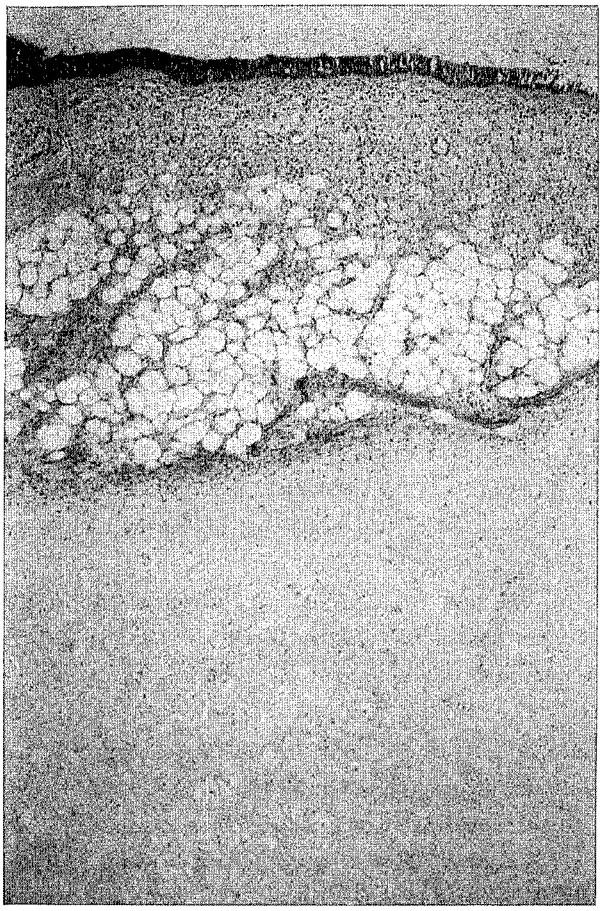

Figure 5. Pathological biopsy showed that there was some fibromyxoid tissue, fat, and cartilage within the nodule which was covered with normal respiratory epithelium (40X).

neoplasms was found [6].

Parenchymal and endobronchial hamartomas both display similar age distribution, sex predilection, and pathological changes. Their difference lies in the site of the lesion only. The former is derived from the peripheral bronchi, while the latter is derived from the major bronchi [24].

Parenchymal hamartoma is often asymptomatic and the majority is found only incidentally in the chest radiograph [25]. Endobronchial hamartoma often has symptoms because of the bronchial obstruction. The most common symptom is coughing, followed by expectoration, hemoptysis, and dyspnea. Sometimes fever and body weight loss associated with obstructive pneumonia are observed [14]. The case presented here exhibited these classic symptoms.

CXRs of endobronchial hamartomas mostly show the imaging of a collapsed lobe, while few display the consolidation of obstructive pneumonia and hyperinflation caused by incomplete obstruction [5]. Calcification is relatively uncommon, seen in only about 10-15.2% of all cases [6, 23]. These findings are inadequate for a confirmed diagnosis of endobronchial hamartoma. Popcorn calcification on X-ray is a feature, but only a few cases have demonstrated such a change [26].

Bronchoscopic biopsy is able to confirm endobronchial hamartoma in only a small percentage of cases. The pathological findings in most biopsies show no more than some inflammatory cells or squamatous metaplasia [10, 11]. In this case, only bronchial mucosa with chronic inflammation was observed.

The CT scan is a useful diagnostic tool because it is more easily interpretes the fat tissue and calcification in the lesion and identifies the presence of lymph node enlargement. It is also helpful in the differential diagnosis. Siegelman et al used CT scans to diagnose 60% of their hamartoma cases, based on three criteria-a tumor size smaller than 2.5cm, a well-defined margin, and a content of fat or fat alternating with areas of calcification, which greatly improved the accuracy of the preoperative diagnosis [12]. In this case, typical findings were observed on the CT scan, and it was easily diagnosed as endobronchial hamartoma before the operation .

The management for endobronchial hamartoma is surgical resection with the preservation of as much of the lung as possible. Depending on the location of the lesion and the pathological change of the terminal lobe obstruction, alternative approaches could include bronchoscopy resection, bronchotomy, sleeve resection, and lobectomy [10,27]. There have been some successful cases using bronchoscopy laser resection [8]. The success rate for hamartoma surgery is high, and relapse is extremely rare. Bosch et al. reported two cases of relapse and

attributed them to incomplete resection [5]. In this case, a sleeve lobectomy was chosen because the upper left lobe orifice was completely blocked by the nodule, and the prevention of post-surgical infection due to the suppuration at the end of the obstructed bronchus was considered.

The most important factors in association with endobronchial hamartoma are the differential diagnosis of the neoplasm and the treatment of symptoms caused by the obstructive lesion. The clinical symptoms, chest radiography manifestation, and bronchoscopic findings of endobronchial hamartoma are non-specific, as in this case. The CT scan can improve the accuracy of the preoperative diagnosis and help the doctor choose the proper surgical approach.

Reference

1. Mc Donald JR, Harrington SW, Clagett OT. Hamartoma (often called chondroma) of the lung. J Thorac Surg 1945;14:128-43.
2. Jones RC, Cleve EA. Solitary circumscribed lesions of the lung. Arch Intern Med 1954;93:842-51.
3. Dounies R, Chwals WJ, Lally KP, et al. Hamartomas of the chest wall in infants. Annals of Thoracic Surgery 1994;57:868-75.
4. Hansen CP, Holtveg H, Francis D, et al. Pulmonary hamartoma. J Thorac Cardiovasc Surg 1992;104:674-8.
5. Van den Bosch JMM, Wagenaar SjSc, Corrin B, et al. Mesenchymoma of the lung (so called hamartoma):a review of 154 parenchymal and endobronchial cases. Thorax 1987;42:790-3.
6. Gjvere JA, Myers JL, Prakash UBS. Pulmonary hamartomas. Mayo clin Proc 1996;71:14-20Miller DR. Benign tumors of lung and tracheobronchial tree. Ann Thorac Surg 1969;8:542-60.
7. Sibala JL. Endobronchial hamartomas. Chest 1972; 62: 631-4.
8. Shah H, Garbe L, Nussbaum E, et al. Benign tumors of the tracheobronchial tree: endoscopic characteristics and role of laser resection. Chest 1995;107:1744-51.
9. Miller DR. Benign tumors of lung and tracheobronchial tree. Ann Thorac Surg 1969;8:542-60.
10. Kui-Chou Huang, Chih-Yi Chen, Chun-Leih Chen. et al. Chin Med J (Taipei) 1988;42:65-70.
11. Davis WK, Roberts L Jr, Foster WL Jr, et al. Computed tomographic diagnosis of an endobronchial hamartoma. Invest Radio 1988 ;23:941-4.
12. Sigelman SS, Khouri NF, Leo FP, et al. Pulmonary hamartoma: CT findings. Radiology 1986;160:313-7.
13. Albrechet E. Ueber Hamartoma. Verh Dtsch Ges Pathol 1904 ;7:153-7.
14. Bateson EM, Abbott EK. Mixed tumors of the lung or hamarto-chondromas. Clin Radiol 1960;11:232-47.
15. Fletcher JA, Longtine J, Wallace K, et al. Cytogenetic and histologic findings in 17 pulmonary chondroid hamartomas: evidence for a pathogenetic relationship with lipomas and leiomyomas. Genes Chromosom Cancer 1995; 12:220-3.
16. Johansson M. Dietrich C, Mandahl N, et al. Recombinations of chromosomal bands 6p21 and 14q24 characterise pulmonary hamartomas.Br J Cancer 1993;67:1236-41.
17. Perez-Atayde AR, Seiler W. Pulmonary hamartoma:An ultrastructural study. Cancer 1984;53:485-92.
18. Salminen US. Pulmonary hamartoma. A clinical study of 77 cases in a 21-year period and review of literature. Eur J Cardio-thorac Surg 1990;4:15-8.
19. Bateson EM. So-call hamartoma of the lung-a true neoplasm of fibrous connective tissue of the bronchi. Cancer 1973;31:1458-67.
20. Poulsen JT, Jacobsen M, Francis D. Probable malignant transformation of a pulmonary hamartoma. Thorax 1979;34:557-8.
21. Karpas CM, Blackman N. Adenocarcinoma arising in a hamartoma (adenolipomyoma) of the bronchus associated with multiple benign tumors. Amer J Clin Pathol 1967;48:383-8.
22. Kojima R, Mizuguchi M, Bessho F, et al. Pulmonary carcinoma associated with hamartoma in an 11-year-old boy. American Journal of Pediatric Hematology-Oncology 1993;15(4):439-42.
23. Karasik A, Modan M, Chaim MSc, et al. Increased risk of lung cancer in patients with chondromatous hamartoma. J Thorac Cardiovasc Surg 1980;80:217-20.
24. Bateson EM. Relationship between intrapulmonary and endobronchial cartilage-containing tumors(so- called hamartomata). Thorax 1965;20: 447- 61.
25. Hamper UM, Khouri NF, Stitik FP, et al. Pulmonary

hamartoma: diagnosis by transthoracic needle-aspiration biopsy. Radiology 1985; 155(1):15-8.
26. Crouch JD, Keagy BA, Starek PJ, et al. A clinical review of patients undergoing resection for pulmonary hamartoma. American surgeon 1988;54(5):297-9.
27. Borro JM, Moya J, Botella JA, et al. Endobronchial hamartoma. Report of 7 cases. Scandinavian Journal of Thoracic & Cardiovascular Surgery 1989;23(3):285-7.

支氣管內過誤瘤－病例報告

黃呈誼 林清基 劉洪彰* 許清寅** 曾岐元***

支氣管內過誤瘤被認為是來自支氣管內結締組織的罕見肺部良性腫瘤。本病例是一位 64 歲男性患者，主述於住院前一個月開始有咳嗽及氣促的現象，痰液為灰白色，偶而併有血絲。胸部 X 光顯示患者有左上肺葉塌陷的現象。支氣管鏡檢查，發現左上肺葉開口被表面平滑呈分葉狀的節結所阻塞，其切片檢查的病理報告為被慢性發炎細胞所浸潤的支氣管黏膜。由於肺部電腦斷層攝影顯示節結內含有脂肪組織及鈣化物，術前診斷為支氣管內過誤瘤。患者隨後接受袖式肺葉切除術。

支氣管內過誤瘤的臨床症狀和支氣管阻塞有關。胸部 X 光的表現及支氣管鏡檢查的發現都不具特殊性。電腦斷層攝影因為較容易發現腫瘤中的脂肪組織及鈣化物，提高了支氣管內過誤瘤的術前正確診斷率。 ***(胸腔醫學 2001; 16: 136-142)***

關鍵詞：支氣管內過誤瘤

台北馬偕紀念醫院 胸腔內科 胸腔外科* 放射科** 病理科***
索取抽印本請聯絡：黃呈誼醫師，台北市中山區中山北路二段 92 號

Chronic Eosinophilic Pneumonia—A Case Report

Chun-Min Chen*, Shin-Hwar Wu, Chih-Mei Huang, Kai-Ming Chang, Chi-Der Chiang

Chronic eosinophilic pneumonia (CEP) is a rare disease. It is characterized by profound systemic symptoms (fever, malaise, weight loss, and anorexia), localized pulmonary manifestations (cough, wheeze with sputum) lasting more than one month, pulmonary infiltrates with eosinophils, and a dramatic response to corticosteroid therapy. We describe a 73-year-old male patient who was referred from a local hospital after 2 months of fever, dry cough, weight loss, and progressive dyspnea. His chest radiograph at admission showed pulmonary infiltrates, predominantly in the periphery of the lower right lung. Laboratory data revealed mild blood eosinophilia (460/cumm). A computed tomography of the chest did not reveal bronchiectasis. Cells from the bronchoalveolar lavage contained 15% eosinophils. A thoracoscopic biopsy showed organizing pneumonia with eosinophilic infiltrations. Under the diagnosis of CEP, prednisolone 40 mg per day was given. This treatment led to defervescence, reduced dyspnea within 48 hours, and radiographic improvement after 1 week. ***(Thorac Med 2001; 16: 143-147)***

Keywords: eosinophilic pneumonia

Introduction

Chronic eosinophilic pneumonia (CEP) is a rare disease characterized by a chronic and ultimately life-threatening illness with high fever, night sweats, weight loss, and severe dyspnea [1]. The etiology is largely unknown [2,3]. Corticosteroid therapy brings about complete clinical recovery and a cleaning of the roentgenogram within a few days. With premature reduction or omission of therapy, symptoms may recur, and infiltrates may reappear precisely in the same location [1]. The long-term prognosis for patients with CEP is excellent, but the majority require long-term low dose oral corticosteroid therapy to prevent relapse [3]. In some cases, high-dose inhaled corticosteroid therapy can allow for a reduction in the maintenance dose of the oral steroid therapy [4]. There is no consistent association with a history of cigarette smoking, but approximately one-third to one-half of patients have antecedent atopy, allergic rhinitis, or nasal polyps [5]. Herein, we describe a case of CEP without atopy.

Case Report

Division of Chest Medicine, Department of Internal Medicine Taichung Veterans General Hospital, *Chest Division, Department of Internal Medicine Armed Forces Hua-lien General Hospital
Address reprint requests to: Dr. Chun-Min Chen, Division of Chest Medicine, Department of Internal Medicine, Taichung Veterans General Hospital, No.160, Section 3, Chung-Kan Road, Taichung City, Taiwan

A 73-year-old male patient was sent to a local hospital because of a cough with scanty sputum and progressive dyspnea that had lasted for more than 2 months. Fever, and weight loss of about 4-5 kg, were noted over the 2 weeks prior to admission. The patient used to be a farmer, and has been retired for more than 10 years. He never smoked cigarettes, and had had no exposure to toxins, or to legal or illegal drugs in the past. He had been operated on for rectal cancer 10 years previous. A chest radiograph showed alveolar opacities predominating in the periphery of the right lung. The bronchoscopy was negative. The patient had been treated as a case of bacterial pneumonia for more than 2 weeks, but the symptoms had exacerbated. He was then referred to our hospital.

On admission to our hospital, his physical examination was unremarkable apart from mildly diminished breathing sounds over the lower right lung field. No lymphadenopathy or skin lesions were found. Laboratory data revealed that the peripheral blood leukocyte count was 8590/cumm (69.6% neutrophils, 16.3% lymphocytes, 10.7% monocytes, 2.9% eosinophils, 5% basophils). Arterial blood gas with O_2 flow 2 L/min by nasal cannula showed pH 7.451, PCO_2 36.5 mmHg, PO_2 67.0 mmHg, $HCO3^-$ 25.6 mEq/L, and SaO_2 94.0%. The serum IgE was 618 IU/ml, and the blood antinuclear antibody (ANA) was negative. A repeated CBC two days later revealed an eosinophil count of 460/cumm. Serum antibodies to common pathogens of atypical pneumonia (*M. pneumoniae, C. pneumoniae* and *Legionella*) were all negative. Serum *cryptococcal* antigen was non-reactive. A stool microscopic examination failed to showed parasite ova. The chest radiograph on admission (fig 1a) showed peripherally predominant pulmonary infiltrates, especially in the right lung base. The computed tomography (CT) scan (fig 2) of the chest revealed multiple subpleural consolidation in both lungs, predominantly in the lower right lung with minimal adjacent pleural effusion. Bronchoalveolar lavage fluid obtained from the lower right lobe showed 78% histiocytes, 15% eosinophils, 4% lymphocytes, and 3% neutrophils (fig 3). The histopathologic examination of the lung tissue, from a thoracoscopic biopsy of the lower right lobe, showed organizing pneumonia with eosinophilic infiltration (fig 4).

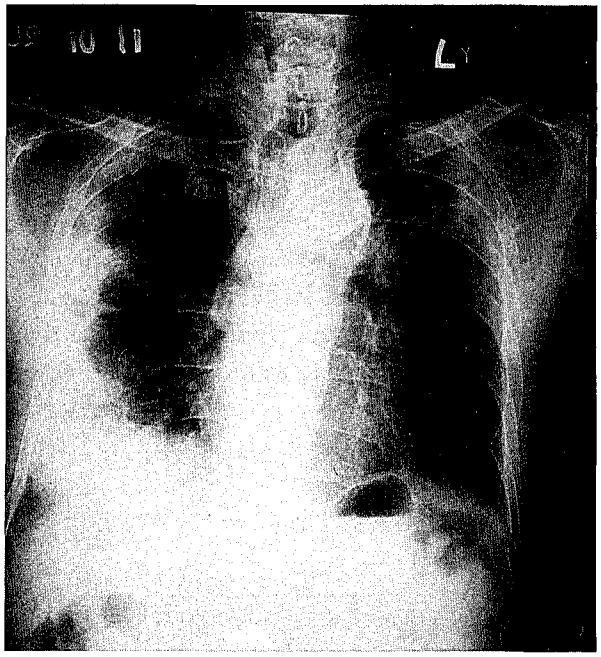

Figure 1. (A) Chest X-ray reveals alveolar opacities predominating in the periphery of the right lung.

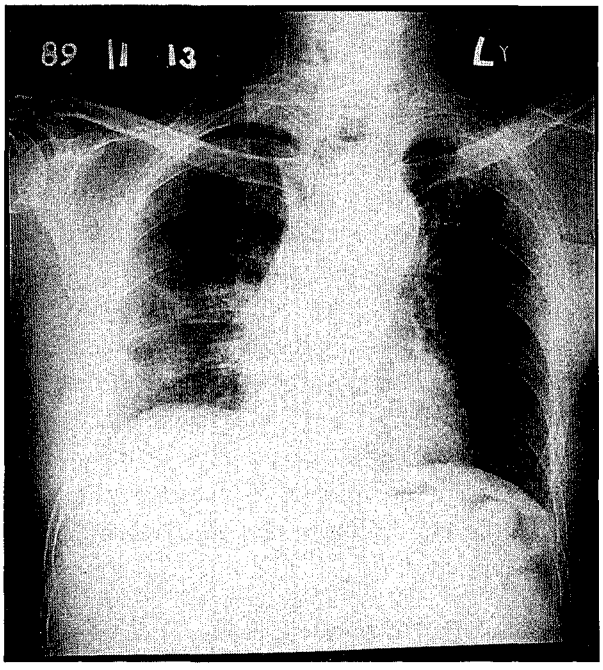

Figure 1. (B) The film after one week of corticosteroid therapy shows a marked resolution of the pulmonary lesions.

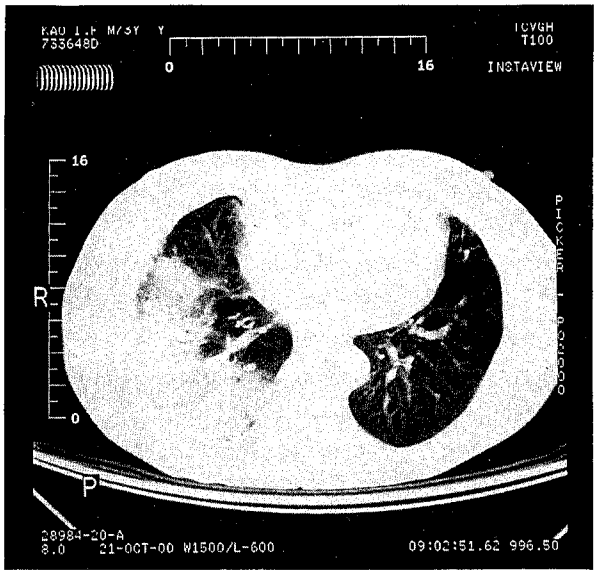

Figure 2. Chest CT scan shows homogenous peripheral airspace consolidation with an air-bronchogram of the right lung.

The patient was started on 40 mg oral prednisolone per day. During the next 72 hours, he improved dramatically. After one week of treatment, the laboratory tests and the pulmonary infiltrates on images had normalized (fig 1b).

Discussion

CEP is a rare disease of unknown cause. It was first defined in 1969 by Carrington et al., who reported their findings of 9 women with a subacute illness characterized by respiratory and severe systemic symptoms, peripheral alveolar infiltrates on imaging, and a dramatic response to corticosteroid therapy [1]. The exact incidence is still not known. Females predominate with a ratio of nearly 2 to 1 [15], but this ratio becomes less conspicuous in patients over 60 years of age. CEP occurs in all age groups. The peak incidence appears among 30-to 39-year olds [7]. Preexisting atopic disease was present in one-half of all patients [7]. The patient in our report is a male who had no atopic history and did not smoke. The pathogenic mechanisms of CEP are poorly understood. Aberrant hypersensitivity responses appear to play important roles [2,6]. T-lymphocytes, GM-CSF, IL-5 and IL-3 mediate

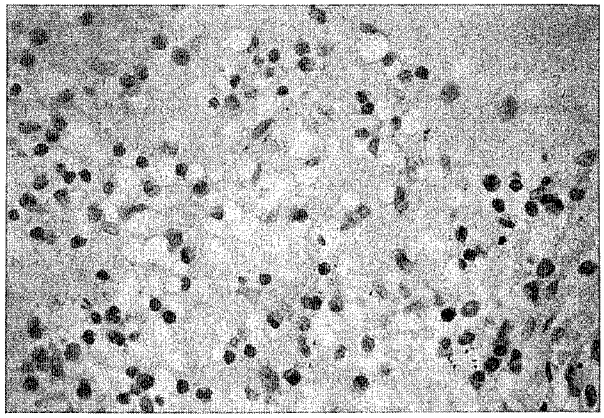

Figure 3. Lung biopsy discloses organizing pneumonia with eosinophilic infiltration (H &E x 400).

the accumulation and proliferation of eosinophils in the pleural cavity [9,13]. Macrophage uptake of lysed eosinophils with released eosinophilic proteins have been detected in patients with CEP, but not in patients with eosinophilic pulmonary infiltrates from other causes [11]. Measuring eosinophilic cation protein concentration seems to be useful for evaluating disease activity [12]. The interval between the onset of symptoms and the diagnosis is often protracted, averaging 4 months [15]. After exclusion of infections (especially pulmonary tuberculosis and fungal disease like cryptococcosis) and other causes of eosinophilic pneumonia (such as Loffler's syndrome, drug-induced pulmonary eosinophilic syndrome, AEP, ABPA, Churg-Strauss syndrome, and idiopathic hypereosinophilc syndrome), the rapid improvement with steroid therapy is of diagnostic value [2]. The pulmonary infiltrates in a chest X-ray can be best described as a "photographic negative of pulmonary edema" [1]. However, a classic radiographic presentation is seen in less than 50 percent of the cases [5]. In one-third of CEP patients, the infiltrates are not distributed peripherally [1,6,14].

Peripheral blood eosinophilia greater than 6%, an elevated white blood cell count (WBC), and a high erythrocyte sedimentation rate (ESR), are found in the majority of patients [7]. Yet, pulmonary eosinophilia does occur without blood eosinophilia [1]. IgE levels are elevated in about

one half of the cases [2]. Bronchoalveolar lavage (BAL) fluid may demonstrate the intra-alveolar exudates of eosinophils and histiocytes. The eosinophilic counts decrease markedly during steroid therapy [8]. In most cases, prednisolone (40 mg a day for 10 to 14 days, followed by a tapering-off over 4-6 weeks) leads to defervescence within 6 hours, reduced dyspnea, cough and blood eosinophilia within 24 to 48 hours, radiographic improvement within 1 to 2 weeks, complete resolution of symptoms within 2 to 3 weeks [2,7], and normalization of the chest radiograph within 2 months [5]. Relapse occurred in most patient (58 to 80%) when steroids were tapered-off or discontinued [3,7]. Seventy-six percent of patients required steroid therapy for more than 6 months [7], a majority of patients require treatment for 1 to 3 years [5,7] and up to 25% may require long-term maintenance treatment (2.5-10 mg prednisolone a day) [3,5]. In some cases, inhaled corticosteroid therapy (1000-1500 μ g/day beclomethasone dipropionate) could permit a reduction in the maintenance dose of oral steroid therapy [4]. The lethality of CEP with treatment is low [1,6,7,10], although repeated episodes may lead to permanent pulmonary damage [1]. In rare instances, patients develop pulmonary fibrosis and honeycombing [5].

In conclusion, most patients with CEP present with subacute respiratory and constitutional symptoms and fail to respond to therapy for presumptive pneumonia. This rare disease should be considered in patients presenting with pulmonary infiltrates and eosinophilia. Eosinophilia occurs in most cases and its absence may be one of the indications for lung biopsy [7].

References

1. Carrington CB, Addington WW, Goff AM et al. Chronic eosinophililc pneumonia. N Engl J Med 1969; 280:787-98.
2. Laufs U, Schneider C, Wassermann K. Chronic eosinophilc pneumonia with atypical radiographic presentation. Respiration 1998; 65: 323-6.
3. Naughton M, Fashy J, FitzGerald MX. Chronic eosinophilic pneumonia. A long-lerm follow-up of 12 patients. Chest 1993; 103: 162-5.
4. Lavandier M, Carre P. Effectiveness of inhaled high-dose corticosteroid therapy in chronic eosinophilic pneumonia [letter]. Chest 1994; 107: 1913.
5. Rochester CL. The eosinophilic pneumonias. In Fishman AP ed. Fishman's pulmonary diseases and disorders. -3rd ed. McGraw-Hill 1998: 1138-40.
6. Umeki S. Reevaluation of eosinophilic pneumonia and its diagnostic criteria. Arch Intern Med 1992; 152: 1913-9.
7. Jederlinic PJ, Sicilian L, Gaensler EA. Chronic eosinophilic pneumonia. A report of 19 cases and a review of the literature. Medicine (Baltimore) 1988; 67: 154-62.
8. Takahashi H, Arakawa Y, Oki K et al. Analysis of bronchoalveolar lavage cells in chronic eosinophilic pneumonia before and during corticosteroid therapy. Int Arch Allergy Immunol 1995; 108(suppl 1): 2-5.
9. Nakamura Y, Ozaki T, Kamei T et al. Factors that stimulate the proliferation and survival of eosinophils in eosinophilic pleural effusion: relationship to granulocyte /macrophage colony-strmulating factors, interleukin-5, and interleukin 3. Am J Resp Cell Mol Biol 1993; 8: 605-11.
10. Chapman BJ, Capewell S, Gibson R et al. Pulmonary eosinophilia with and without allergic bronchopulmonary aspergillosis. Thorax 1989; 44: 919-24.
11. Janin A, Torpier G, Courtin P et al. Segregation of eosinophil proteins in alveolar macrophage compartments in chronic eosinophilic pneumonia. Thorax 1993; 48: 57-62.
12. Shijubo N, Shigehara K, Hirasawa M et al. Eosinophilic cationic protein in chronic eosinophilc pneumonia and eosinophilic granuloma. Chest 1994; 106: 1481-6.
13. Kita H, Sur S, Hunt LW et al. Cytokine production at the site of disease in chronic eosinophilic pnemonitis. Am J Respir Crit Care Med 1996;153: 1437-41.
14. Ebara H, Ikezoe J, Johkoh T et al. Chronic eosinophilic pneumonia: evolution of chest radiograms and CT features. J Comput Assist Tomogr 1994; 18: 737-44.
15. Eric M, Martine RG, Dominique L. Idiopathic chronic eosinophilic pneumonia: A clinical and follow-up study of 62 cases. Medicine 1998; 77(5): 299-312.

慢性嗜伊紅白血球性肺炎－病例報告

陳俊民* 吳莘華 黃枝梅 張開明 江自得

慢性嗜伊紅白血球性肺炎為一罕見疾病，特徵為持續一個月以上之全身(發燒，倦怠，體重減輕，厭食)和肺部(咳嗽，喘鳴，多痰)症狀，肺部伊紅性血球浸潤，以及對類固醇治療有快速反應。本文描述一位 73 歲男性病人，因發燒，乾咳，體重減輕及呼吸困難約 2 個月而由其他醫院轉診至本院。入院時之胸部 x 光呈現右下肺野邊緣性浸潤。實驗室檢查發現伊紅性血球增多(460/cumm)，血清 IgE 上升(618 IU/ml)。胸部電腦斷層掃瞄顯示無支氣管擴張，支氣管肺泡灌洗呈現 15%之伊紅性血球，胸腔鏡肺部組織病理檢查證實為慢性嗜伊紅性白血球肺炎。投予每日 40 mg 之 prednisolone 48 小時後病人症狀改善，1 週後胸部 x 光浸潤消退。 ***(胸腔醫學 2001; 16: 143-147)***

關鍵詞：嗜伊紅白血球性肺炎

台中榮民總醫院 胸腔內科 國軍花蓮總醫院 內科部*
索取抽印本請聯絡：陳俊民醫師，台中市中港路三段 160 號 台中榮民總醫院 胸腔內科